BH binaries

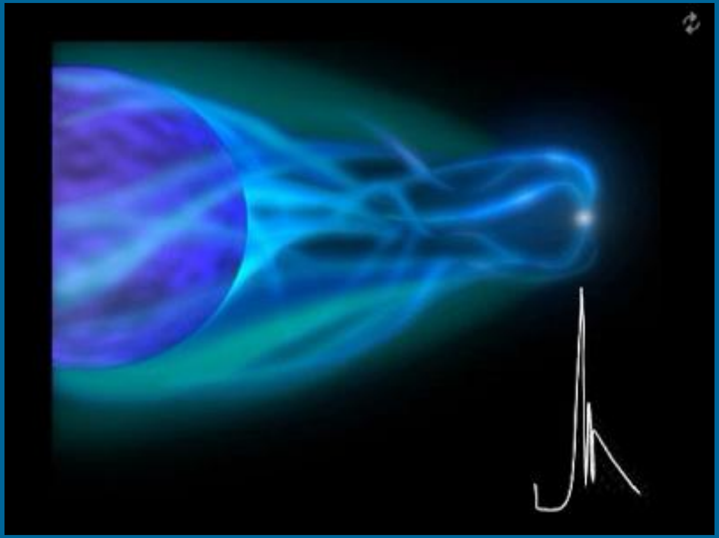

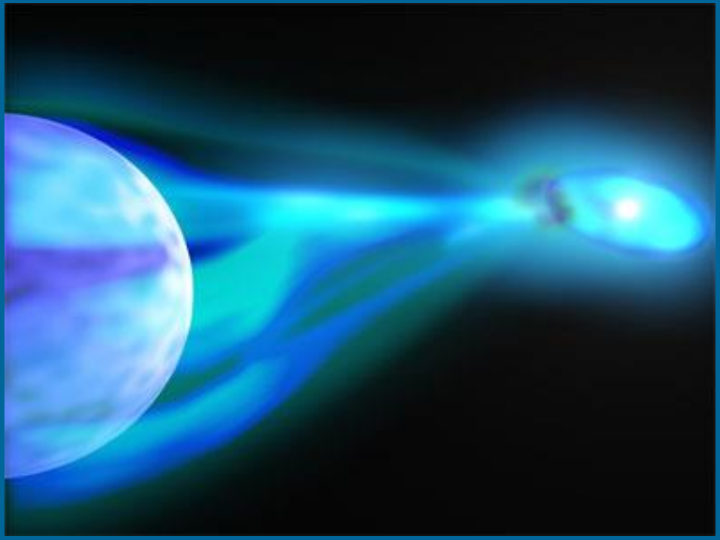

Black hole binaries

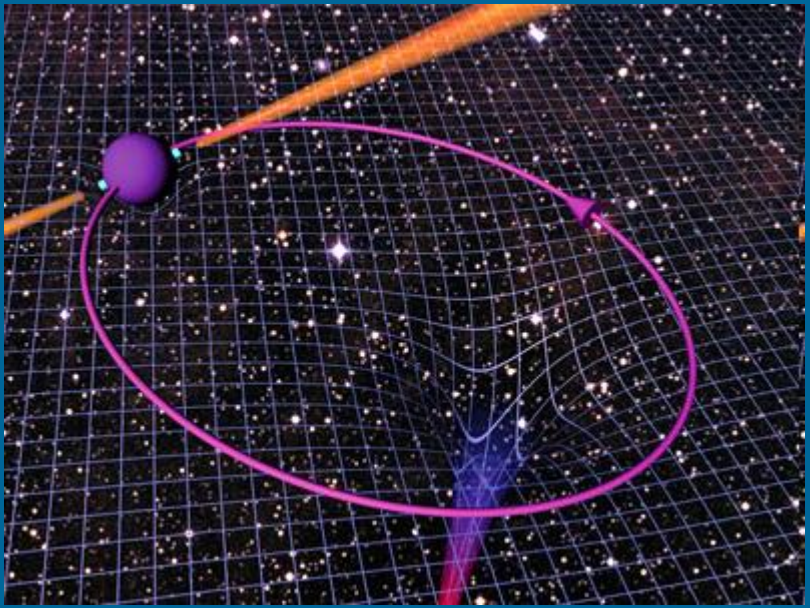

- Dormant BHs
- High mass (few)
- Low-mass (majority)
- ULX – ultraluminous X-ray sources

Most of low-mass are transients.

Microquasars.

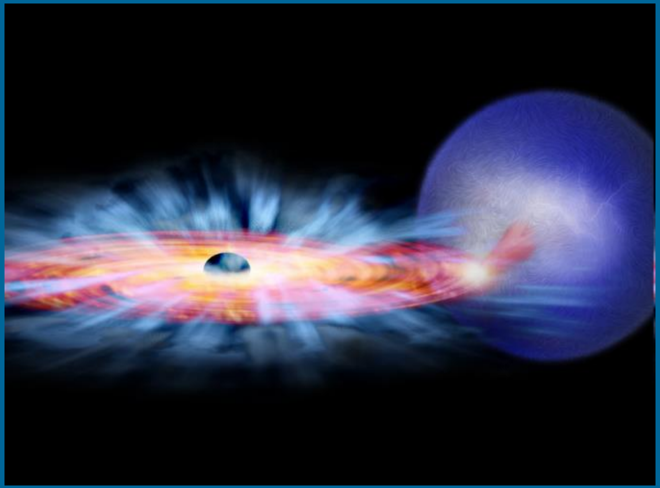

A hope for PSR+BH binary
- Either due to evolution
  (one per several thousand normal PSRs)
- Either due to capture
  (then – few in the central pc,
  see arXiv: 1012.0573)

BH1 – the first Gaia BH in a binary

Gaia DR3
d = 468 pc

$M_* = 0.91\ M_\odot$
M_{bh}~9-12$M_\odot$
P_{orb}=185 d
e=~0.46

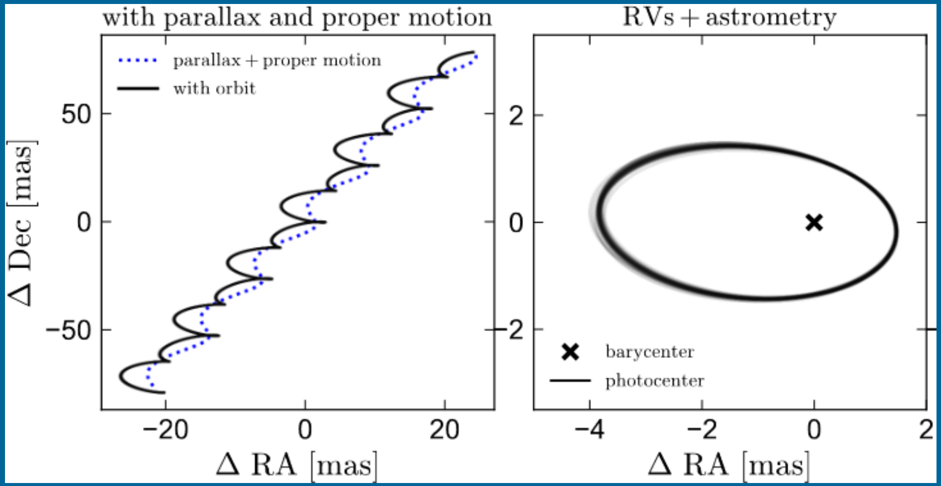

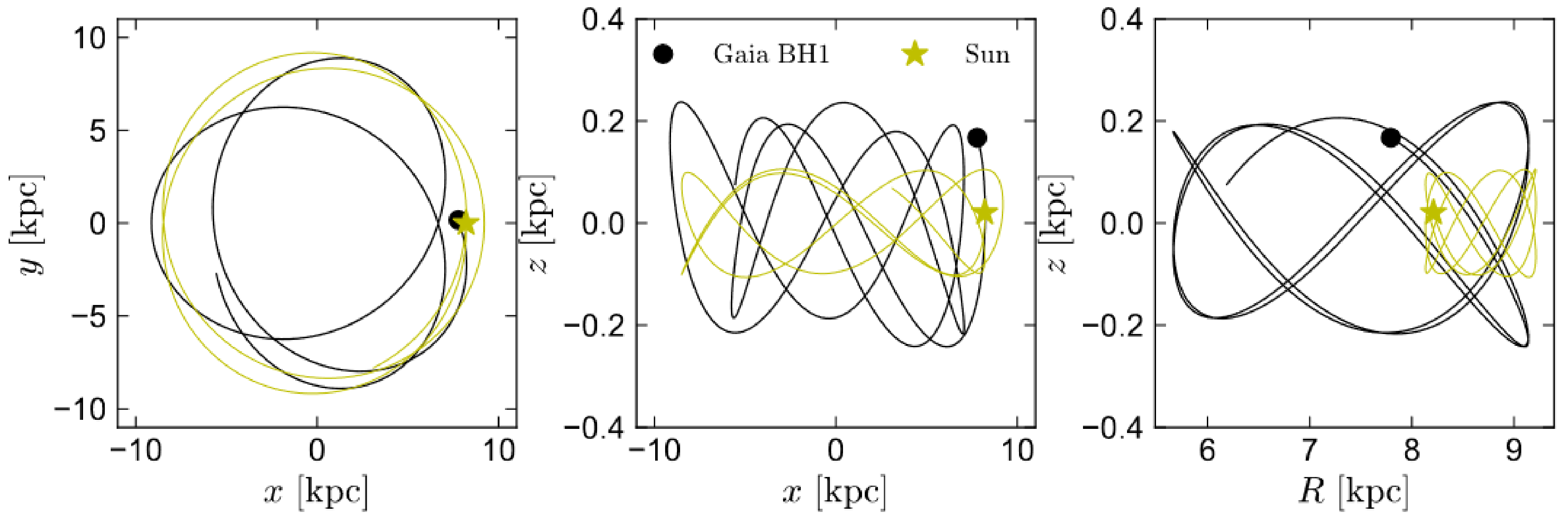

2209.06833, 2210.05003

BH2 – the system with a red giant

d=1.16 kpc

$M_* \sim 1 M_{sun}$
$M_{bh} \sim 9\ M_{sun}$
P_{orb}=1227 d

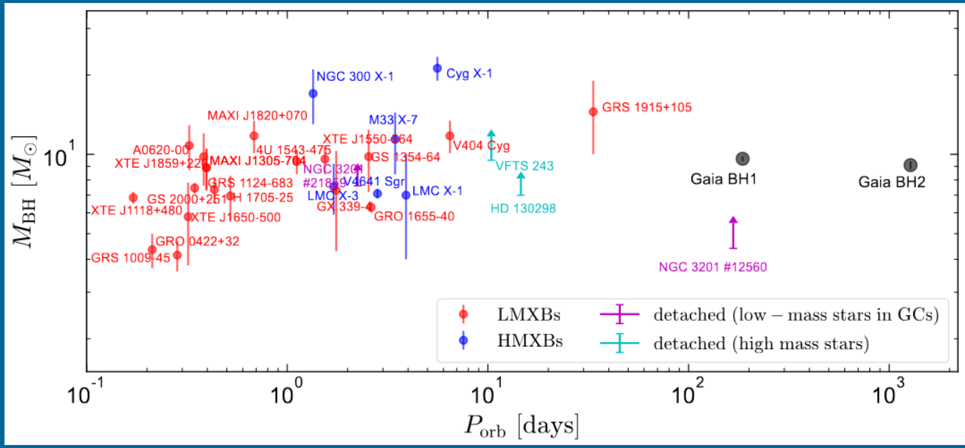

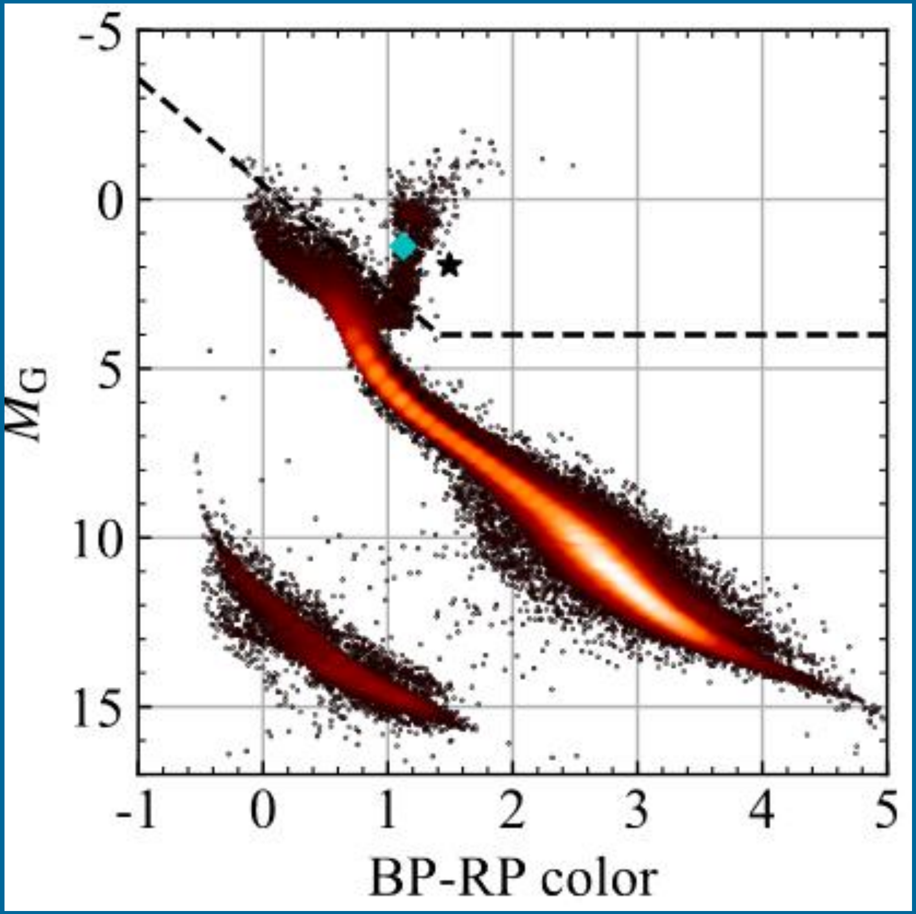

No X-rays detected from BH1, BH2 (2311.05685)
About the origin of BH1 and BH2 see 2403.13579

2302.07880 2209.05632

BH3 – a massive dormant BH in a binary

d=590 pc

M_*~

M_{bh}~32-33 M_{sun}

Porb~11.6 yrs

Visible star is has a low metallicity.

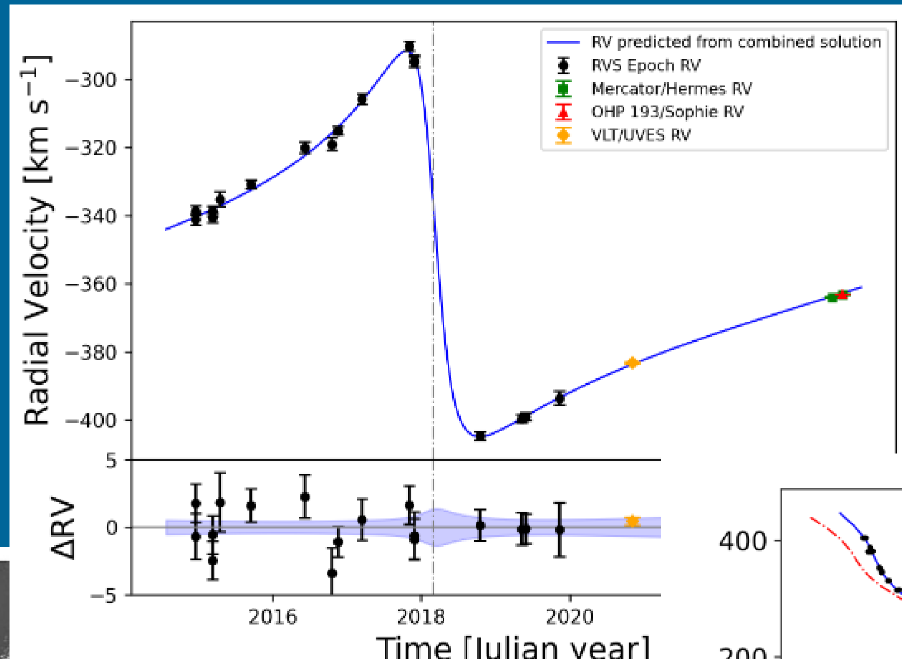

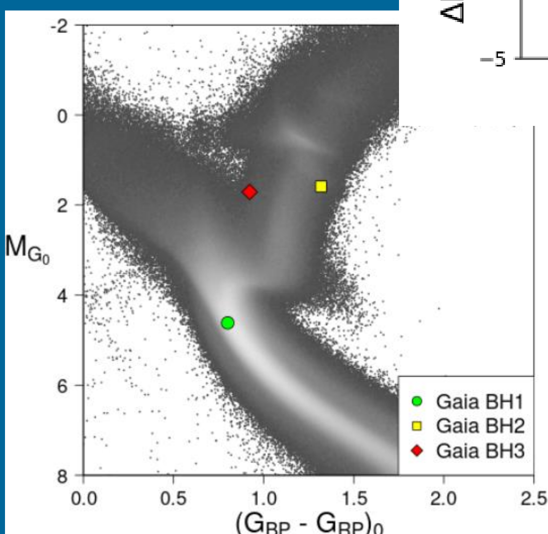

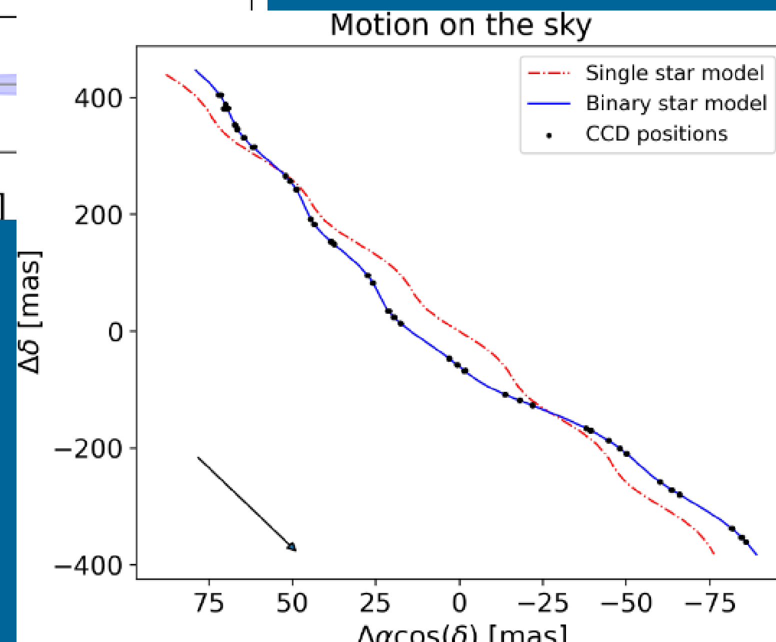

2404.10486 About the formation of this system see 2404.13047, 2404.17568

X-ray observations: Cyg X-1

"In the case of Cyg X-1 black hole – is the most conservative hypothesis"
Edwin Salpeter

The history of exploration of binary systems with BHs started about 40 years ago...

Recent mass measurement for Cyg X-1 can be found in arXiv:1106.3689

X-ray novae

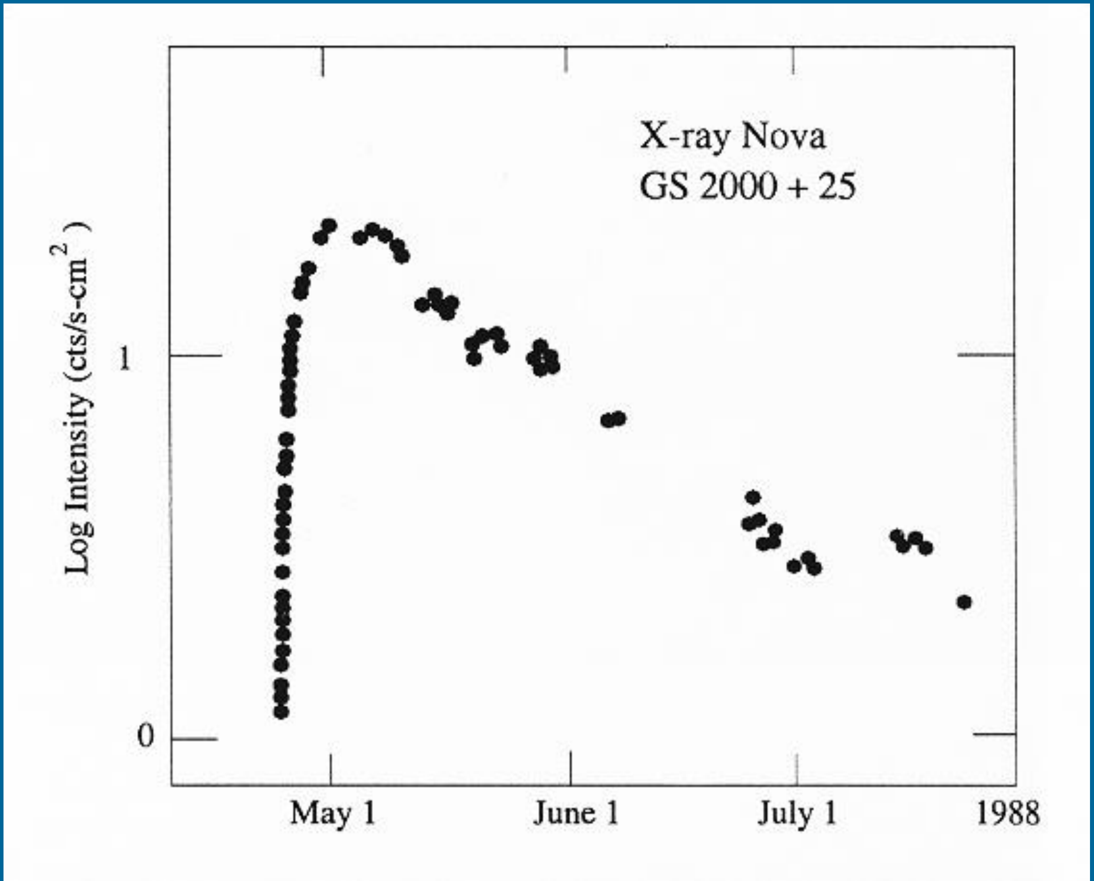

Low-mass binaries with BHs

One of the best candidates

In the minimum it is possible to see the secondary companion, and so to get a good mass estimate for a BH.

BH candidates

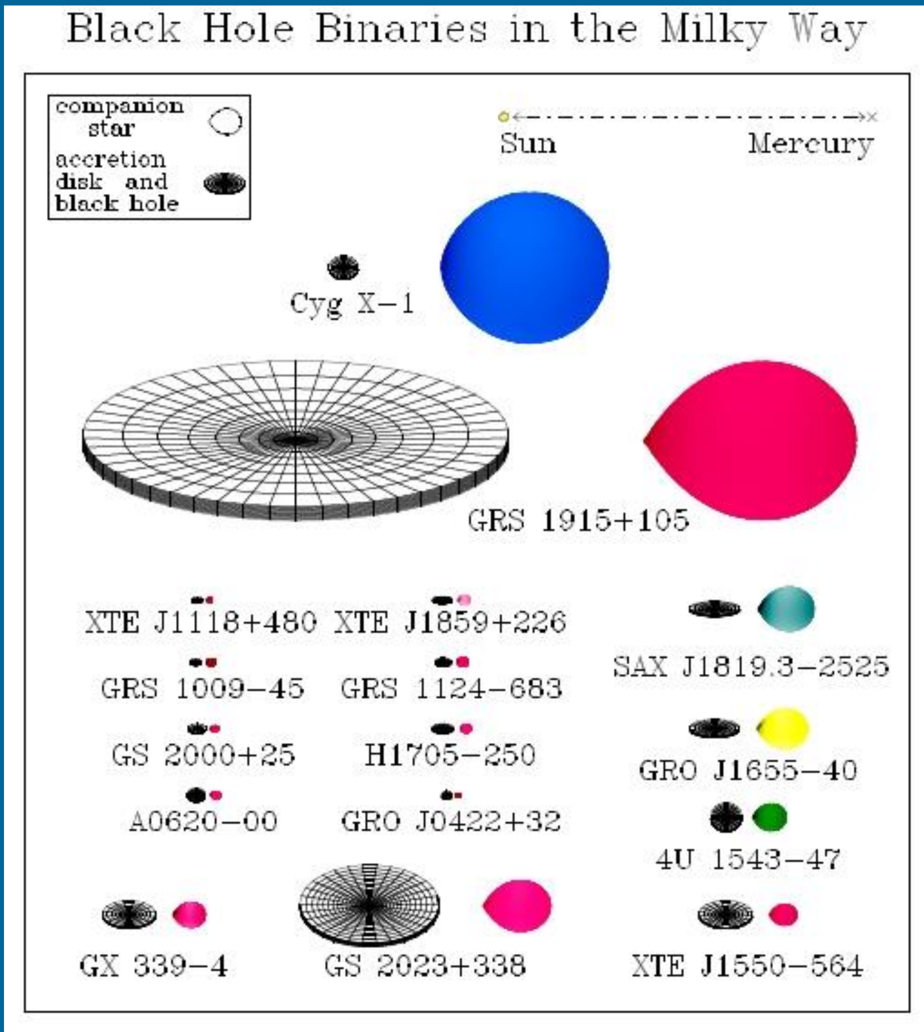

Among 20 good galactic candidates
17 are X-ray novae.
3 belong to HMXBs
(Cyg X-1, LMC X-3, GRS 1915+105).

New candidates still appear.

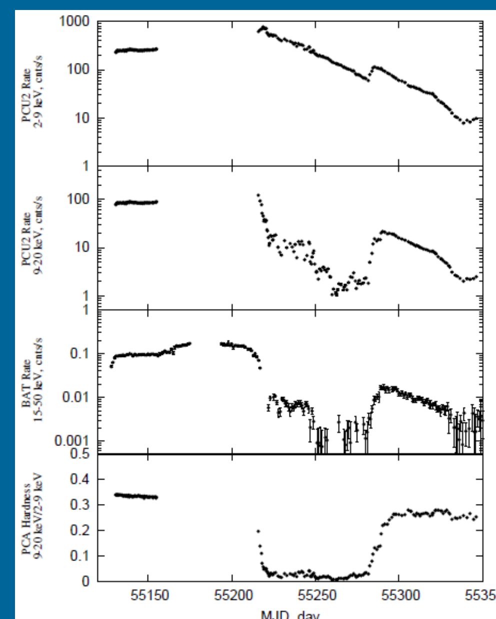

J. Orosz, from astro-ph/0606352

Candidates properties

Table 1: Twenty confirmed black holes and twenty black hole candidates[a]

Coordinate Name	Common[b] Name/Prefix	Year[c]	Spec.	P_{orb} (hr)	f(M) ($M_\odot$)	M_1 ($M_\odot$)
0422+32	(GRO J)	1992/1	M2V	5.1	1.19±0.02	3.7–5.0
0538–641	LMC X–3	–	B3V	40.9	2.3±0.3	5.9–9.2
0540–697	LMC X–1	–	O7III	93.8[d]	0.13±0.05[d]	4.0–10.0:[e]
0620–003	(A)	1975/1[f]	K4V	7.8	2.72±0.06	8.7–12.9
1009–45	(GRS)	1993/1	K7/M0V	6.8	3.17±0.12	3.6–4.7:[e]
1118+480	(XTE J)	2000/2	K5/M0V	4.1	6.1±0.3	6.5–7.2
1124–684	Nova Mus 91	1991/1	K3/K5V	10.4	3.01±0.15	6.5–8.2
1354–64[g]	(GS)	1987/2	GIV	61.1[g]	5.75±0.30	–
1543–475	(4U)	1971/4	A2V	26.8	0.25±0.01	8.4–10.4
1550–564	(XTE J)	1998/5	G8/K8IV	37.0	6.86±0.71	8.4–10.8
1650–500[h]	(XTE J)	2001/1	K4V	7.7	2.73±0.56	–
1655–40	(GRO J)	1994/3	F3/F5IV	62.9	2.73±0.09	6.0–6.6
1659–487	GX 339–4	1972/10[i]	–	42.1[j,k]	5.8±0.5	–
1705–250	Nova Oph 77	1977/1	K3/7V	12.5	4.86±0.13	5.6–8.3
1819.3–2525	V4641 Sgr	1999/4	B9III	67.6	3.13±0.13	6.8–7.4
1859+226	(XTE J)	1999/1	–	9.2:[e]	7.4±1.1:[e]	7.6–12.0:[e]
1915+105	(GRS)	1992/Q[l]	K/MIII	804.0	9.5±3.0	10.0–18.0
1956+350	Cyg X–1	–	O9.7Iab	134.4	0.244±0.005	6.8–13.3
2000+251	(GS)	1988/1	K3/K7V	8.3	5.01±0.12	7.1–7.8
2023+338	V404 Cyg	1989/1[f]	K0III	155.3	6.08±0.06	10.1–13.4

(astro-ph/0606352)   Also there are about 20 “candidates to candidates”.

Detector MAXI recently added several new BH candidates

New mass and spin estimates for Cyg X-1

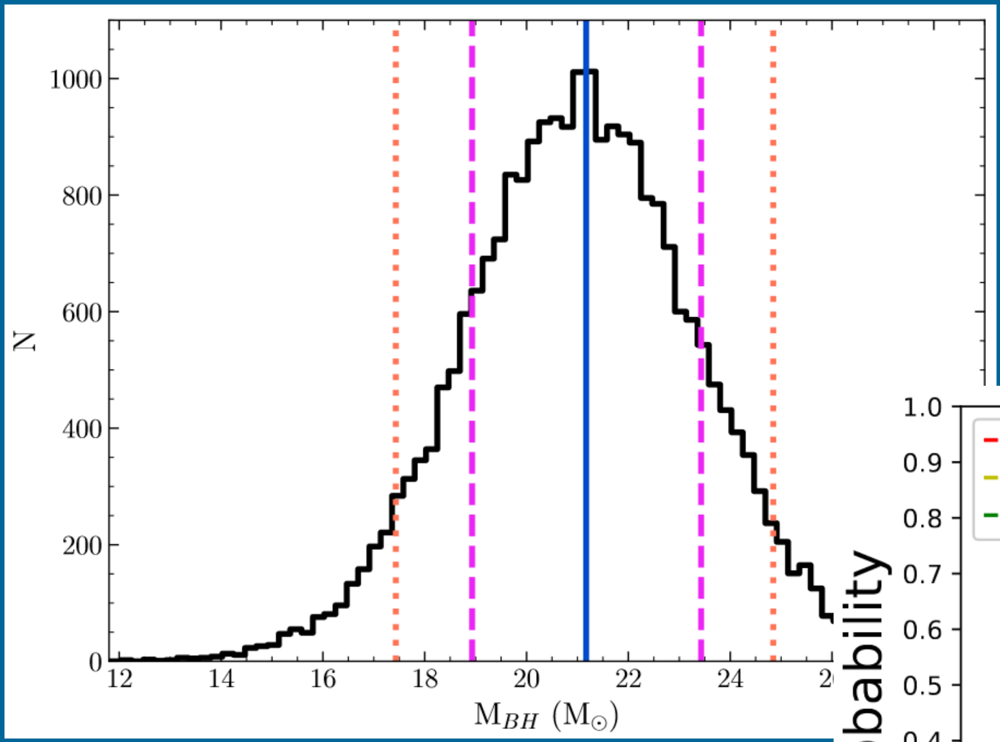

New distant measurements (VLBA)

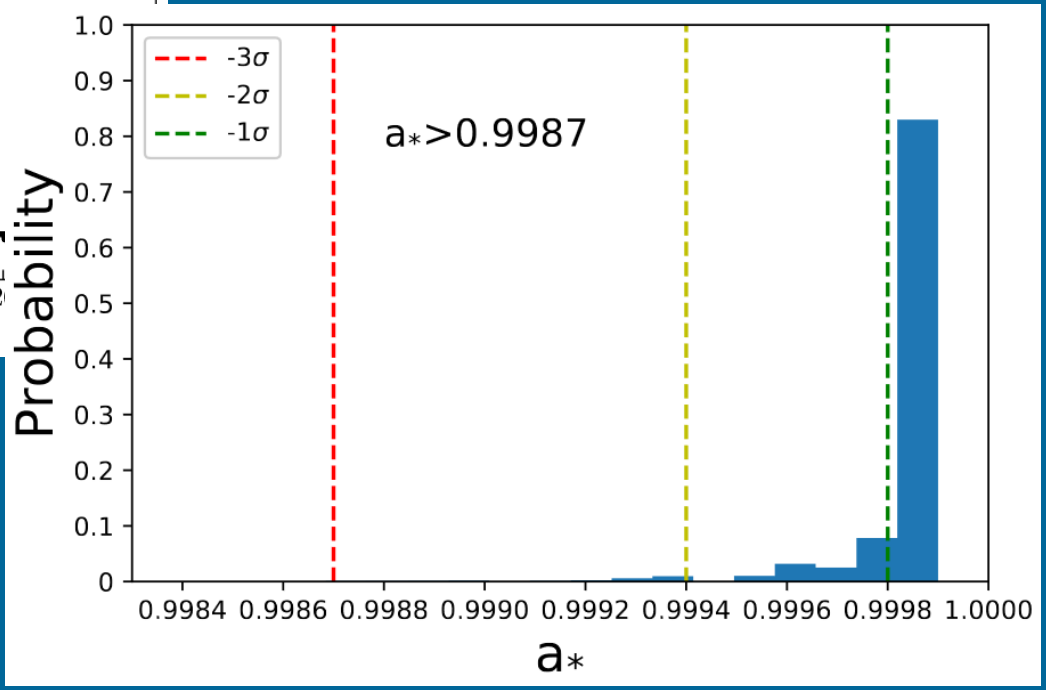

2102.09091-2102.09093

The first Be-BH binary: MWC 656

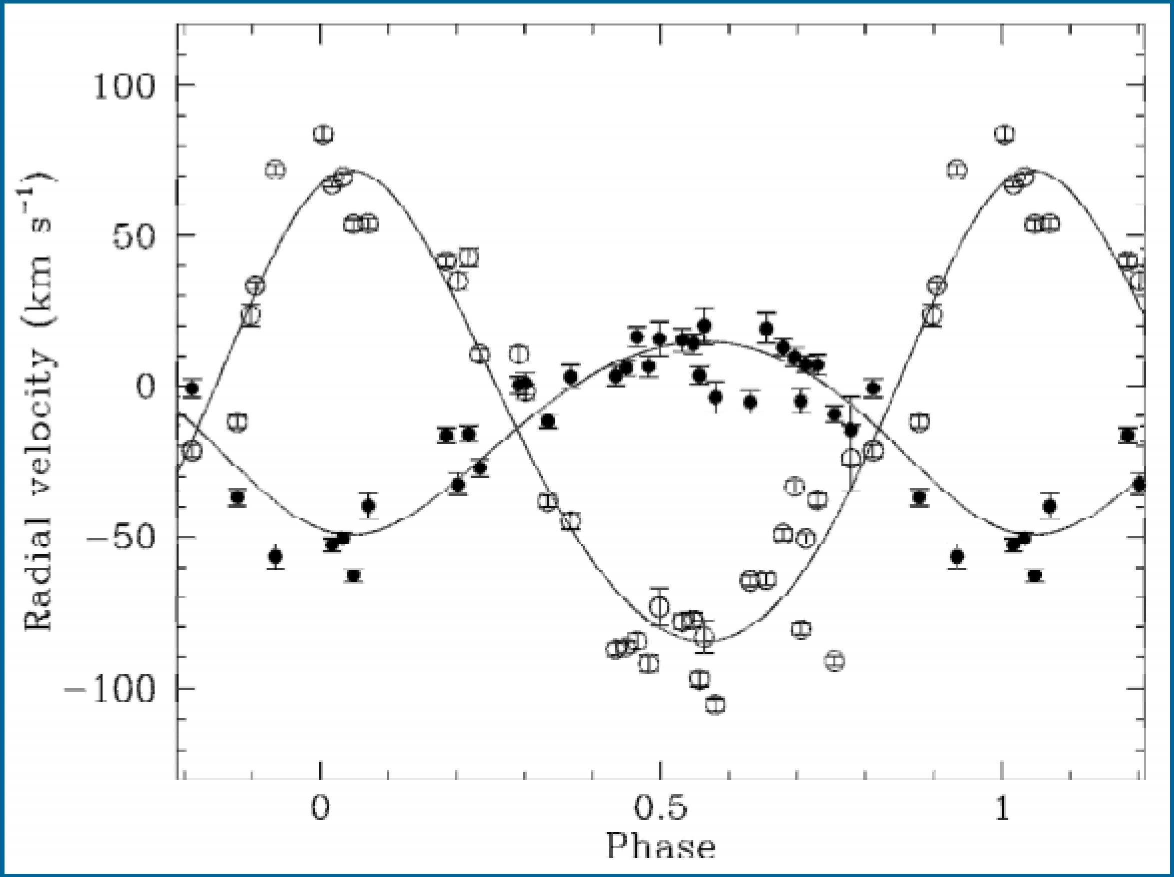

Compact object has a mass 3.8 – 6.9 Msolar.

X-ray luminosity is low

1401.3711

X-rays from MWC656

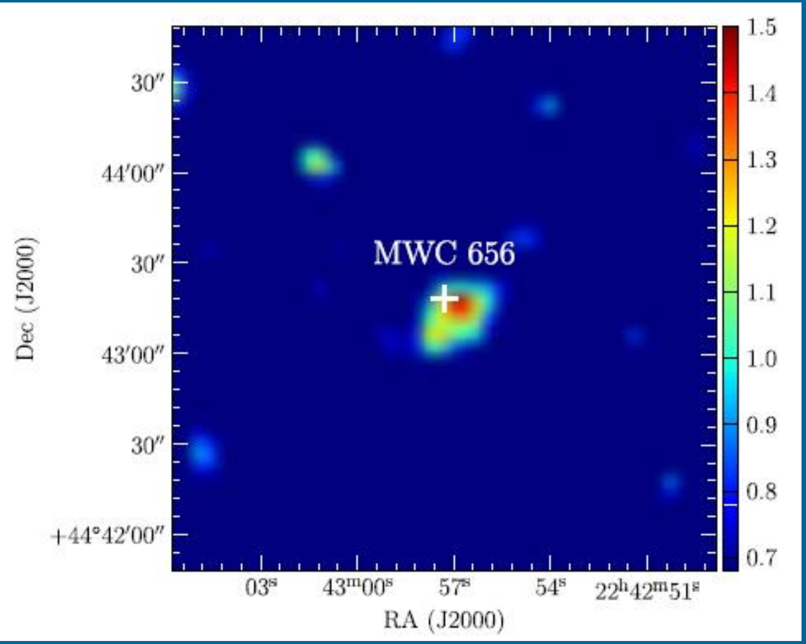

XMM-Newton

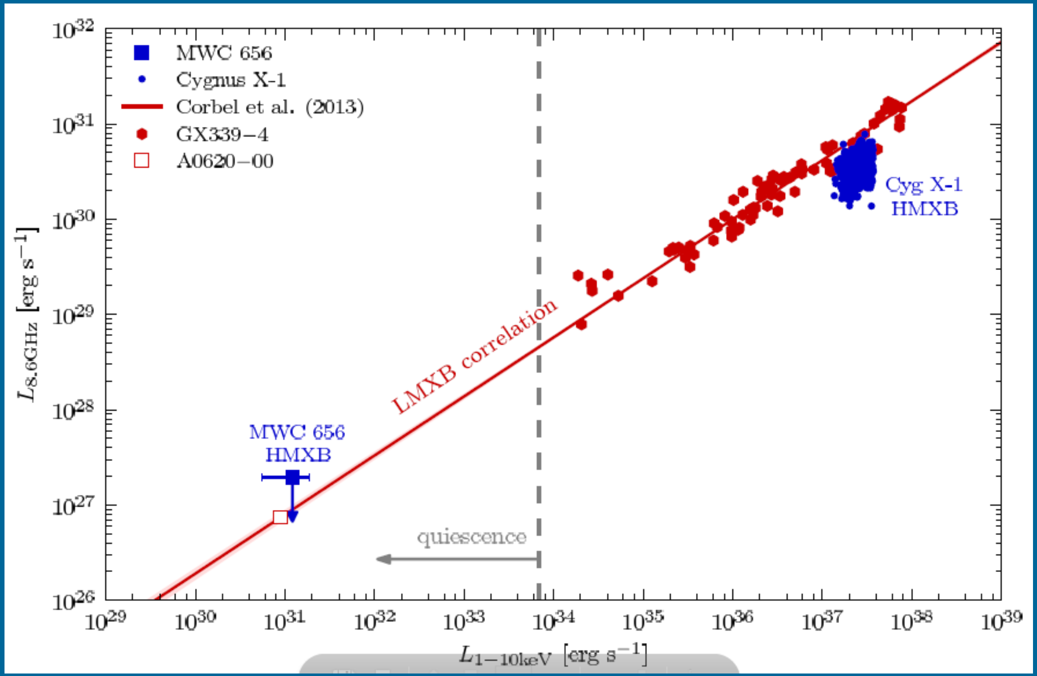

Became fainter since 2014.

1404.0901

BH/Be are fainter than NS/Be

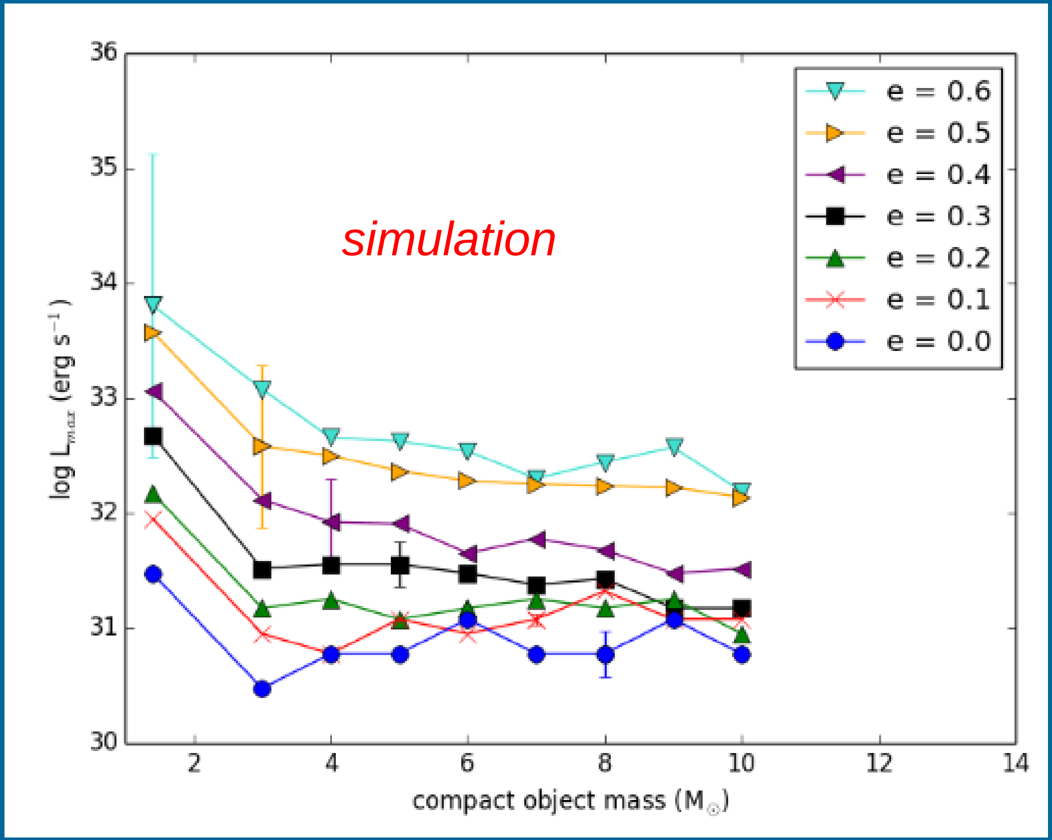

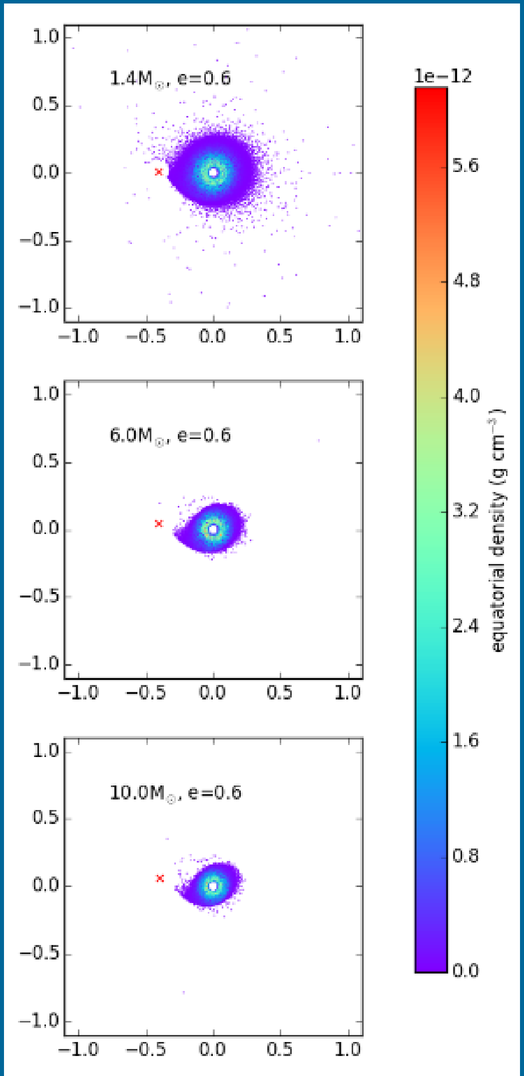

BH systems are fainter even for the same efficiency due to truncation of a disc around the Be-star.
Lower efficiency can help to
explain better why BH/Be systems are rarer than NS/Be.

1804.05749

Quescent luminosity vs. Orbital period

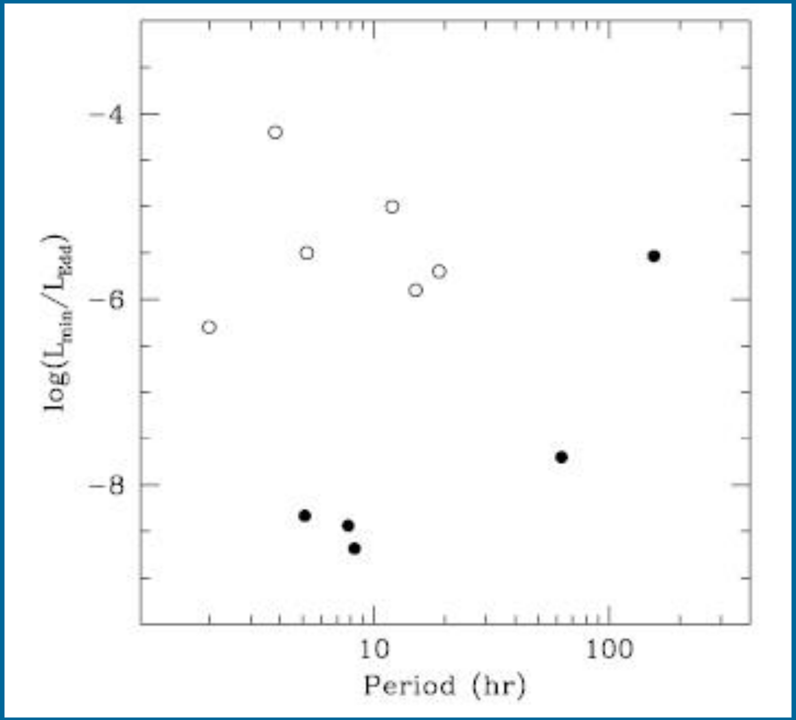

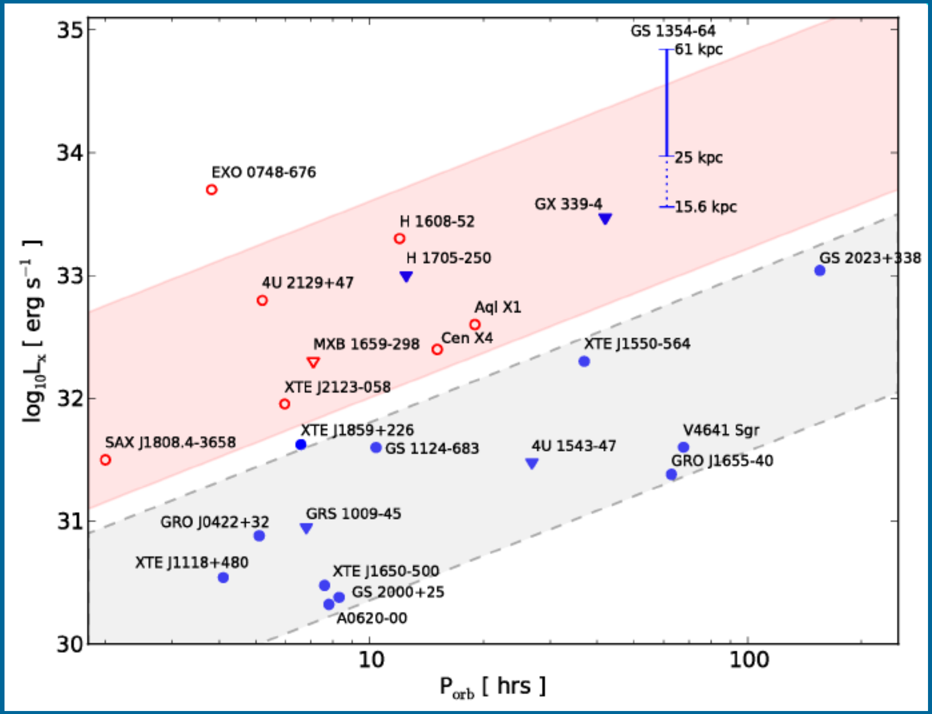

Open symbols – neutron stars
black symbols – black holes.

Red – NS systems.
Blue – BHs.
arXiv: 1105.0883

Garcia et al. 2001, see Psaltis astro-ph/0410536

Distance to V404 Cyg

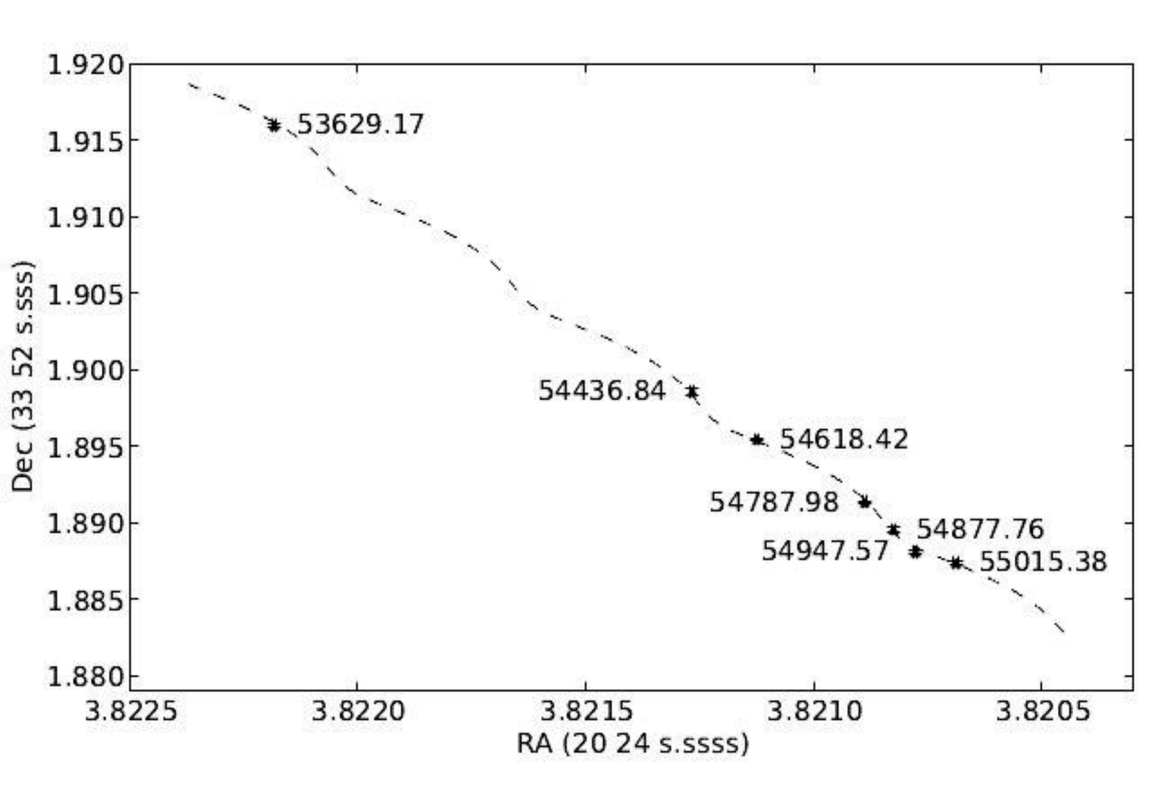

The parallax was measured.
The new distance estimate is 2.25-2.53 kpc.
It is smaller than before.
Correspondently,
flares luminosity is lower,
and so they are subEddington.

arXiv:0910.5253

Parallax is also measured for Cyg X-1 (arXiv:1106.3688)

V404 Cyg is a triple!

A known LMXB. M_{bh}~$9M_{sun}$
The inner binary ~0.14 au.
The third component at >3500 au.
As a wide binary survived,
the kick of the BH might be
very low. Plus, the mass loss
might be very small.

As the third star is evolved,
it is possible to estimate
the age of the system as
> (3-5) Gyrs.

Interaction with the third star
can also explain misalignment
between the jet and the
orbital spin axis.

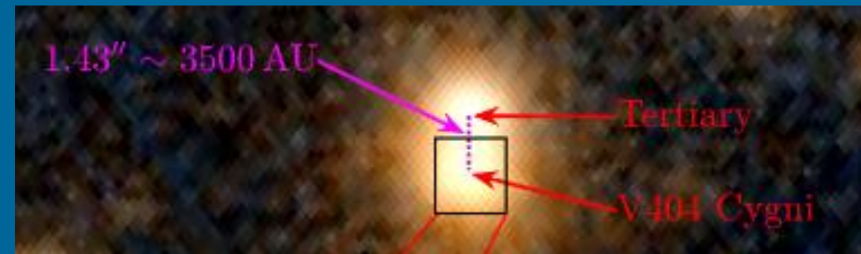

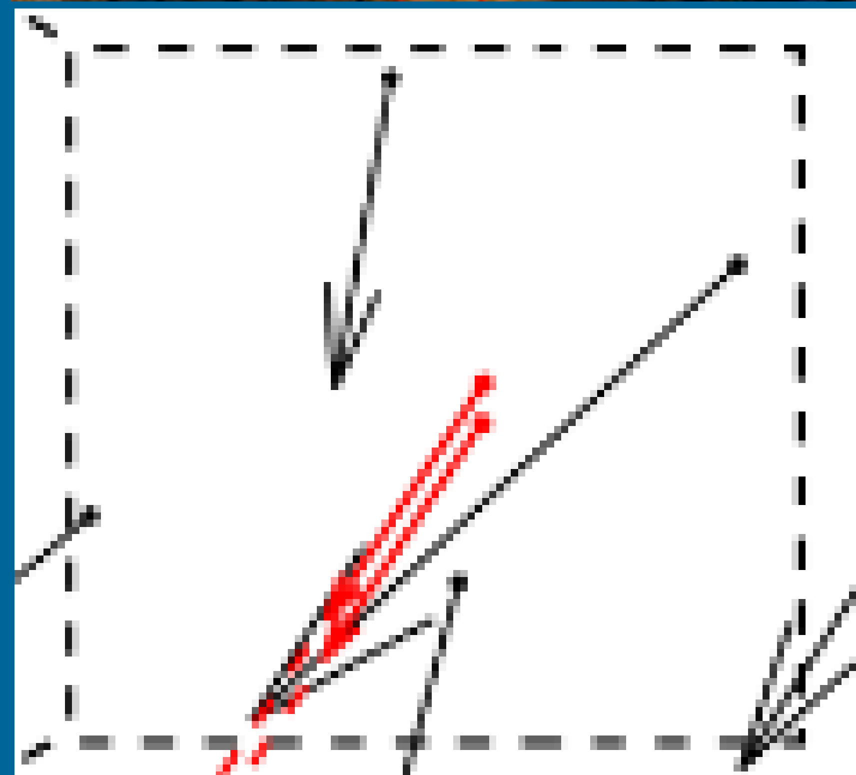

2404.03719

Mass determination

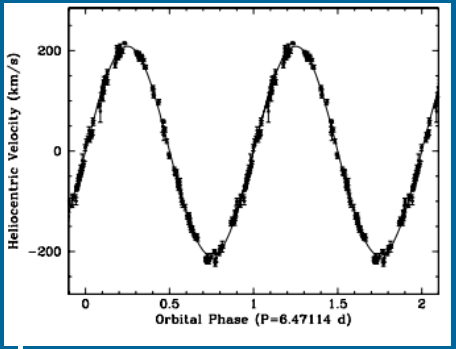

$$f_v(m)\frac{m_x^3 \sin i^3}{(m_x+m_v)^2} = 1,038\cdot 10^{-7} K_v^3 P (1-e^2)^{3/2}\,,$$

here m_x, m_v - masses of a compact object and of a normal (in solar units), K_v – observed semi-amplitude of the line of sight velocity of the normal star (in km/s), P – orbital period (in days), e – orbital eccentricity, i – orbital inclination (the angle between the line of sight and the normal to the orbital plane).

As one can see, the mass function of the normal star is the absolute lower limit for the mass of the compact object.

The mass of the compact object can be calculated as:

$$m_x = f_v(m)\left(1+\frac{m_v}{m_x}\right)^2 \frac{1}{\sin i^3}\,.$$

So, to derive the mass of the compact object in addition to the line of sight velocity it is necessary to know independently two more parameters: the mass ratio $q=m_x/m_v$, and the orbital inclination i.

Mass estimates for BHs (including IMBHs) are well reviewed recently in 1311.5118

Black hole masses

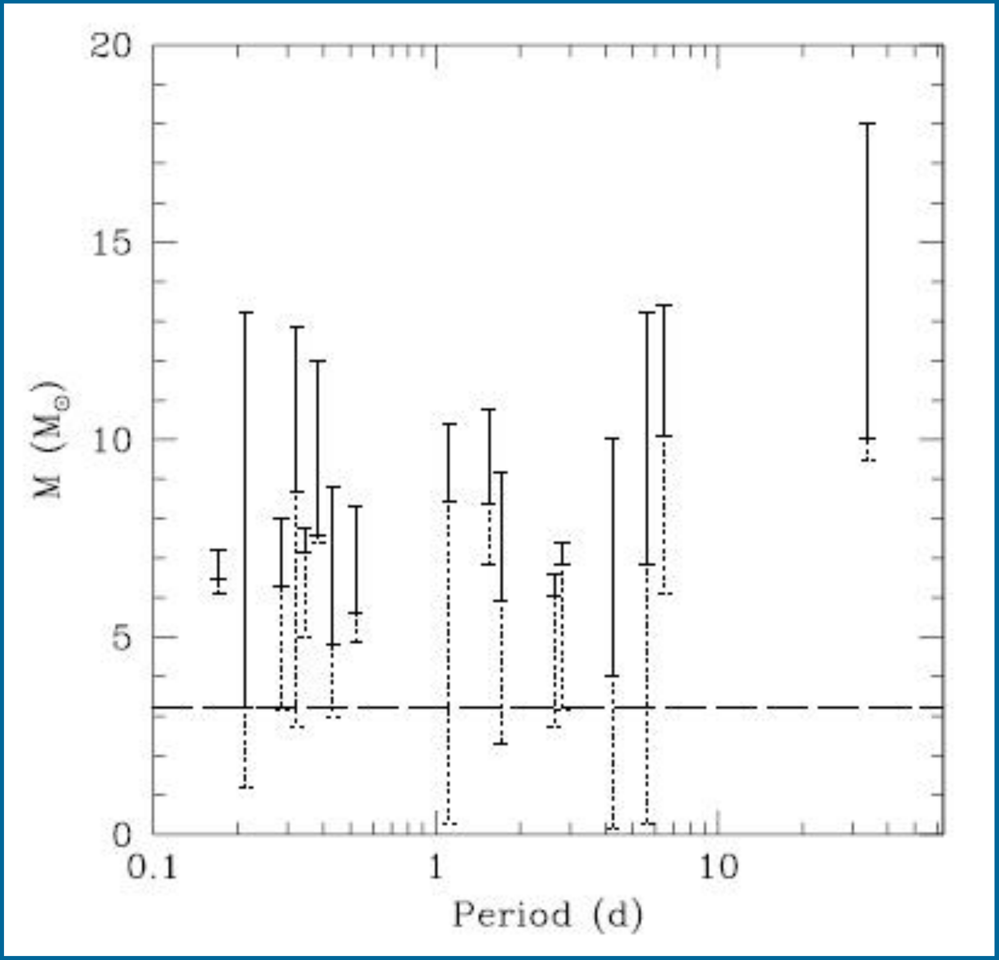

The horizontal line corresponds to the mass equal to 3.2 solar.

New technics are used to determine BH masses in binaries.
For example, reverberation mapping was used for Cyg X-1 (1906.08266).
The result (16+/-5 Msun)
is compatible with dynamical measurements.

Orosz 2002, see also Psaltis astro-ph/0410536

Some more results on masses

Paredes
arXiv: 0907.3602

System	$P_{\rm orb}$ [days]	$f(M)$ [$M_\odot$]	Donor Spect. Type	Classification	M_x [$M_\odot$]
GRS 1915+105	33.5	9.5 ± 3.0	K/M III	LMXB/Transient	14 ± 4
V404 Cyg	6.471	6.09 ± 0.04	K0 IV	”	12 ± 2
Cyg X-1	5.600	0.244 ± 0.005	09.7 Iab	HMXB/Persistent	10 ± 3
M33 X-7[a]	3.453	–	O7 III	–	15.65 ± 1.45
LMC X-1	4.229	0.14 ± 0.05	07 III	”	> 4
XTE J1819-254	2.816	3.13 ± 0.13	B9 III	IMXB/Transient	7.1 ± 0.3
GRO J1655-40	2.620	2.73 ± 0.09	F3/5 IV	”	6.3 ± 0.3
BW Cir	2.545	5.74 ± 0.29	G5 IV	LMXB/Transient	> 7.8
GX 339-4	1.754	5.8 ± 0.5	–	”	–
LMC X-3	1.704	2.3 ± 0.3	B3 V	HMXB/Persistent	7.6 ± 1.3
XTE J1550-564	1.542	6.86 ± 0.71	G8/K8 IV	LMXB/Transient	9.6 ± 1.2
IC 10 X-1[b]	1.455	7.64 ± 1.26	–	Wolf-Rayet	32.7 ± 2.6
4U 1543-475	1.125	0.25 ± 0.01	A2 V	IMXB/Transient	9.4 ± 1.0
H1705-250	0.520	4.86 ± 0.13	K3/7 V	LMXB/Transient	6 ± 2
GS 1124-684	0.433	3.01 ± 0.15	K3/5 V	”	7.0 ± 0.6
XTE J1859+226	0.382	7.4 ± 1.1	–	”	–
GS2000+250	0.345	5.01 ± 0.12	K3/7 V	”	7.5 ± 0.3
A0620-003	0.325	2.72 ± 0.06	K4 V	”	11 ± 2
XTE J1650-500	0.321	2.73 ± 0.56	K4 V	”	–
GRS 1009-45	0.283	3.17 ± 0.12	K7/M0 V	”	5.2 ± 0.6
GRO J0422+32	0.212	1.19 ± 0.02	M2 V	”	4 ± 1
XTE J1118+480	0.171	6.3 ± 0.2	K5/M0 V	”	6.8 ± 0.4

M33 X-7 15.65+/-1.45 M_{solar} (Orosz et al. 2007).
Eclipsing binary IC10 X-1 32+/- 2.6 (Silverman and Filippenko 2008)

Systems BH + radio pulsar: a Holy Grail

The discovery of a BH in pair with a radio pulsar can provide the most direct proof of the very existence of BHs.
Especially, it would be great to find a system with a millisecond pulsar observed close to the orbital plane.
Computer models provide different estimates of the abundance of such systems.

Lipunov et al (1994) give an estimate about one system (with a PSR of any type) per 1000 isolated PSRs.

Pfahl et al. (astro-ph/0502122) give much lower estimate for systems BH+mPSR: about 0.1-1% of the number of binary NSs.
This is understandable, as a BH should be born by the secondary (i.e. initially less massive) component of a binary system.

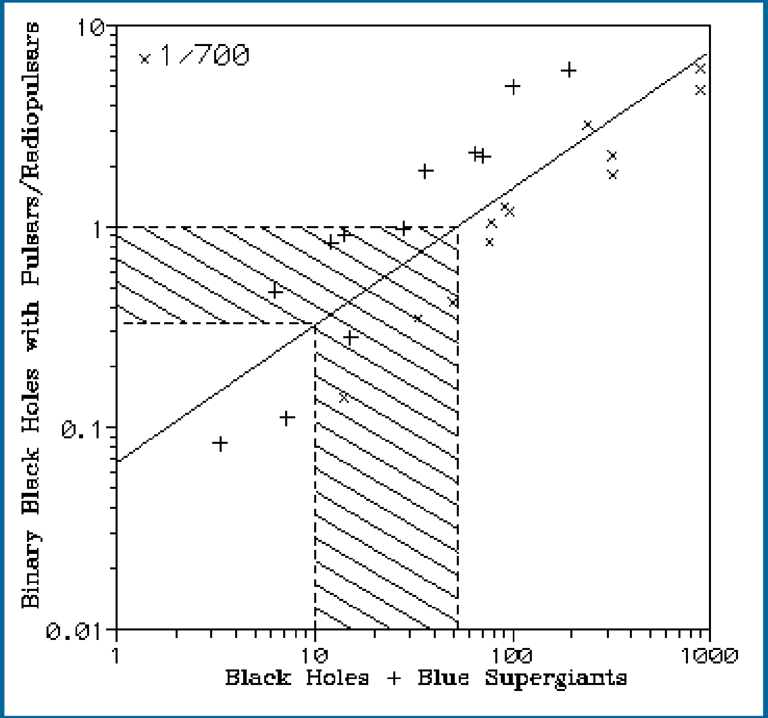

What can be done with such systems if they are detected by SKA was studied in 1409.3882. Mainly related to gravity tests.

BH+pulsar binaries and FAST

Birth rate of NS+BH binaries ~0.6-13 Myr^{-1}
Thus, ~10^4 -10^5 in the Galaxy.
Difficult to have a msecPSR.
Thus, typical spin periods ~1 s.
3-80 BH+PSR binaries.
~10% of them can be detected by FAST.

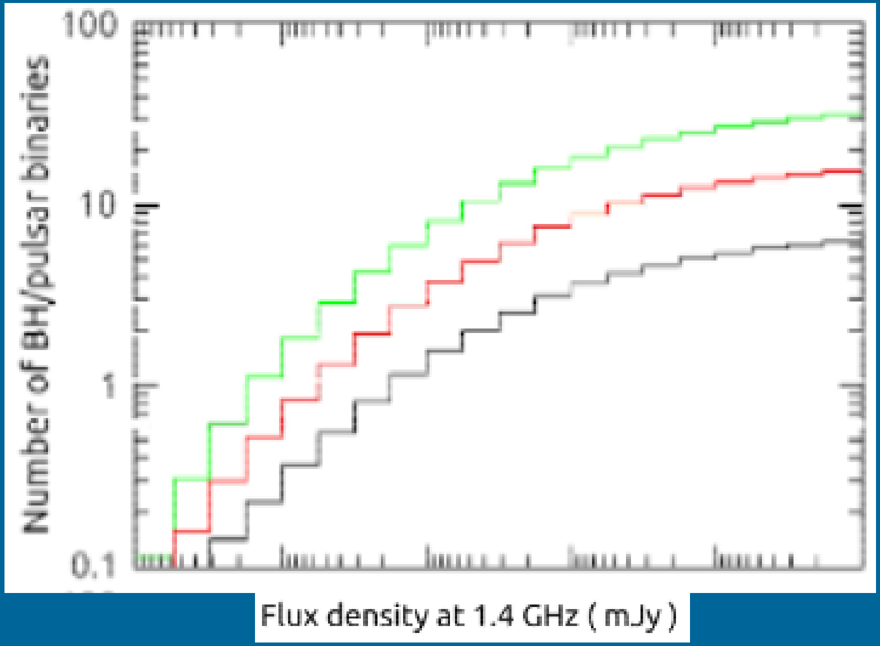

σ_{NS_kick} = 150 km/s

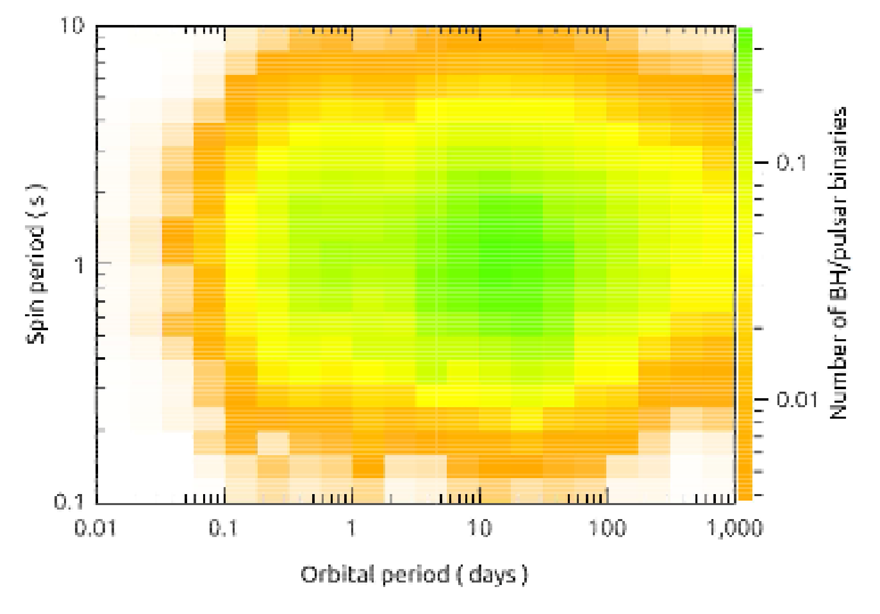

1804.06014

New estimates of BH+PSR systems

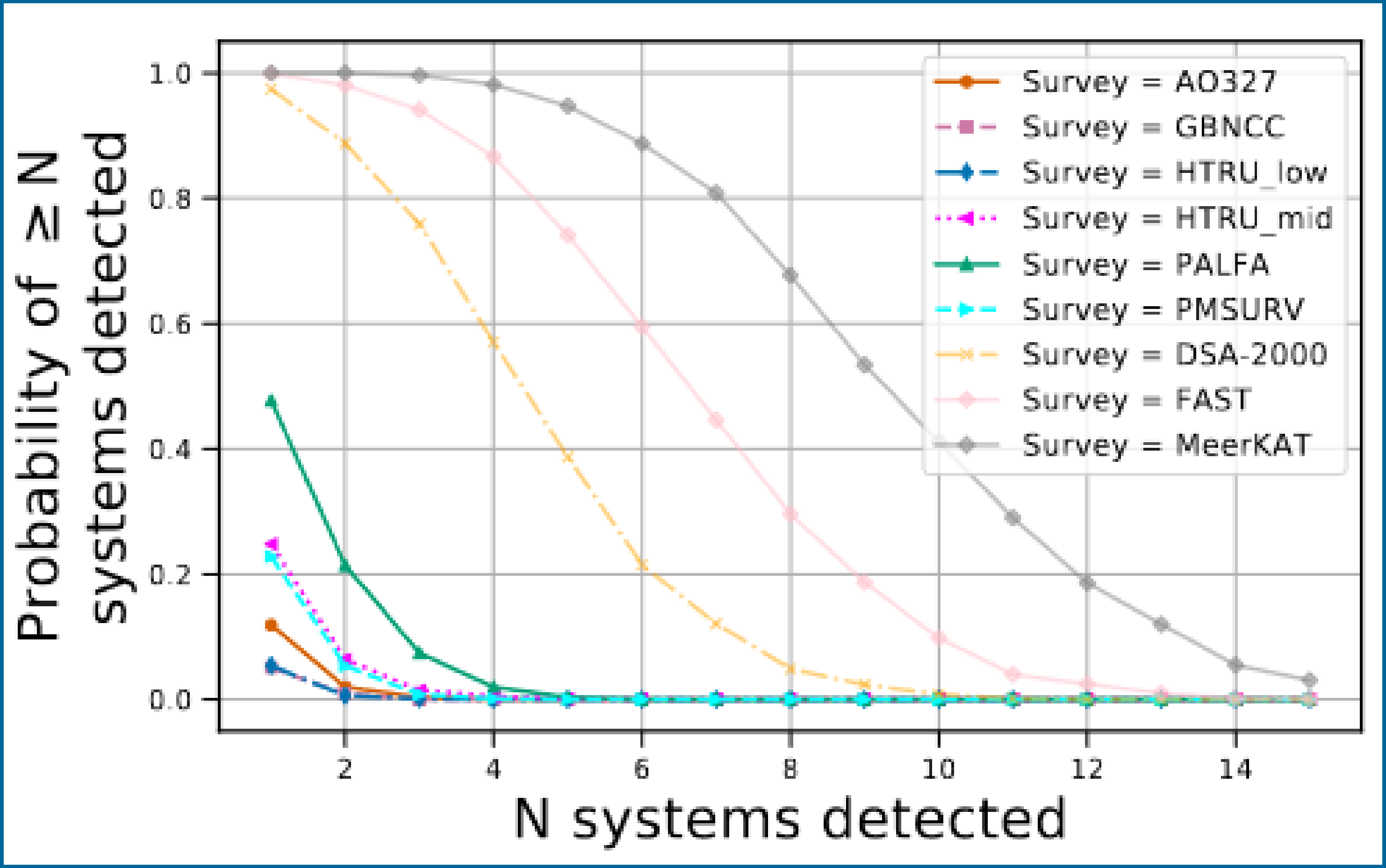

<10 detectable systems in the Galaxy are expected.
New survey might discover at least one with ~100% probability.

2109.04512

Population synthesis of PSR+BH binaries

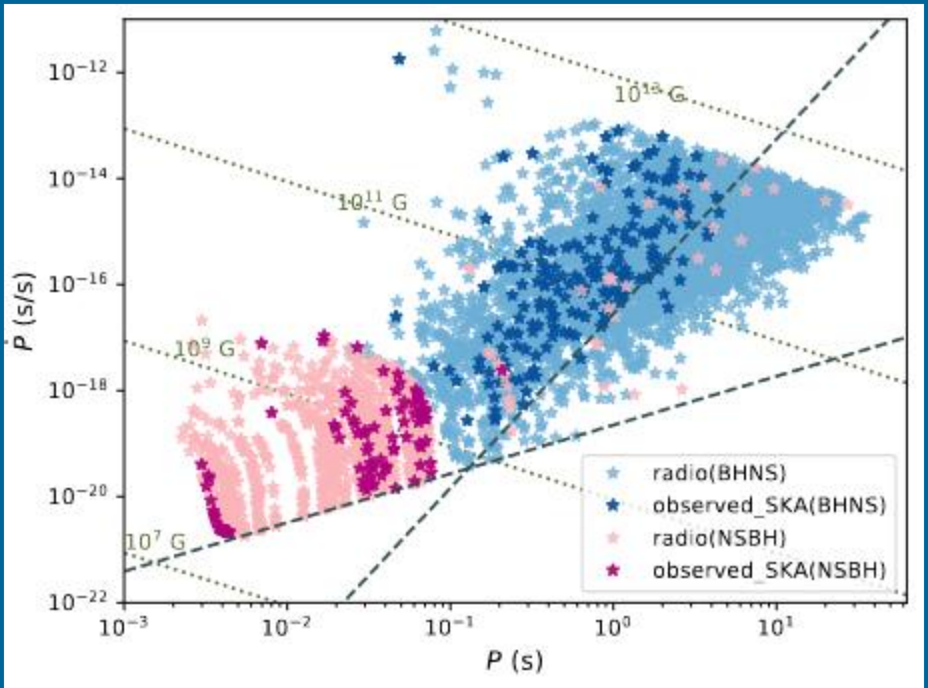

Normalized to 10 Milky Ways

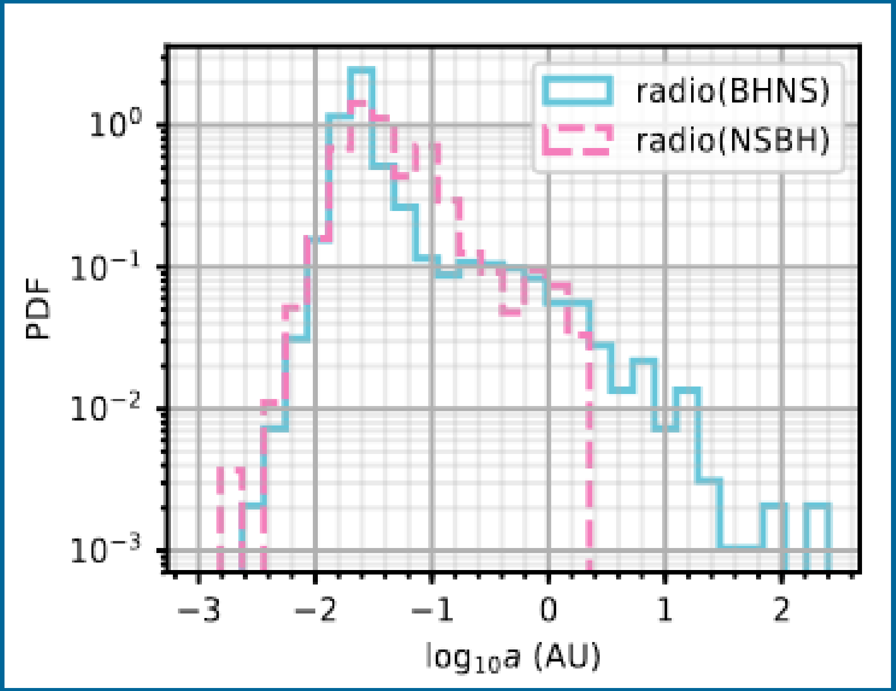

2011.13503

The first candidate?

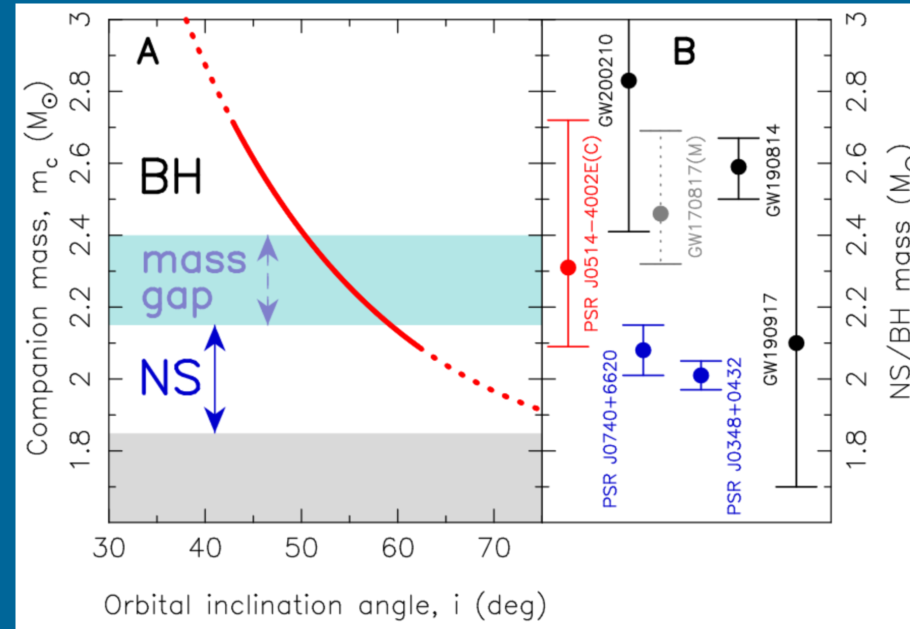

PSR J0514−4002E

Total binary mass 3.9 M_{sun}

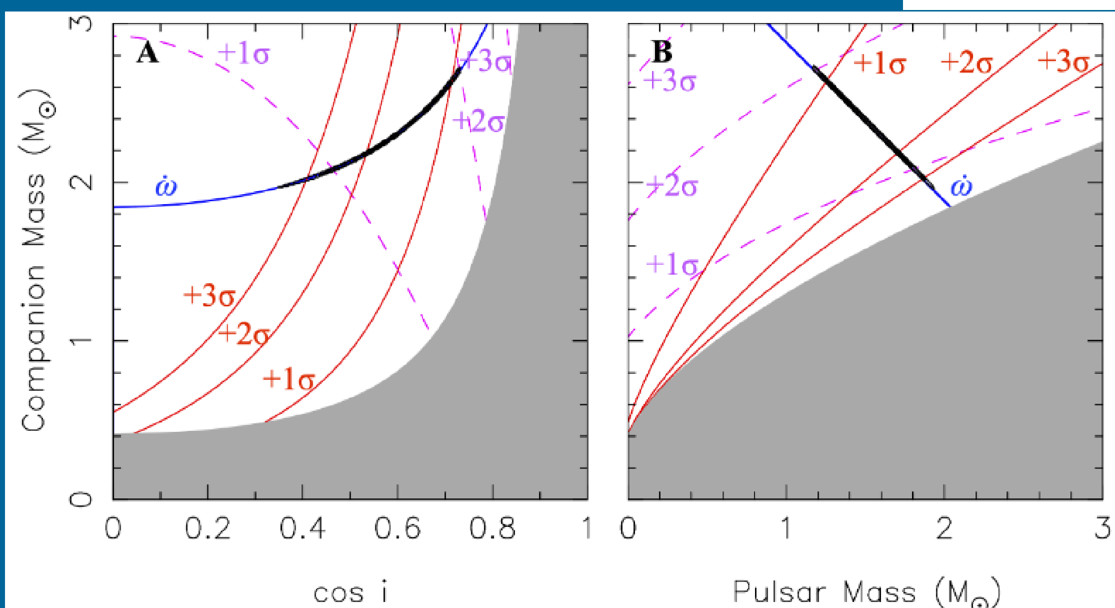

MeerKAT observations

P~5 msec

P_{orb}~7.4 d

e~0.7

2401.09872

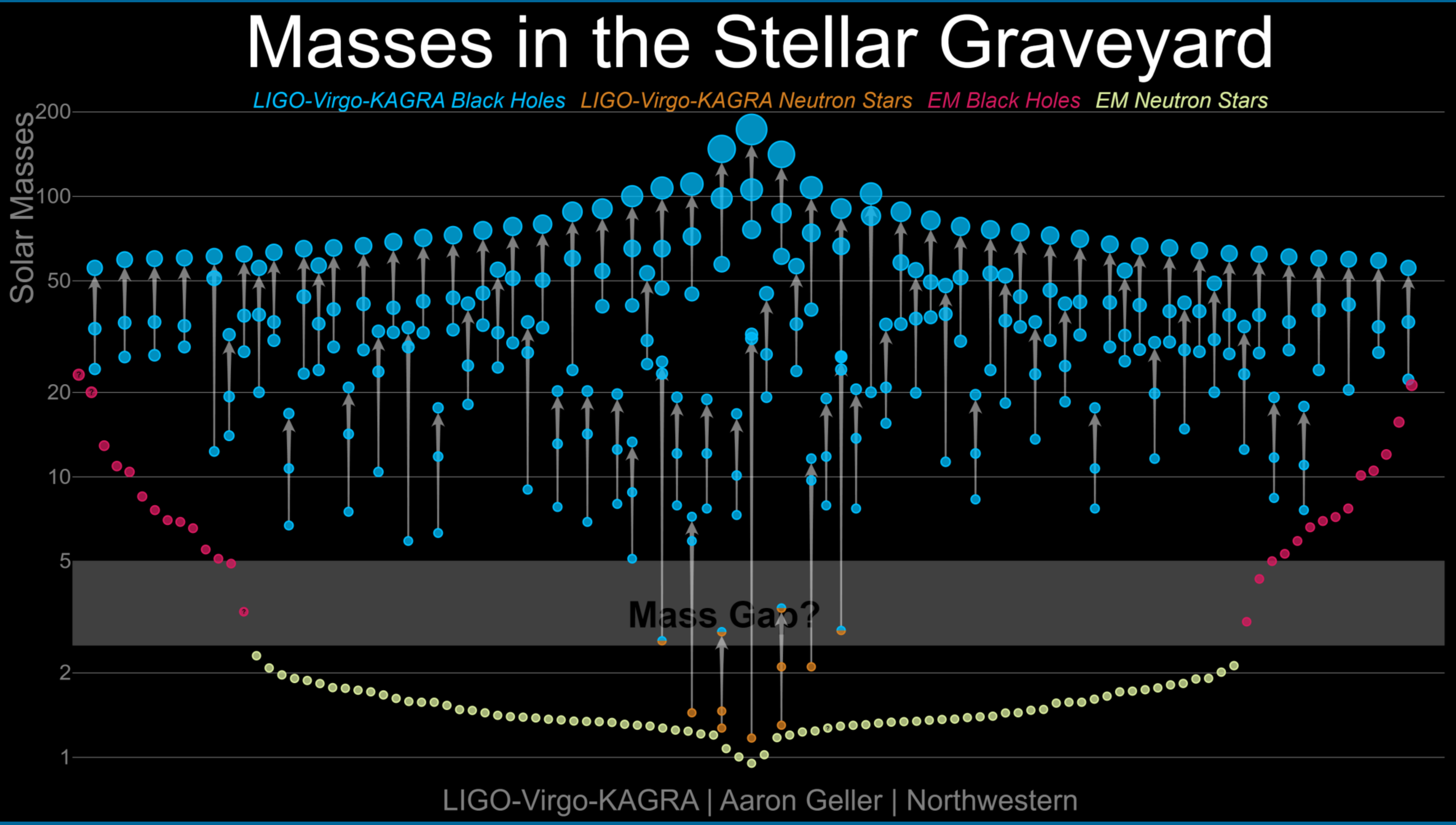

Masses in the Stellar Graveyard
LIGO-Virgo-KAGRA Black Holes
LIGO-Virgo-KAGRA Neutron Stars
EM Black Holes
EM Neutron Stars
Solar Masses
200
100
50
20
10
5
2
1
Mass Gap?
LIGO-Virgo-KAGRA | Aaron Geller | Northwestern

Jet from GRS 1915+105

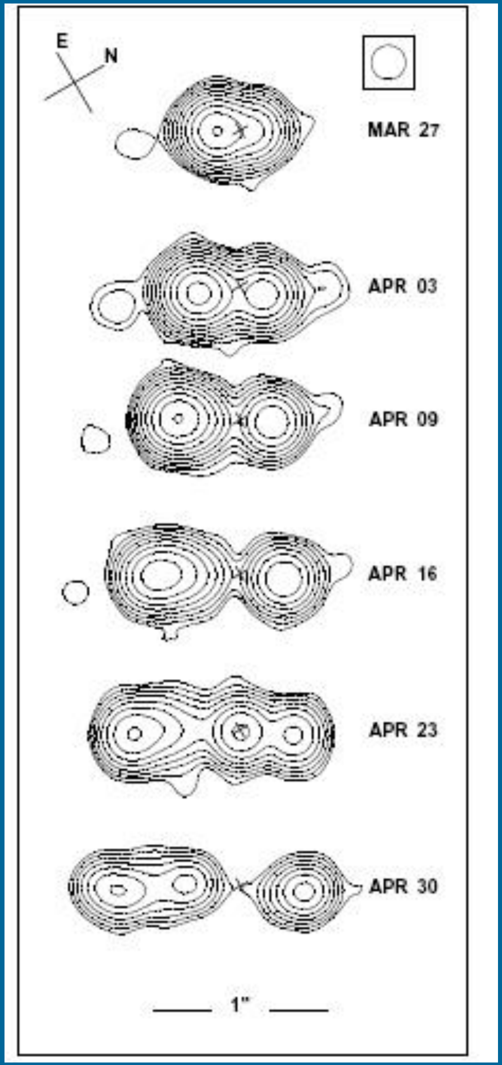

VLA data. Wavelength 3.5 cm.

Mirabel, Rodrigez 1994, see Psaltis astro-ph/0410536

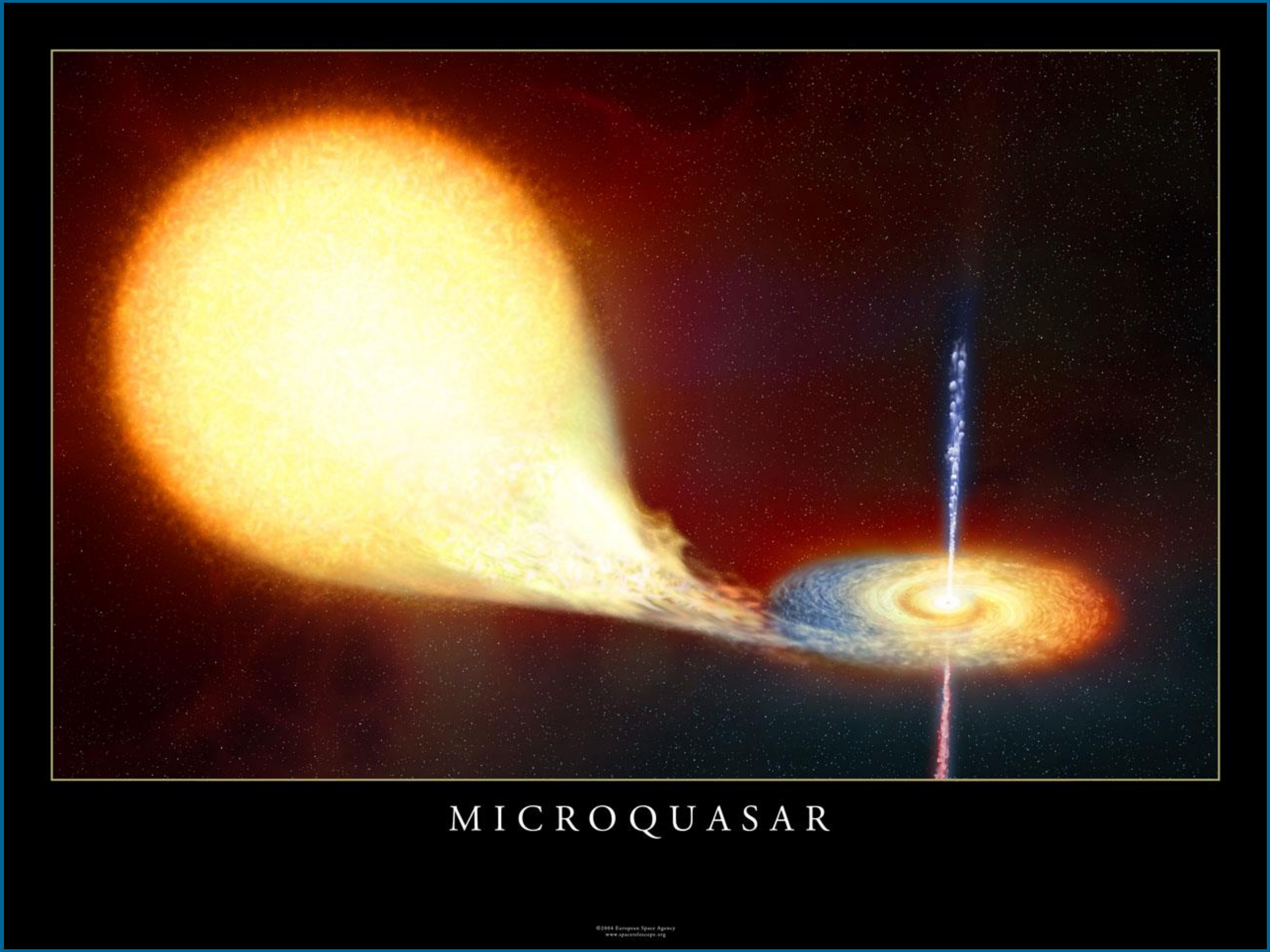

See a brief review in 1106.2059

$T \sim 10^7$ K $M^{-1/4}$ – last stable orbit temperature at Eddington luminosity

Optics/UV – QSO
X-ray - μQSO

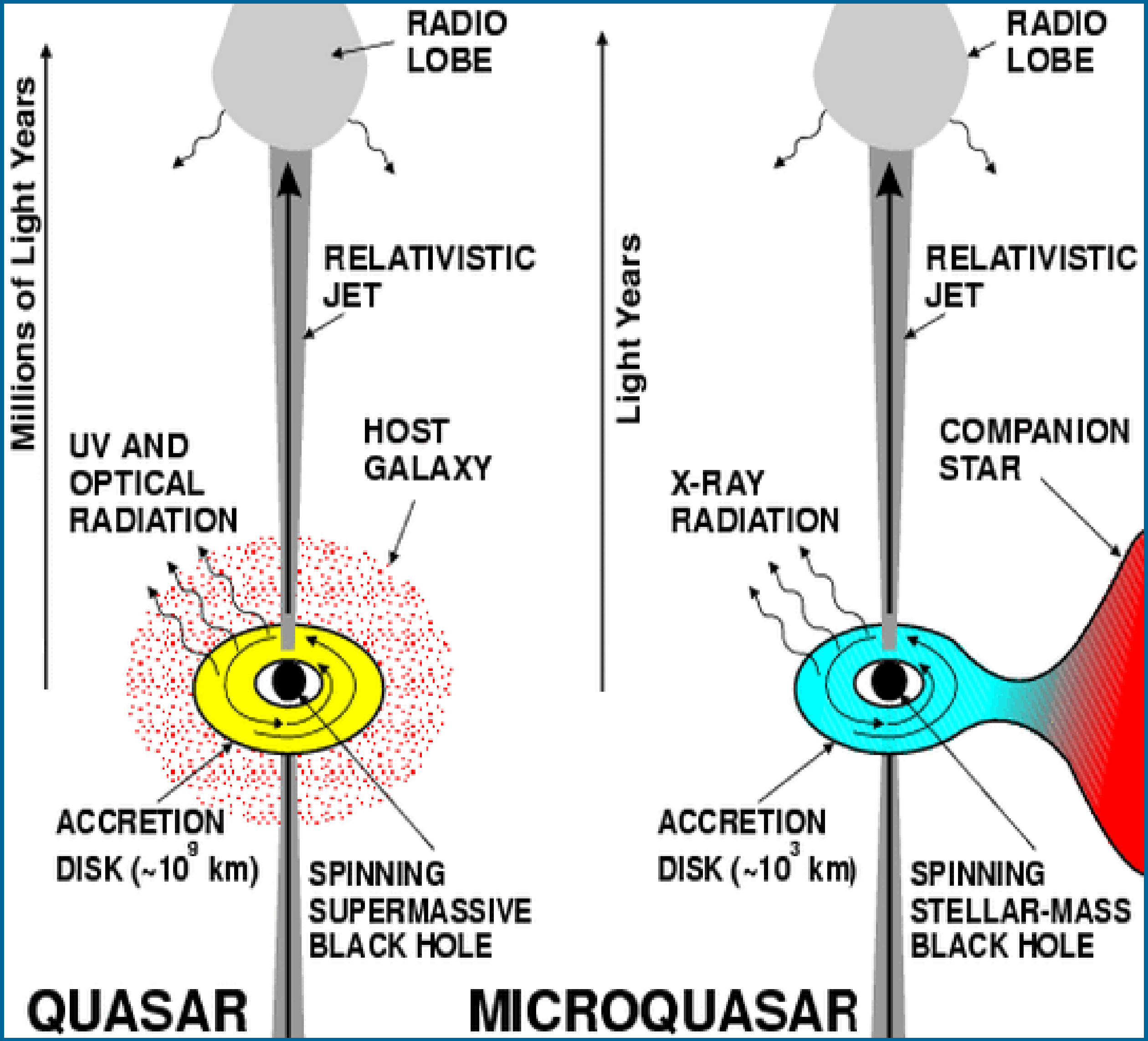

Jet-luminosity relation

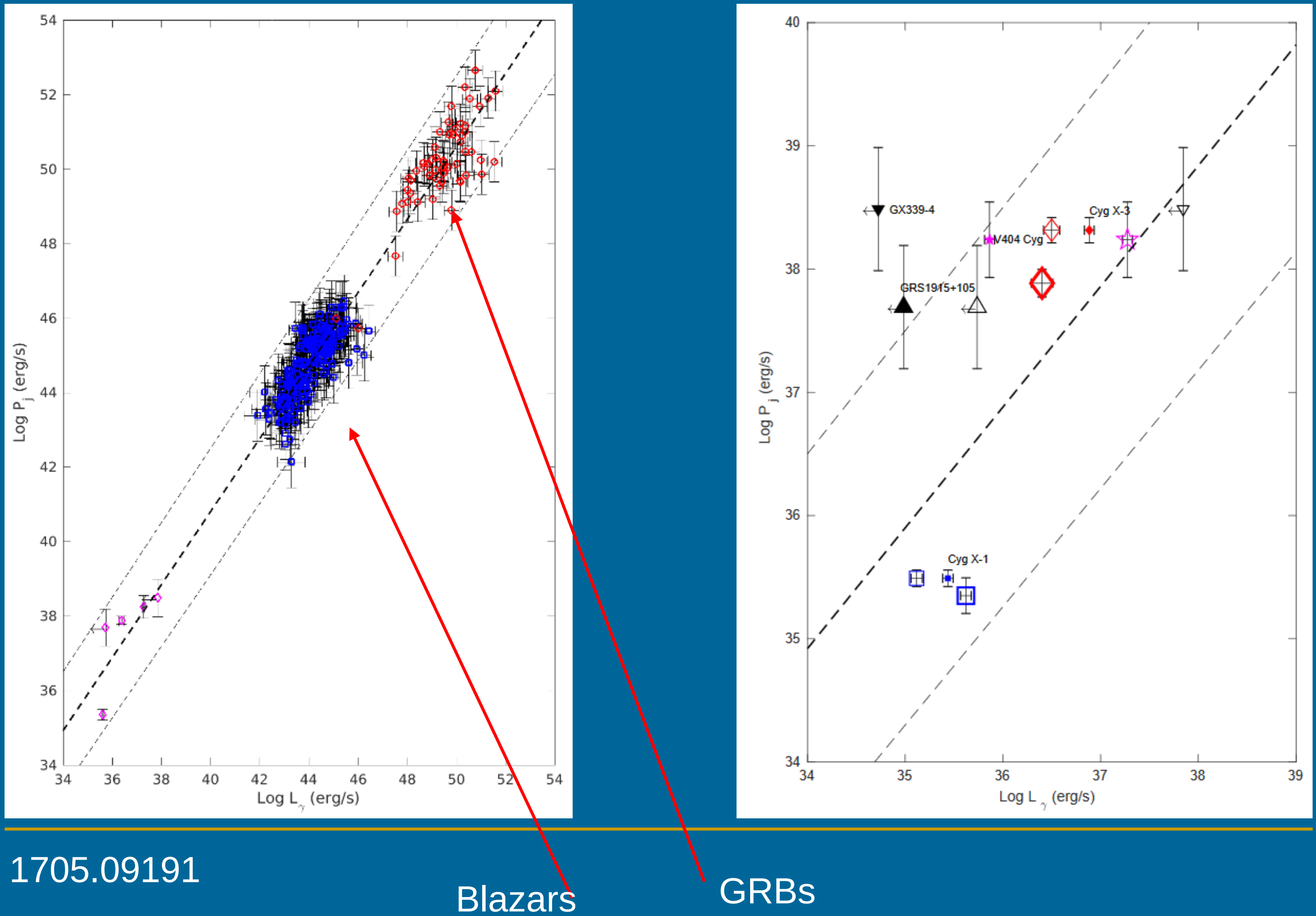

1705.09191

Large jet in Swift J1727.8-1613

BH LMXB.

Jet was observed during an outburst.

Jet length >100 au.

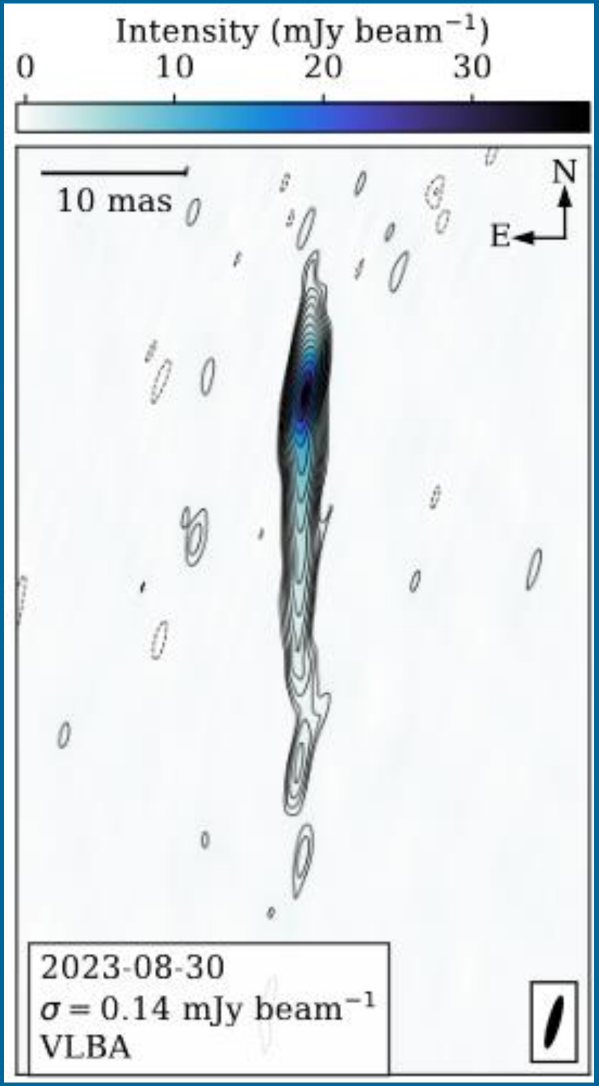

2405.12370

Jets behaviour in BH binaries

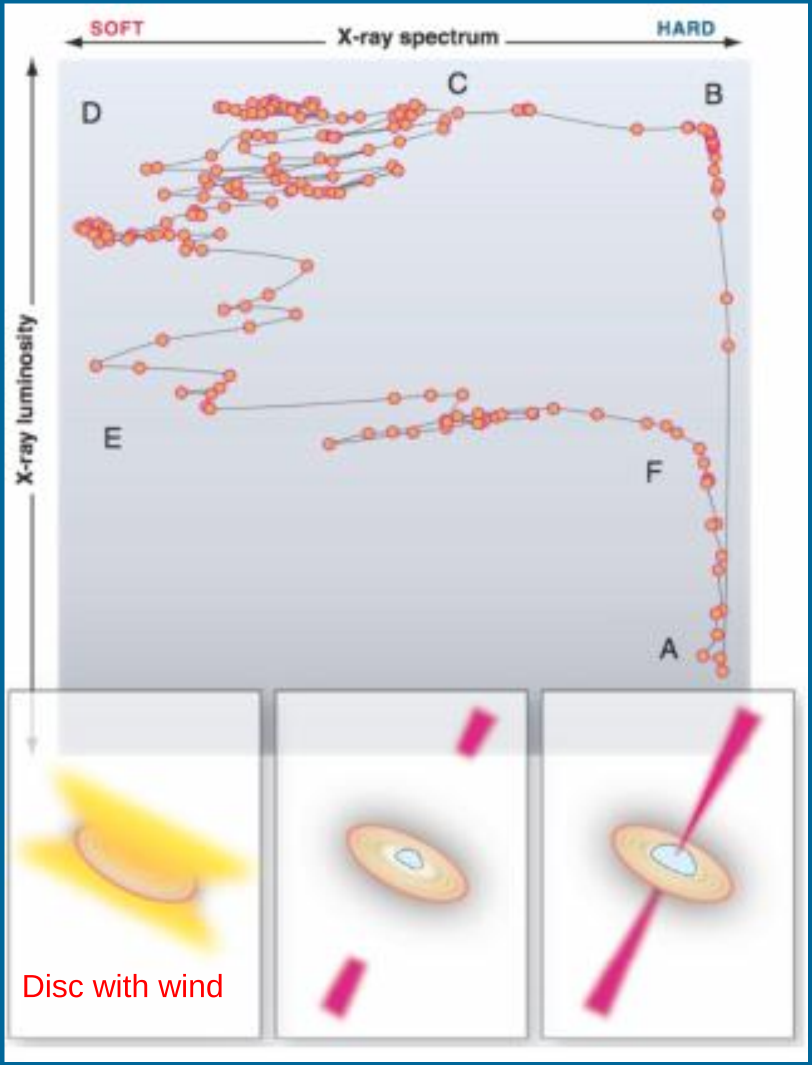

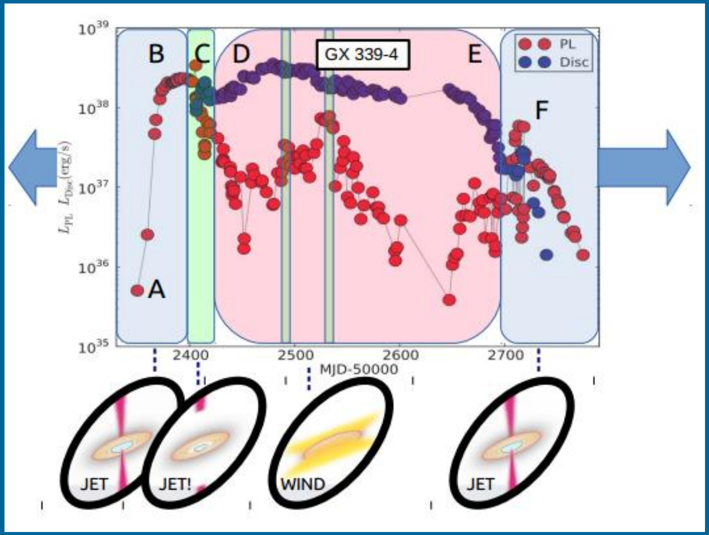

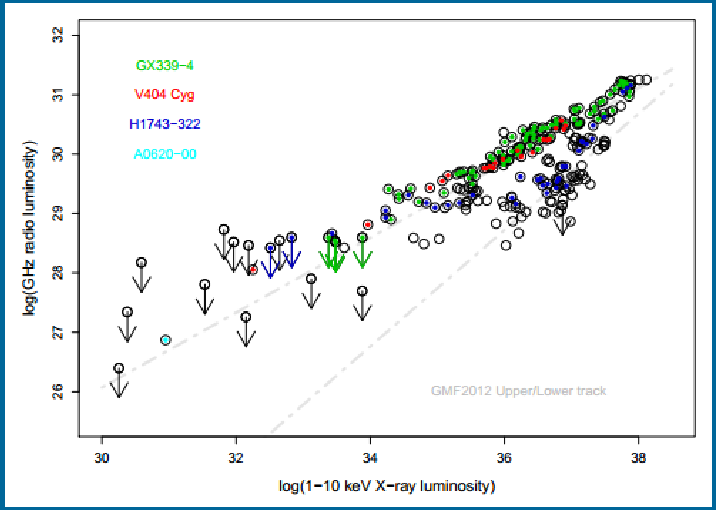

A large review can be found in 1407.3674

States (luminosity+spectrum+jet+variability)

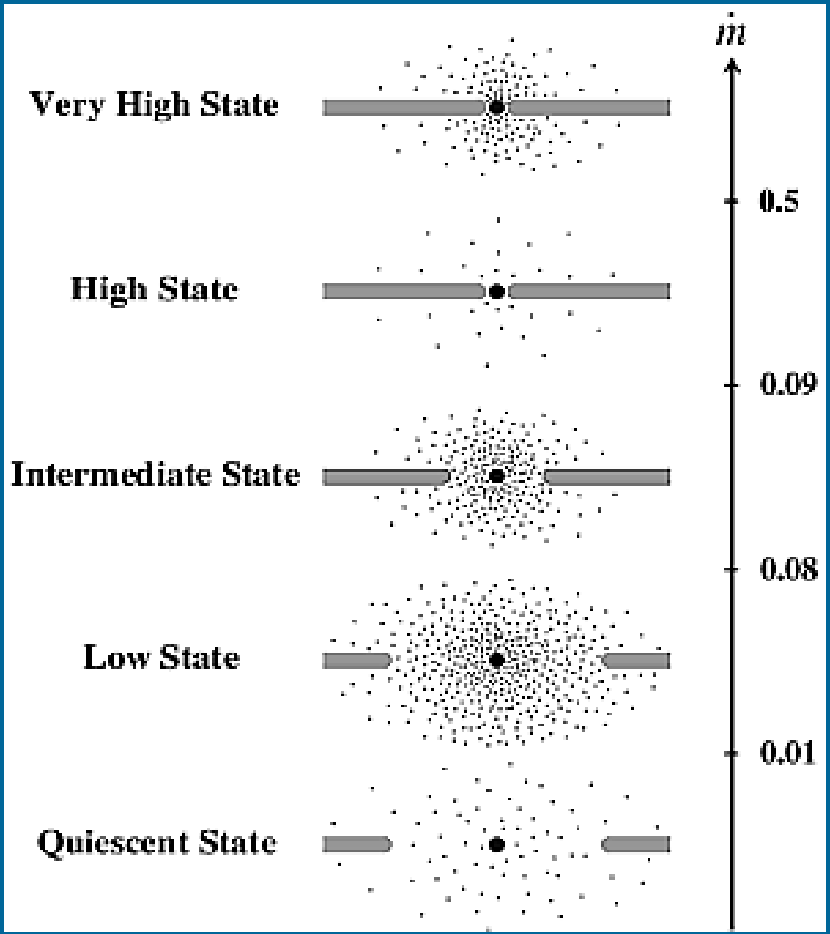

The understanding that BH binaries can pass through different “states” (characterized by luminosity, spectrum, and other features, like radio emission) appeared in 1972 when Cyg X-1 suddenly showed a drop in soft X-ray flux, rise in hard X-ray flux, and the radio source was turned on.

Now there are several classifications of states of BH binaries.

astro-ph/0306213 McClintock, Remillard
Black holes on binary systems

Accretion onto BHs was reviewed in details in 1304.4879

Spectra of BH candidates

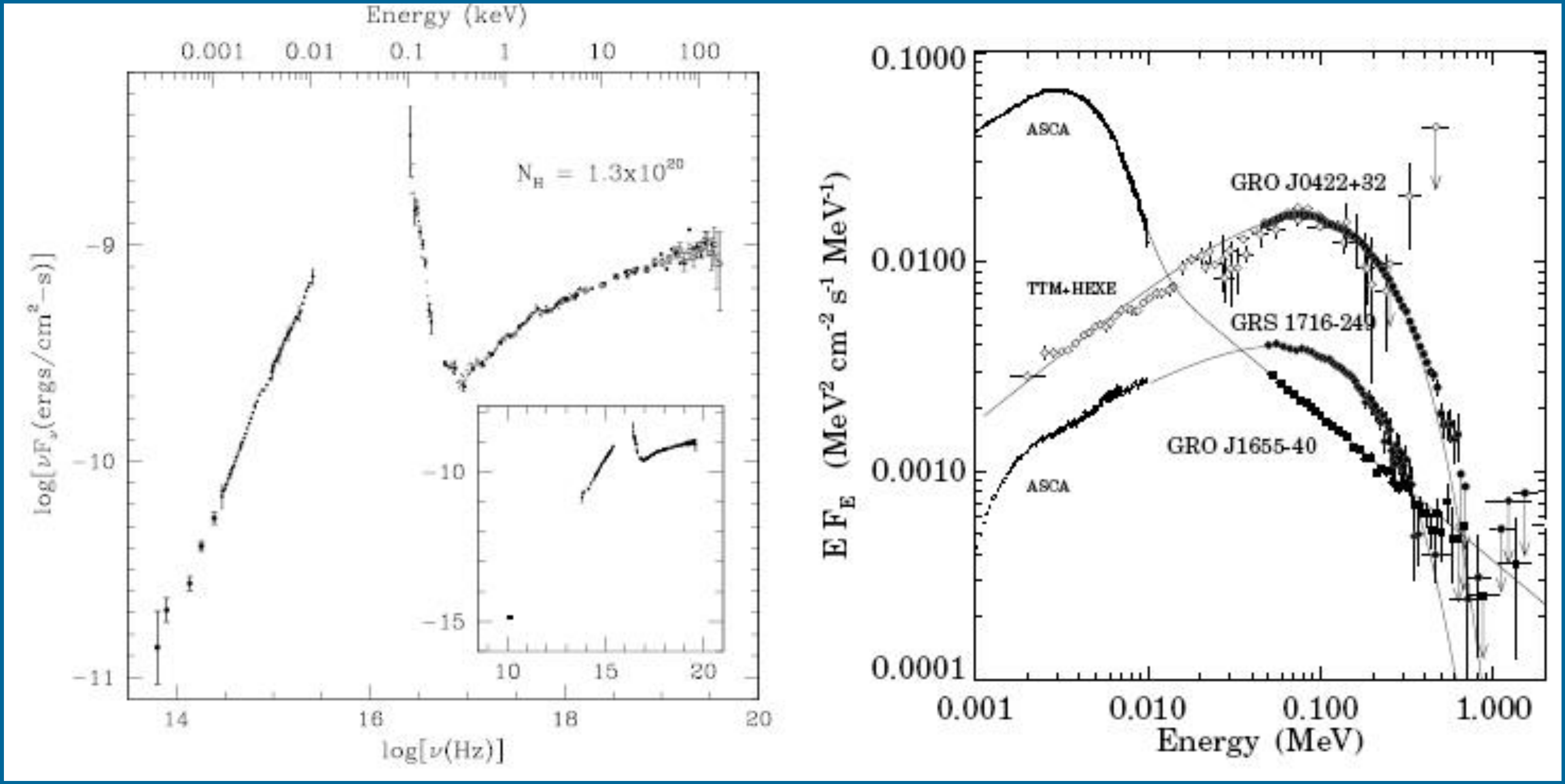

(Psaltis astro-ph/0410536)

Different components of a BH spectrum

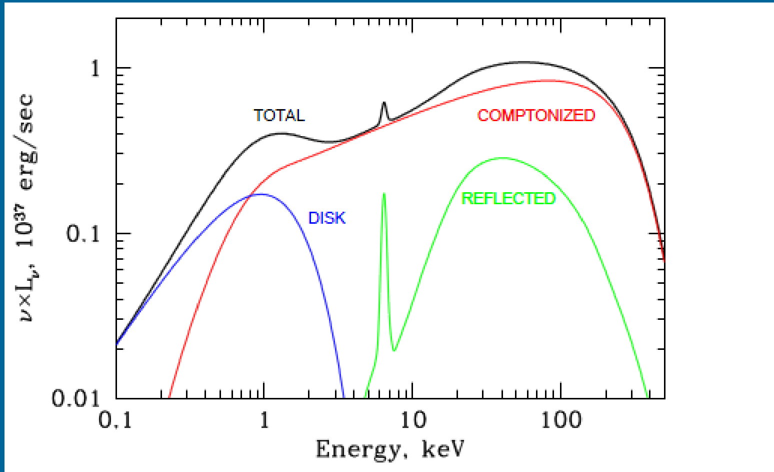

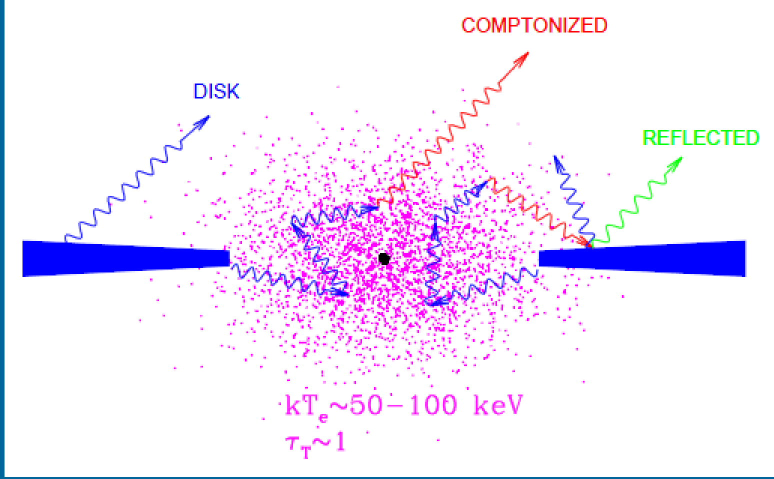

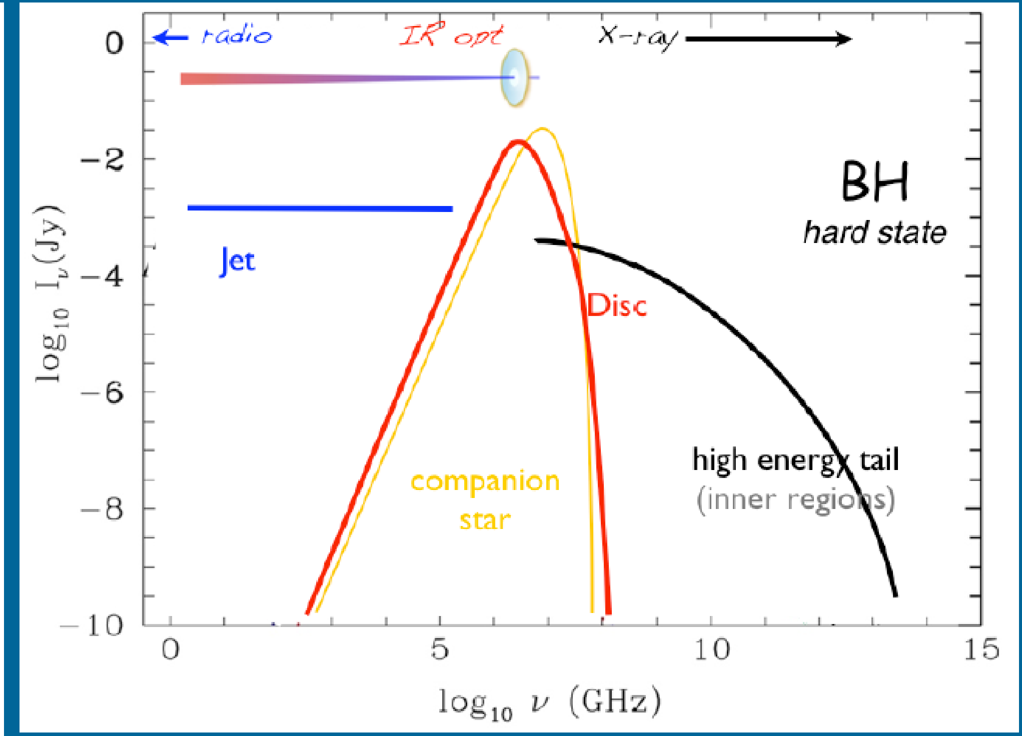

1104.0097

Accretion geometry and photon paths at the hard state

0909.2567

Three-state classification

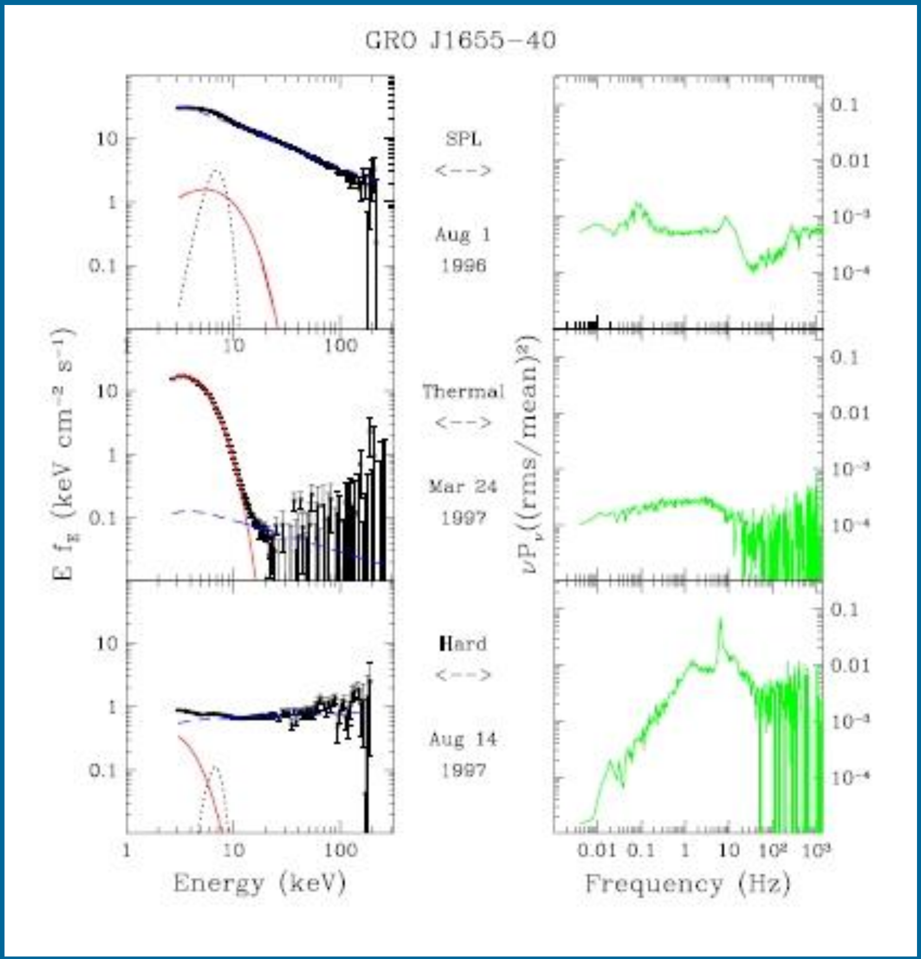

Table 2: Outburst states of black holes: nomenclature and definitions

New State Name (Old State Name)	Definition of X-ray State[a]
Thermal (High/Soft)	Disk fraction $f^b > 75\%$ QPOs absent or very weak: $a^c_{\max} < 0.005$ Power continuum level $r^d < 0.075^e$
Hard (Low/Hard)	Disk fraction $f^b < 20\%$ (i.e., Power-law fraction $> 80\%$) $1.4^f < \Gamma < 2.1$ Power continuum level $r^d > 0.1$
Steep Power Law (SPL) (Very high)	Presence of power-law component with $\Gamma > 2.4$ Power continuum level $r^d < 0.15$ *Either* $f^b < 0.8$ and 0.1–30 Hz QPOs present with $a^c > 0.01$ *or* disk fraction $f^b < 50\%$ with no QPOs

In this classification the luminosity is not used as one of parameters.

(Remillard, McClintock astro-ph/0606352)

Discs and jets

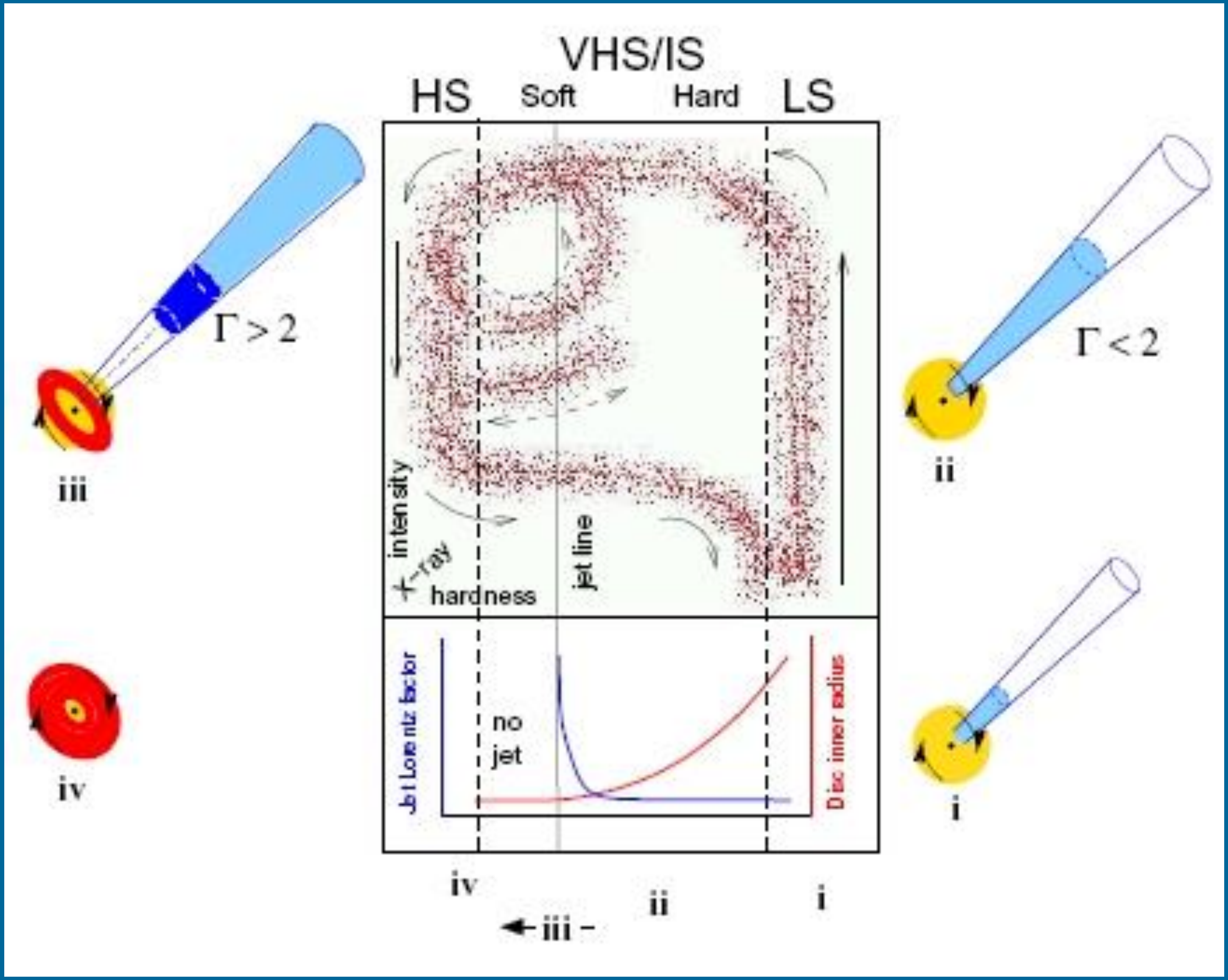

The model for systems with radio jets

LS – low/hard state
HS – high/soft state
VHS/IS –very high and intermediate states

The shown data are for the source GX 339-4.

(Fender et al. 2004, Remillard, McClintock astro-ph/0606352)

Hardness vs. flux: state evolution

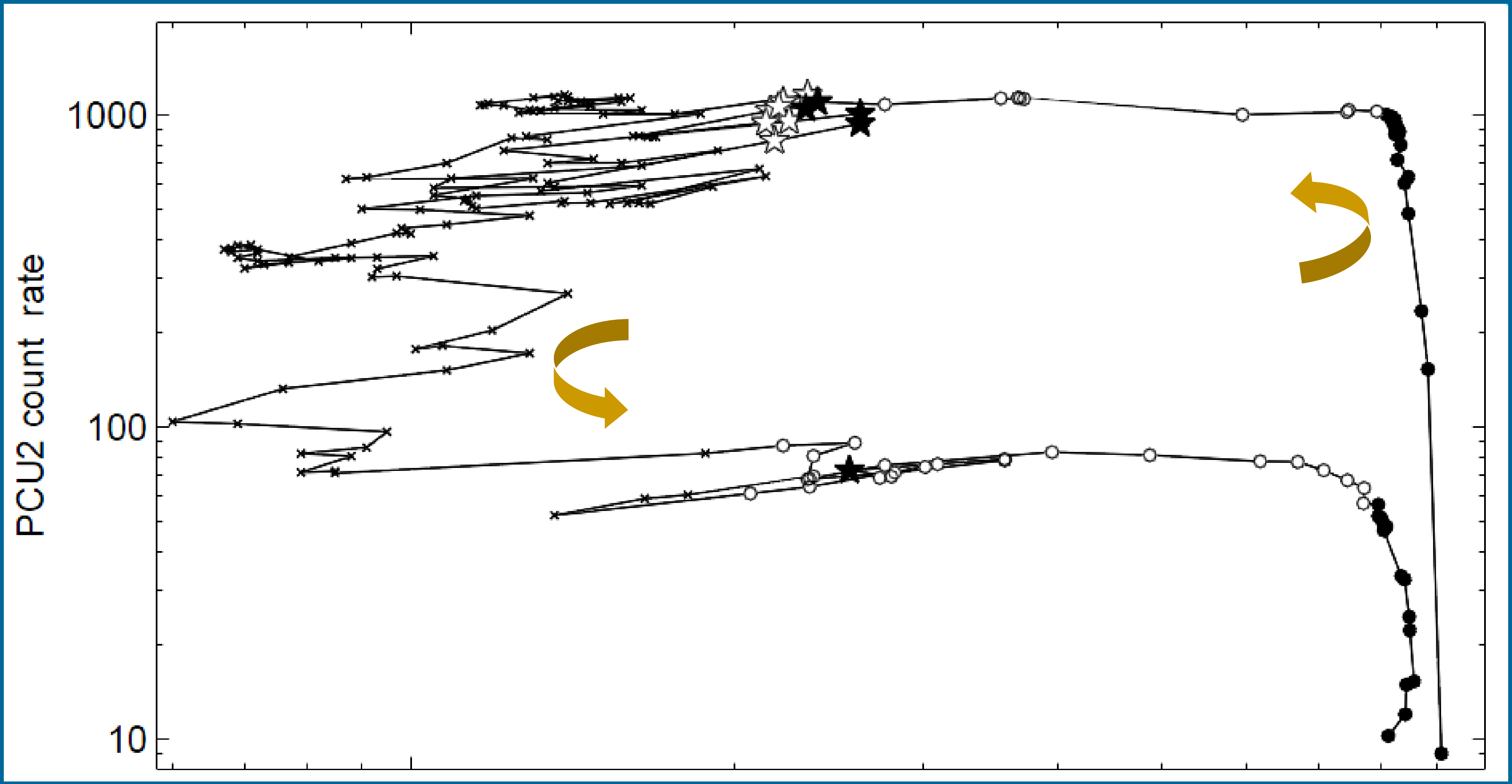

0909.2474

GRO J1655-40 during a burst

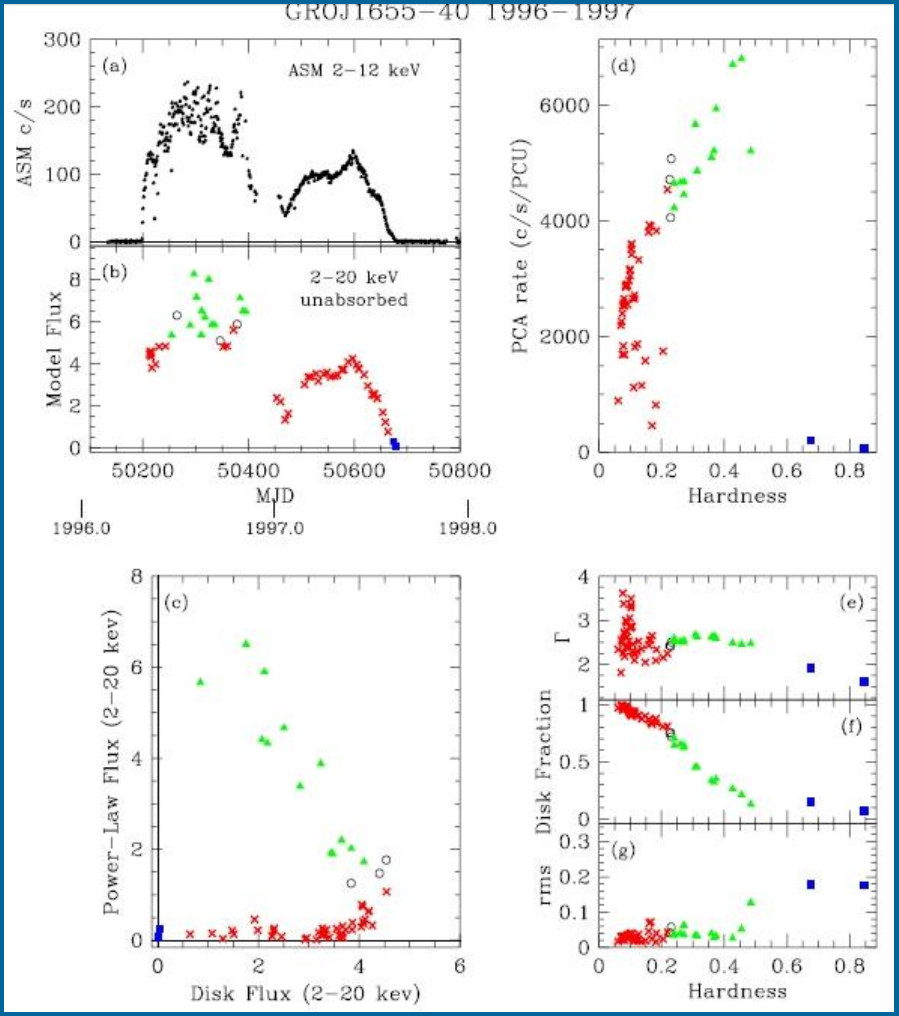

Red crosses – thermal state,
Green triangles – steep power-law (SPL),
Blue squares – hard state,
circles - intermediate.

(Remillard, McClintock astro-ph/0606352)

4U 1543-47 and H1743-322

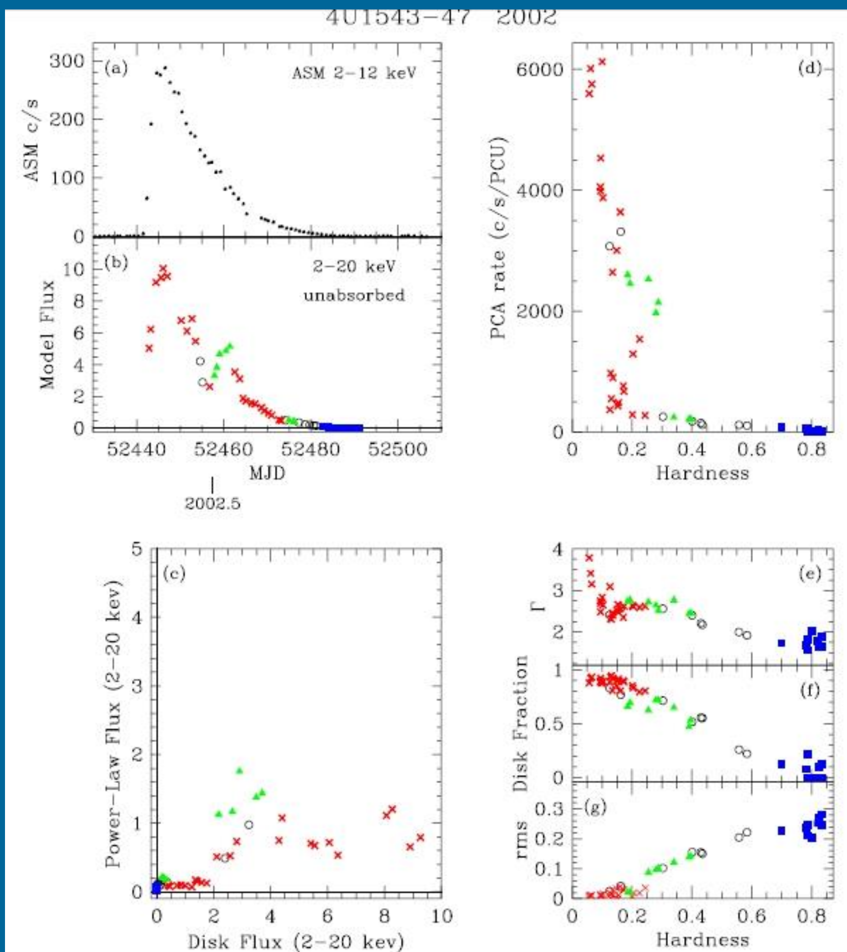

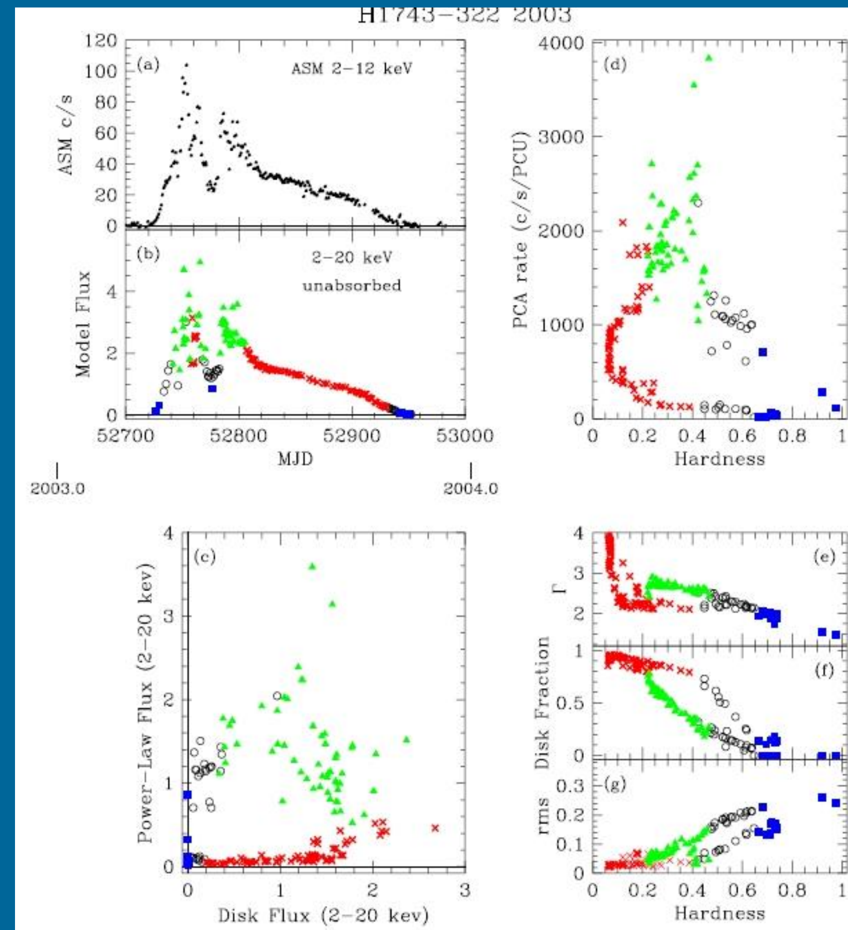

(Remillard, McClintock astro-ph/0606352)

XTE J1550-564 and XTE J1859-226

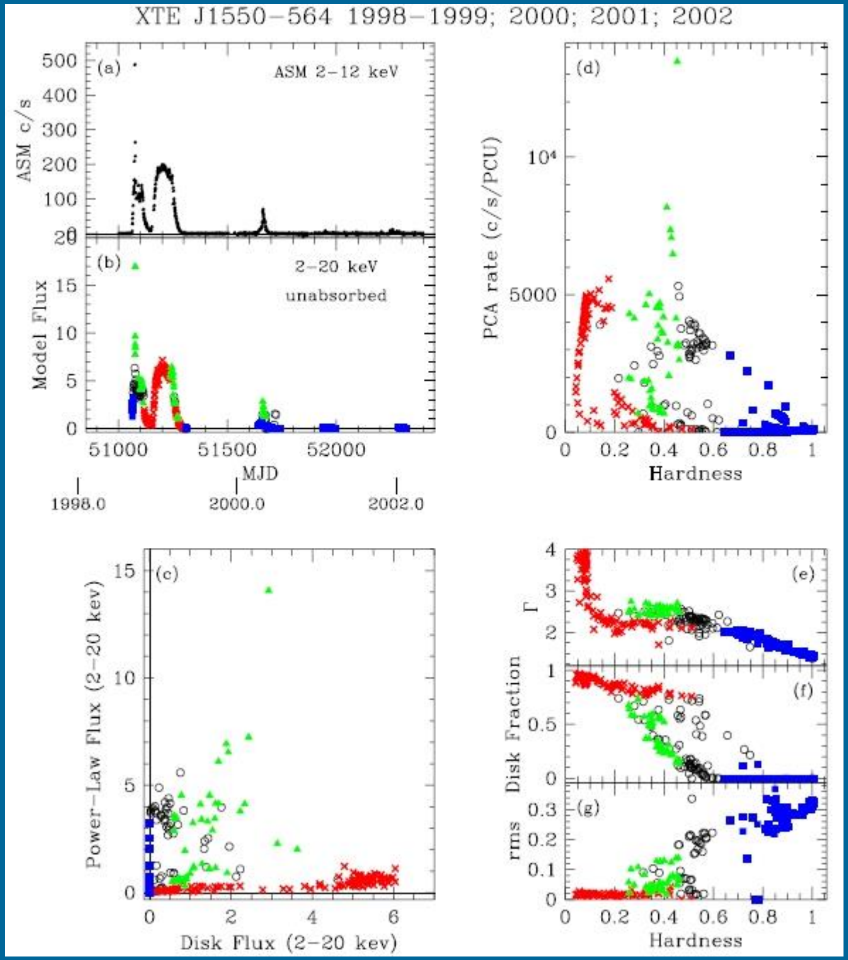

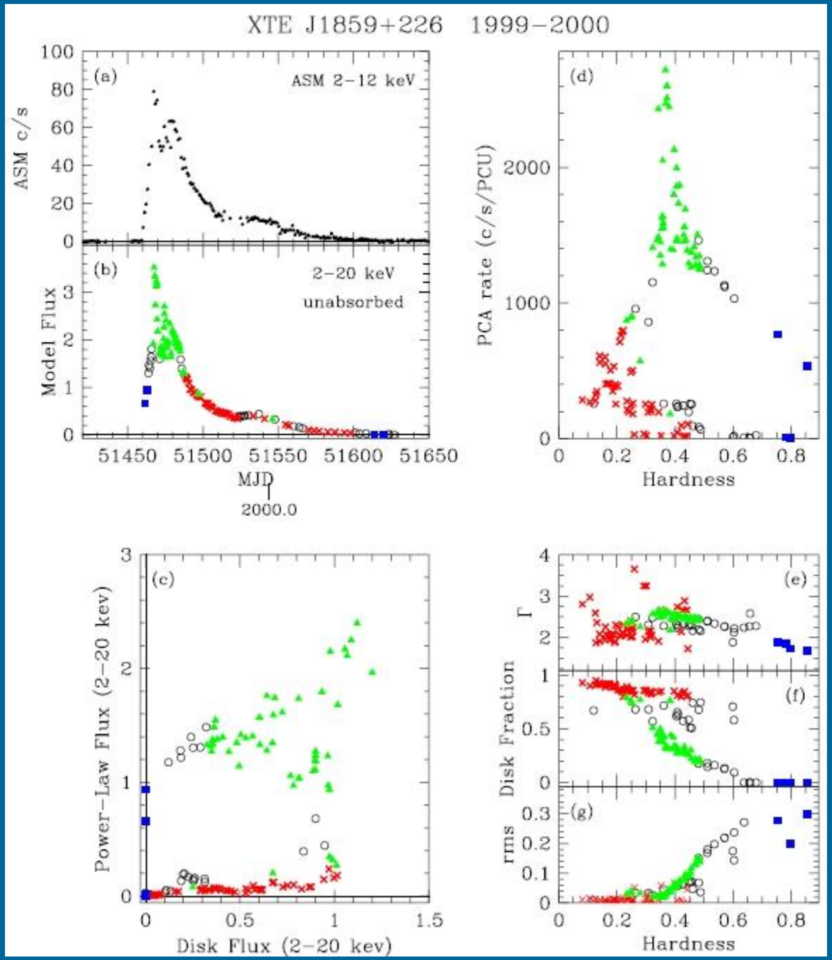

Recent large set of data

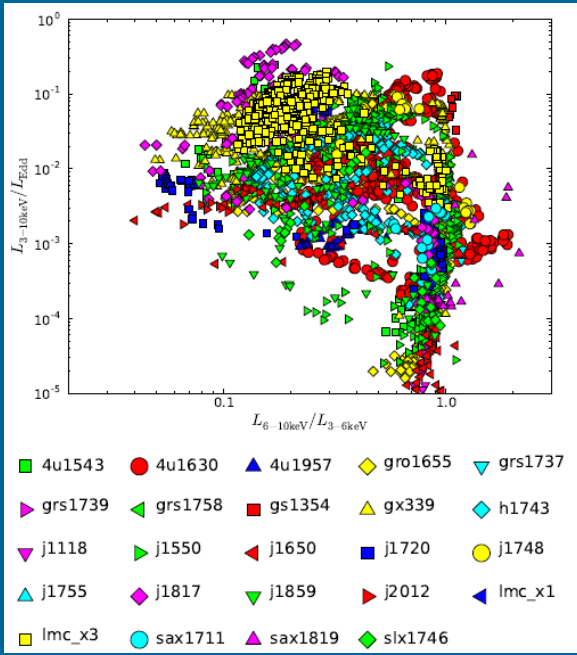

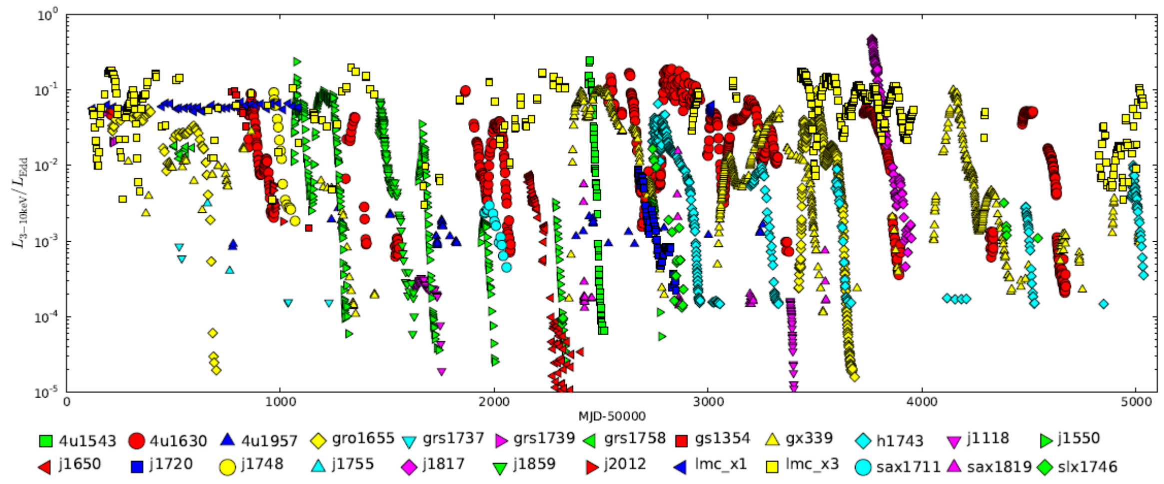

RXTE data
25 LMXBs

0912.0142

Hardness Intensity Diagram (HID) and Disc Fraction Luminosity Diagram (DFLD)

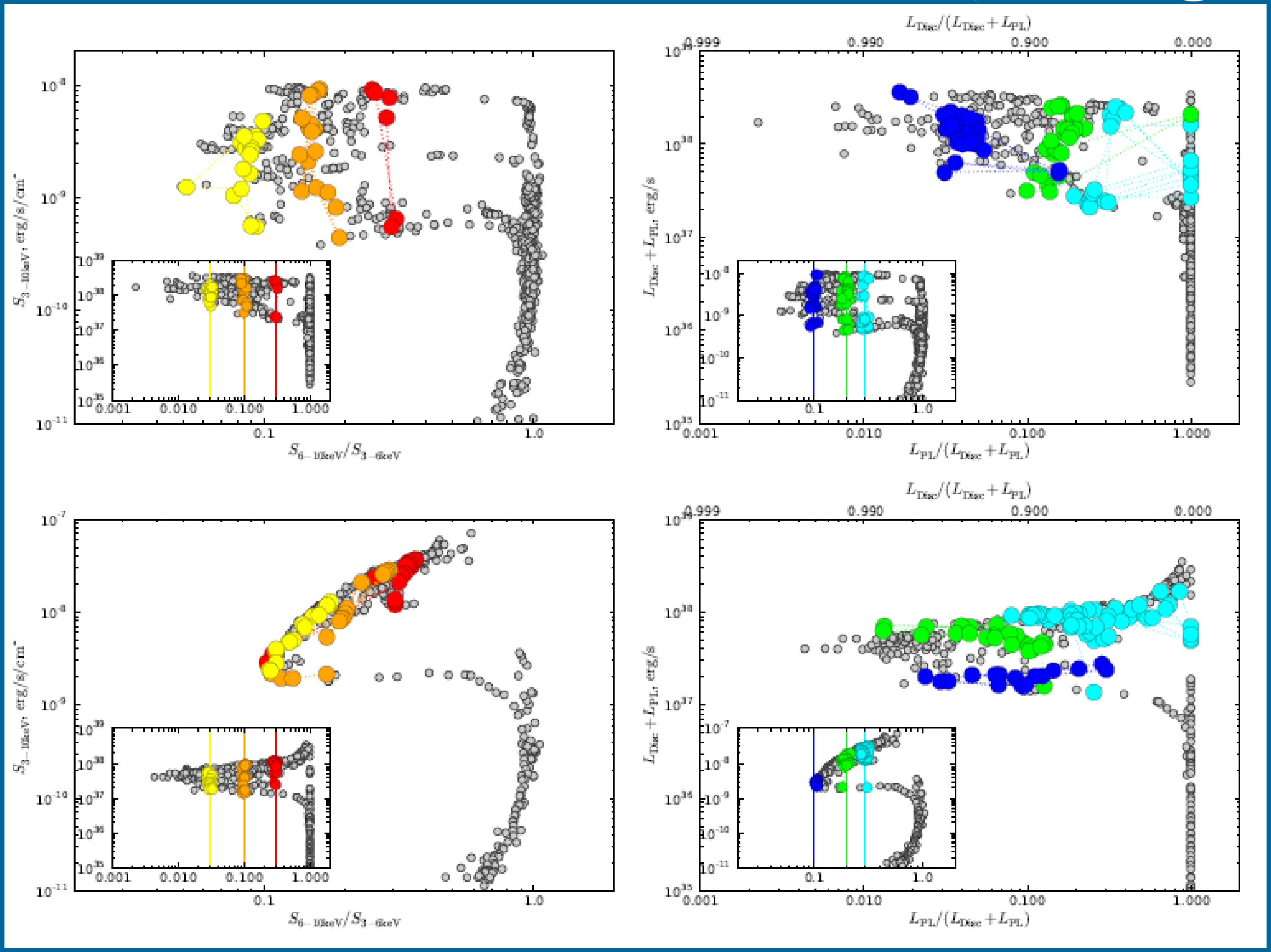

LEFT: HID with specific disc fractions highlighted
RIGHT: DFLD with specific X-ray colours highlighted.
The highlighted disc fractions are red 0.3, orange 0.1, yellow 0.03; and the highlighted X-ray colours are cyan 0.3, green 0.2, blue 0.1.
TOP: GX 339-4,
DOWN: GRO 1655-40

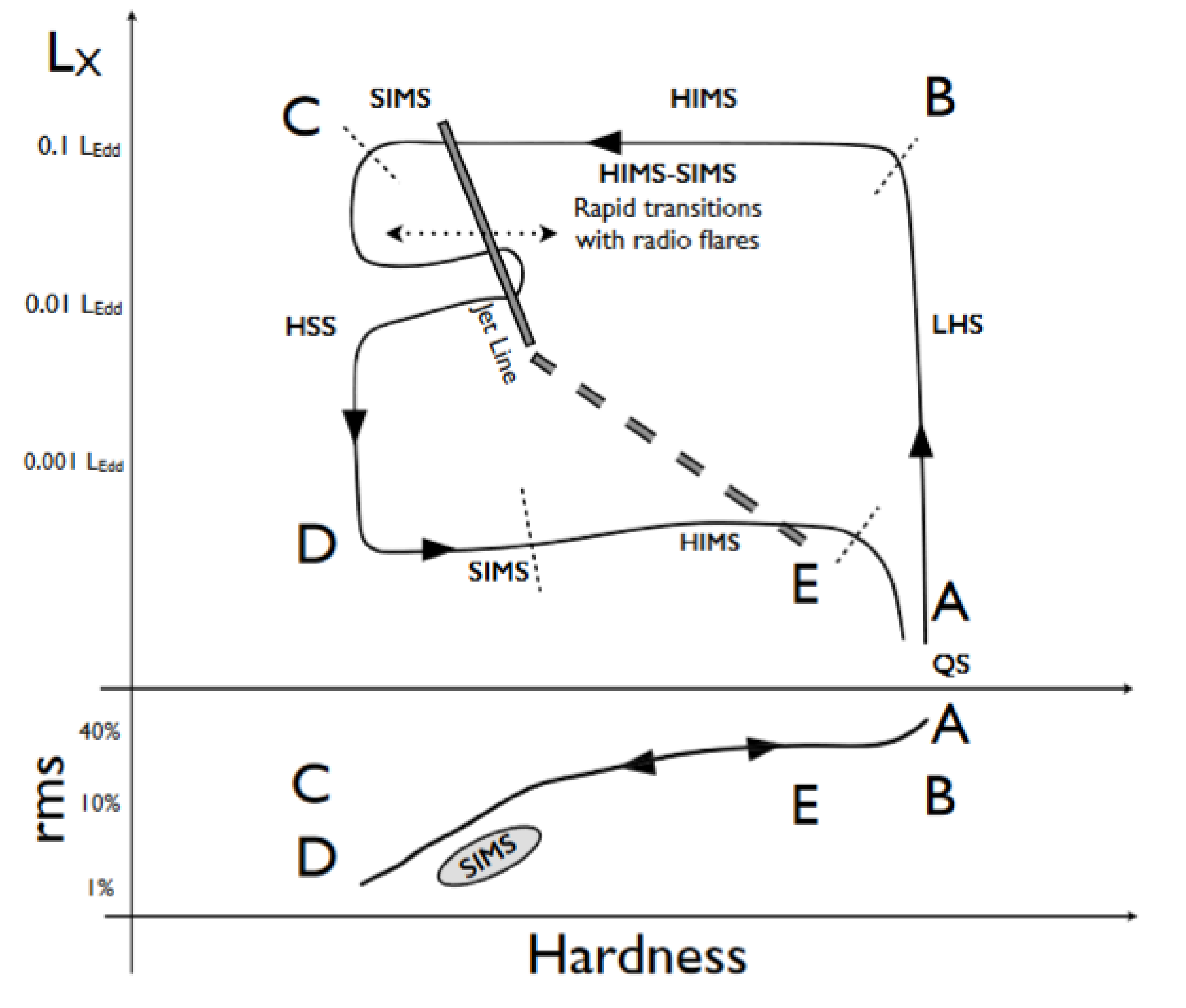

See p.17-19 for a very clear description.

1603.07872

Summary of the main states

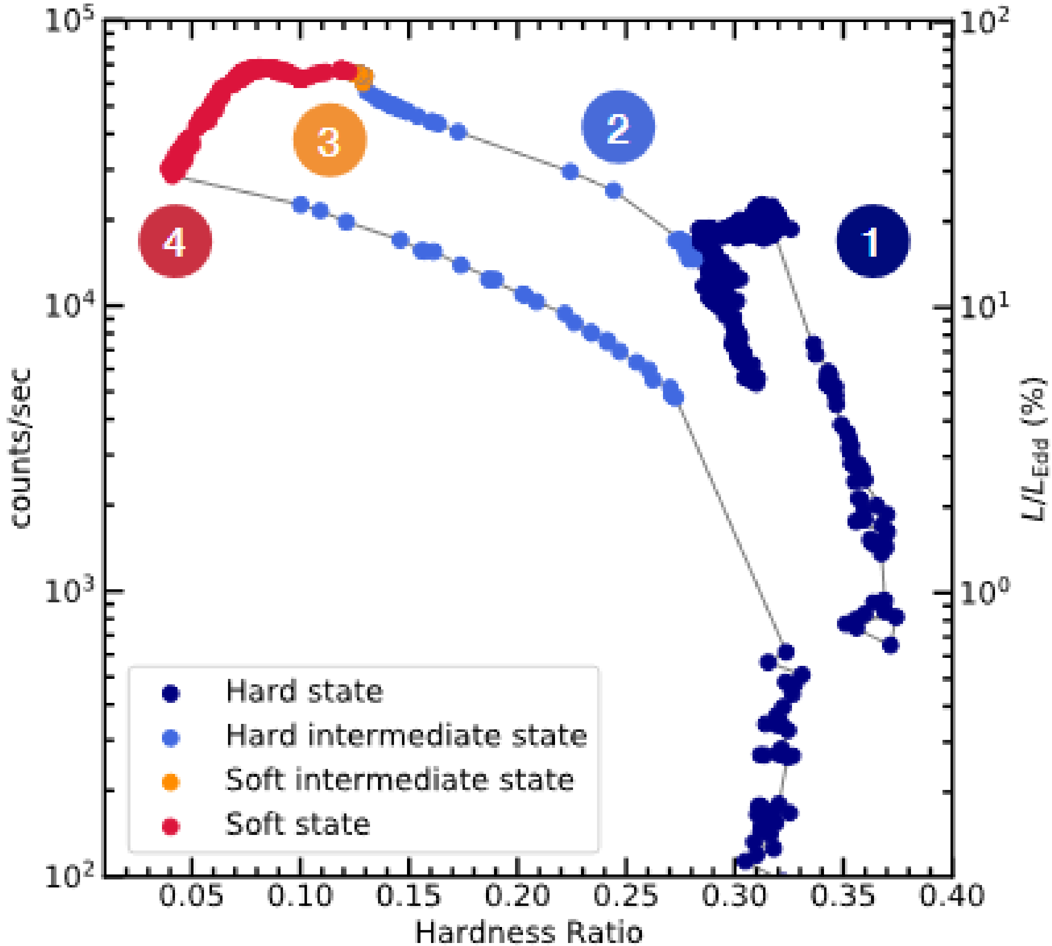

1 Hard State

- Hardest corona, weak disk
- Compact radio jet
- Iron line and Compton hump
- Highest RMS: Type C QPOs, Reverberation lags

2 Hard Intermediate State (HIMS)

- Softening corona, stronger disk
- Compact radio jet shuts down
- Iron line and Compton hump
- High RMS: Type C QPOs, Reverberation lags

3 Soft Intermediate State (SIMS)

- Still softer corona, stronger disk
- Ballistic radio jet
- Iron line and Compton hump
- Low RMS: Transition from Type C to B QPOs

4 Soft State

- Weak corona, strong disk
- No radio jet, equatorial winds
- Less prominent iron line and Compton hump
- Low RMS: Rarely Type A QPOs, no lags

2206.14410

X-ray – radio correlation

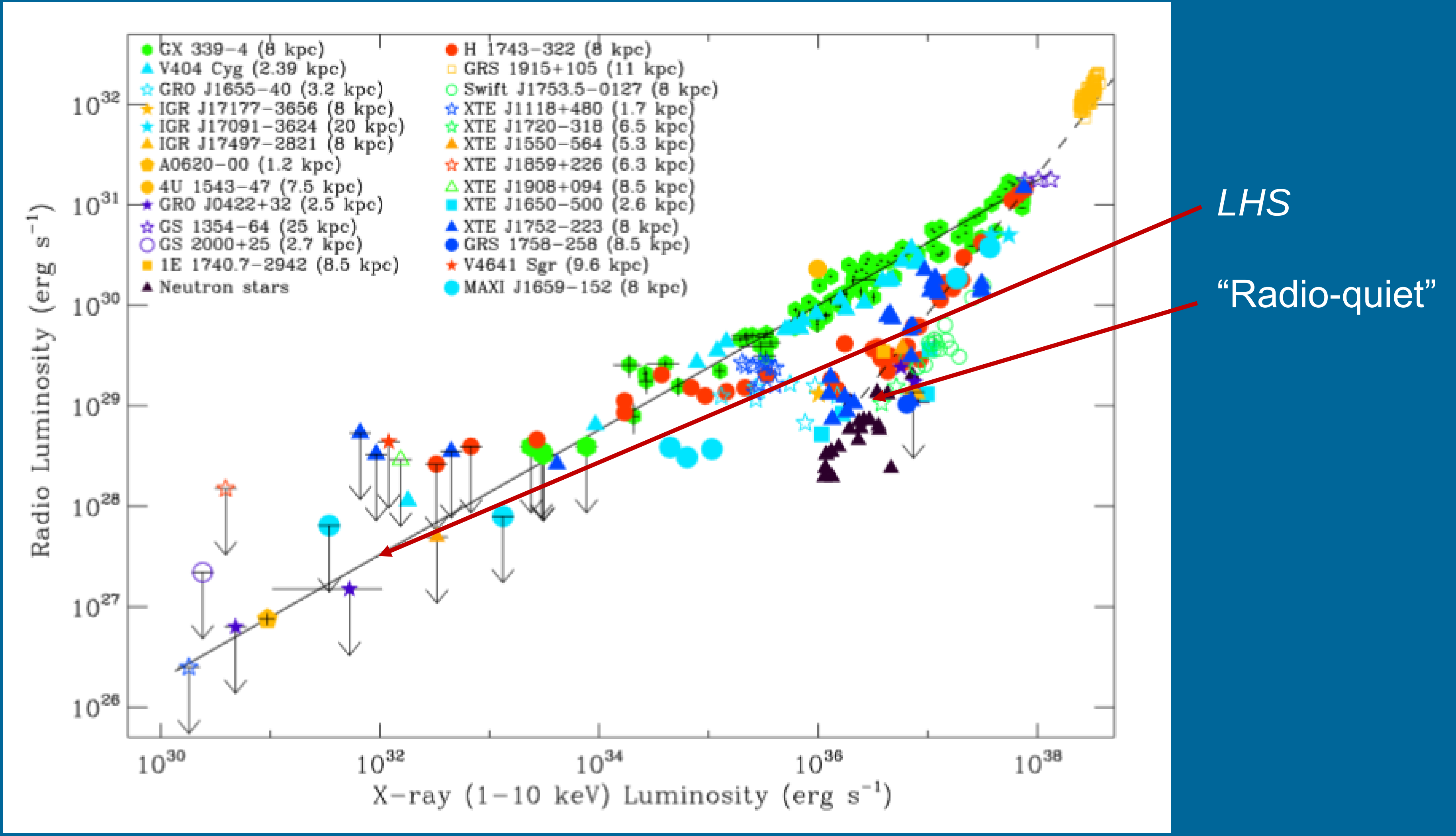

1603.07872

Jet variation in Cyg V404 during outburst

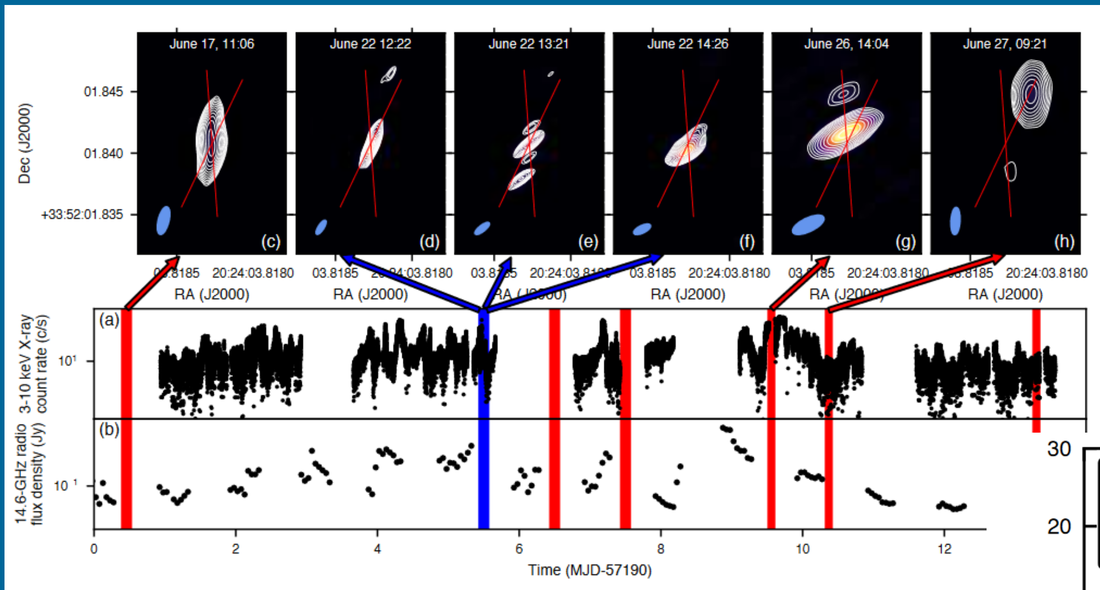

Rapid jet direction variability during an outburst can be due to Lense-Thirring precession of the inner disc.

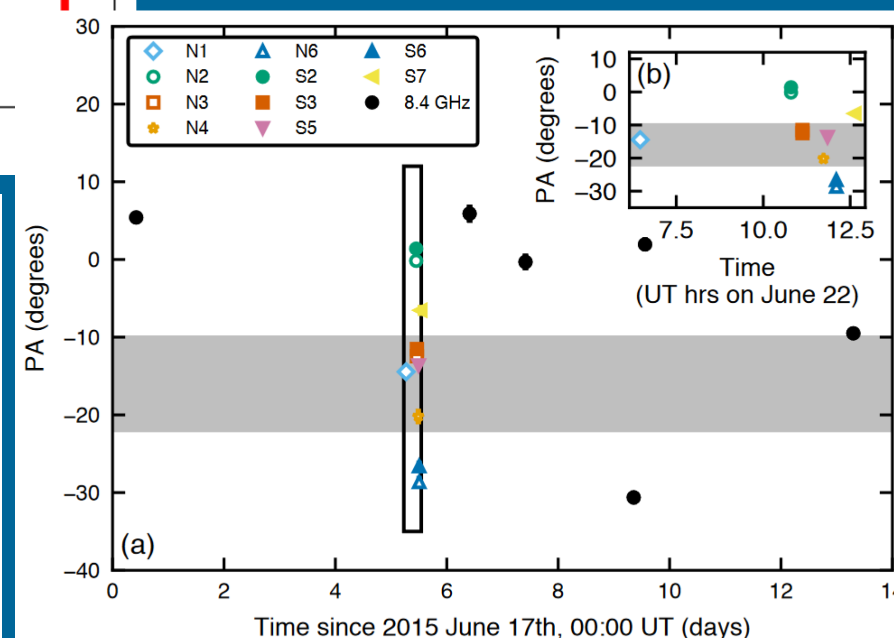

Timescale: minutes to hours.

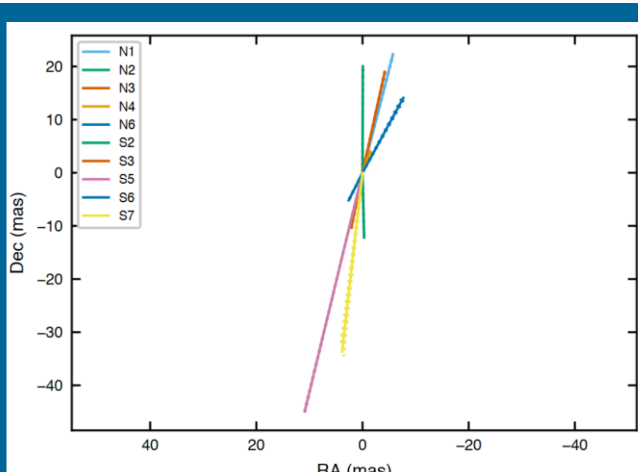

1906.05400

Inner disk boundary in GX 339-4

In BH binaries there are different spectral and luminosity states. It was suggested that the inner disk boundary moves significantly from stage to stage.

For the first time the effect was measured thanks to the iron line data.

At low luminosity the inner disk boundary is far from the BH.

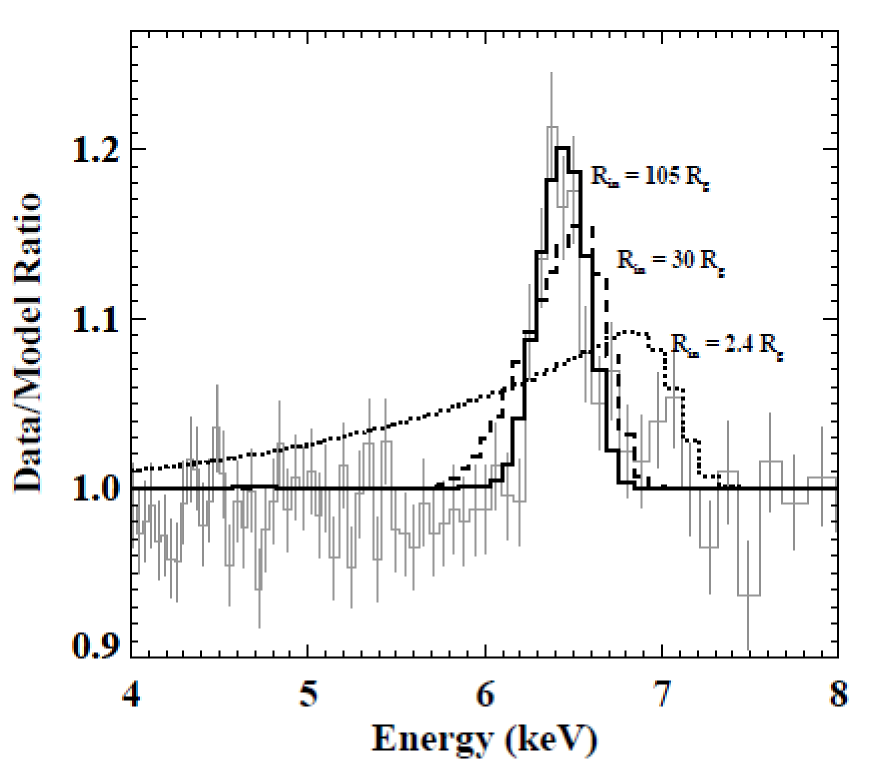

0911.2240

Inner disc boundary vs. luminosity

Position of the inner disc boundary is clearly different at different luminosities: from 0.1 to 0.001 L_{Edd}.

In a separate paper another group of scientists put constraints on the spin rate of the BH in this system.

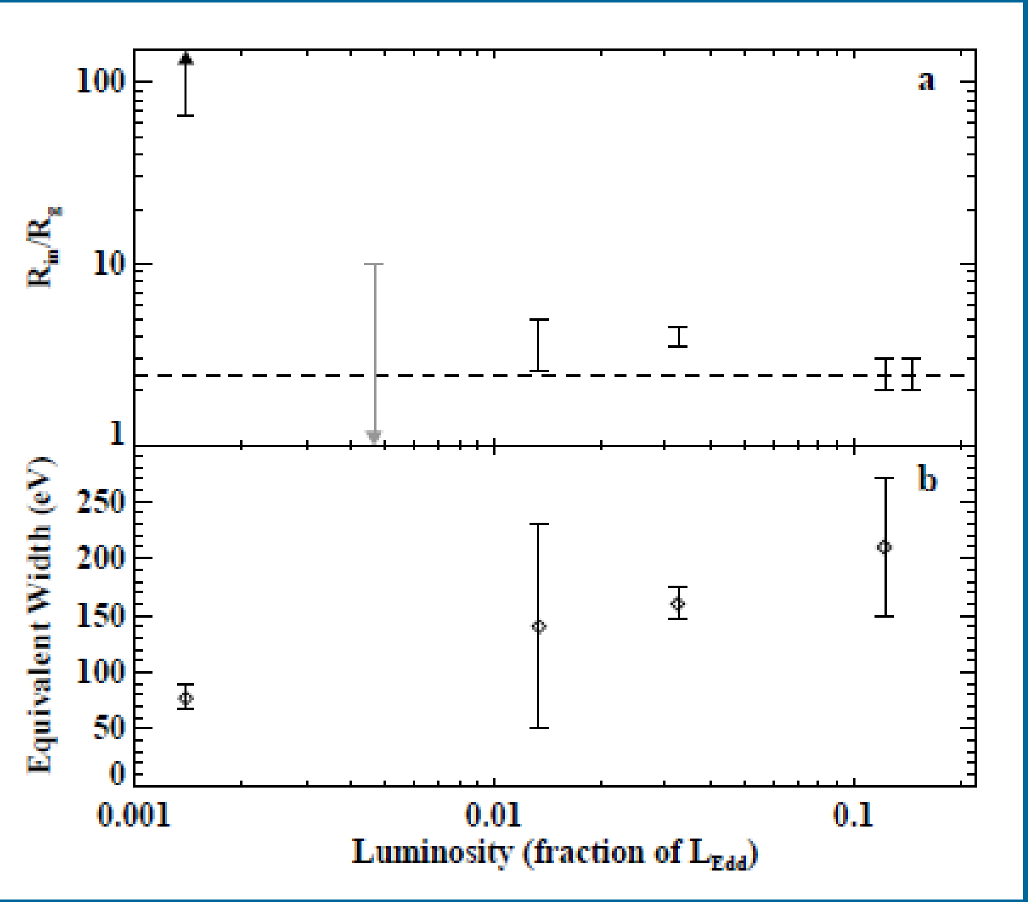

0911.2240

GX 339–4

Disc truncation or corona expansion?

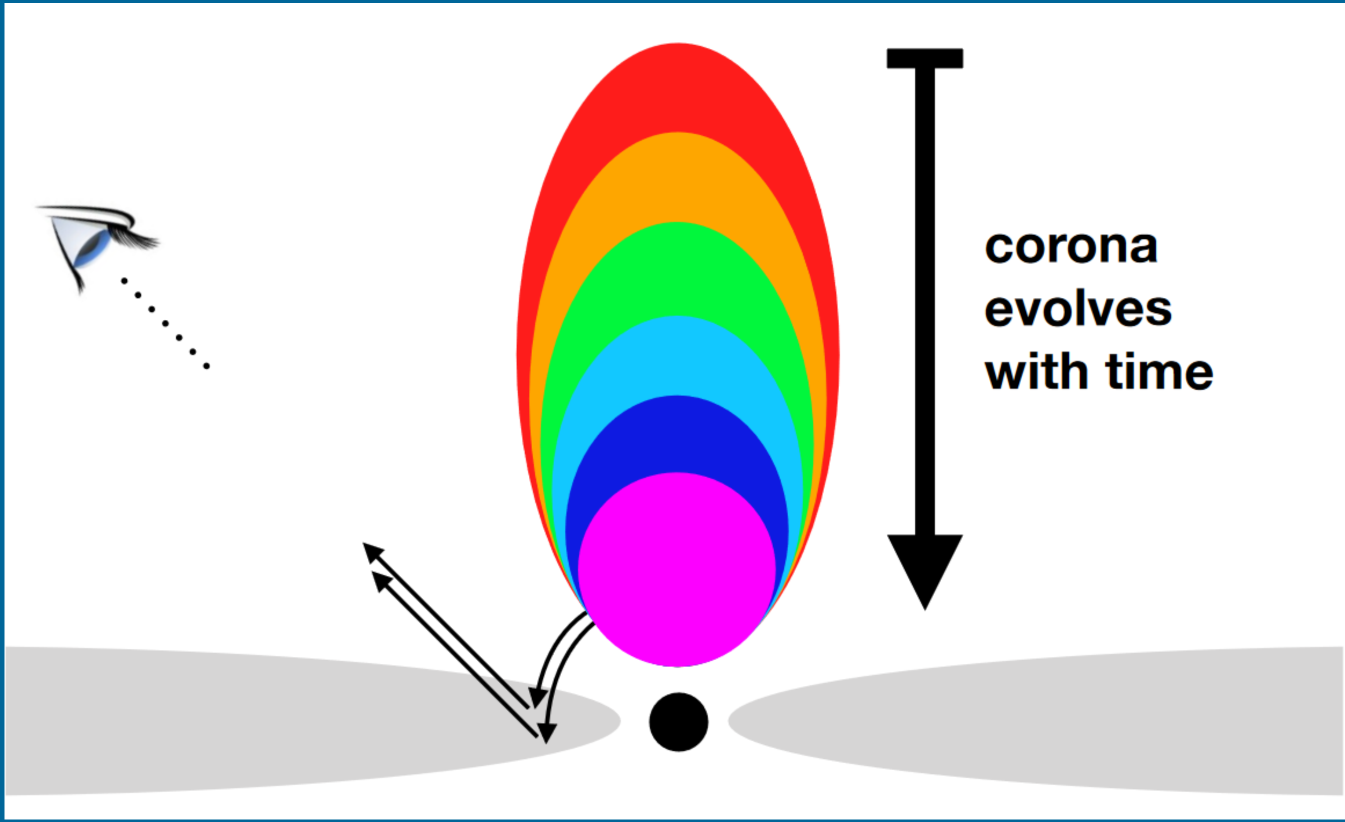

In the case of MAXI J1820+070 observations suggest that stage (and spectral) changes are mostly not due to modification of the inner disc radius, but due to changes in the hot corona size. The result is based on time lags between corona and disc emission.

1901.03877

Scheme of time lags

Low-frequency hard lags (soft before hard)
is due to propagation of disturbances in the disc

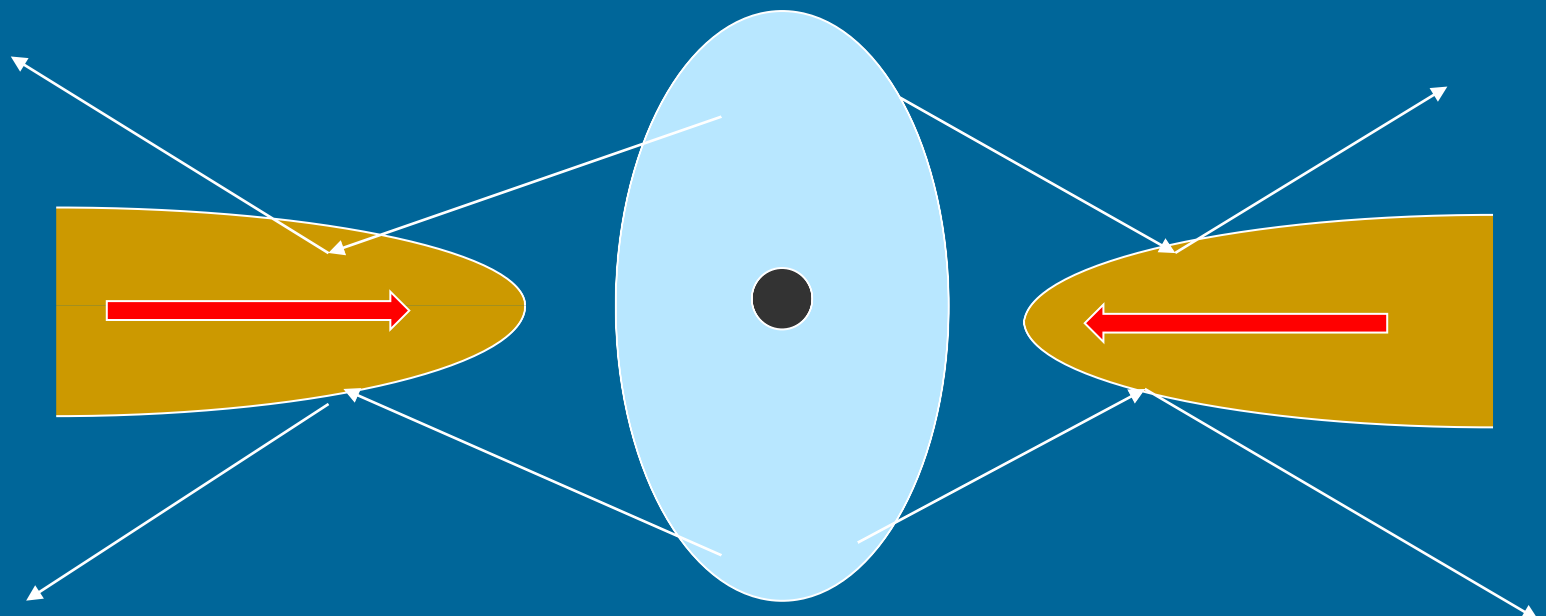

High-frequency soft lag (hard before soft) is due to irradiation of the disc by corona

Hard lags and soft lags

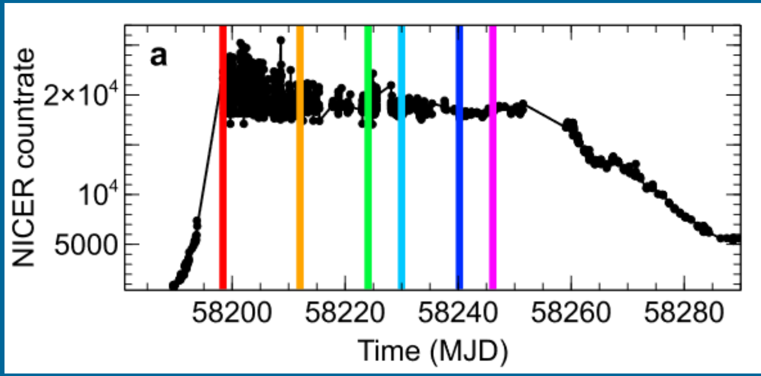

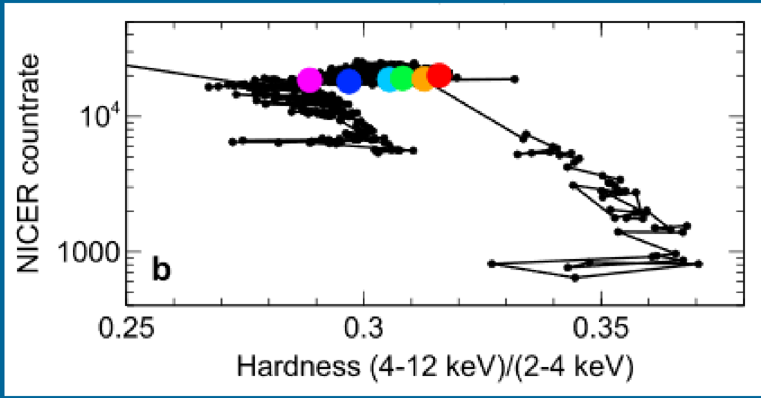

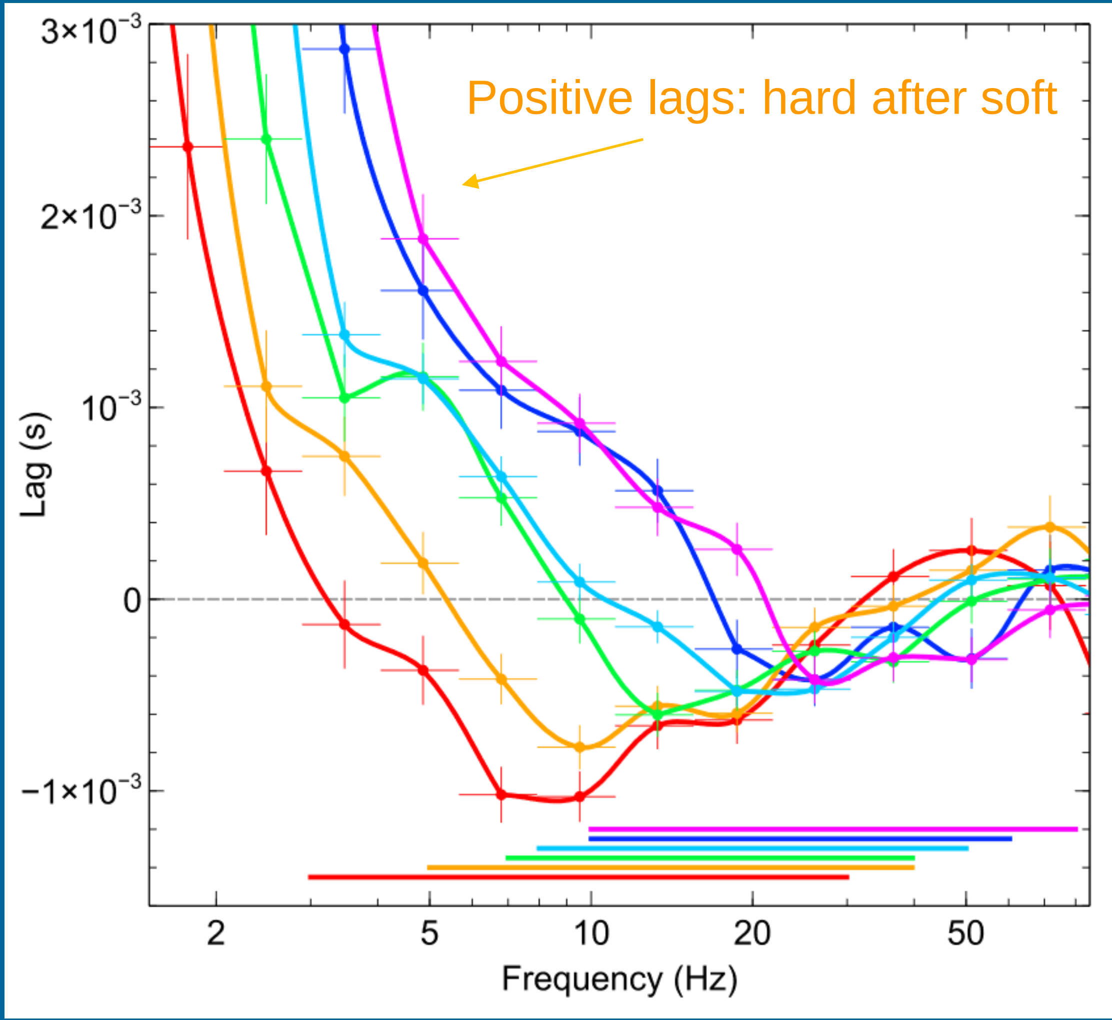

1901.03877

NS jets

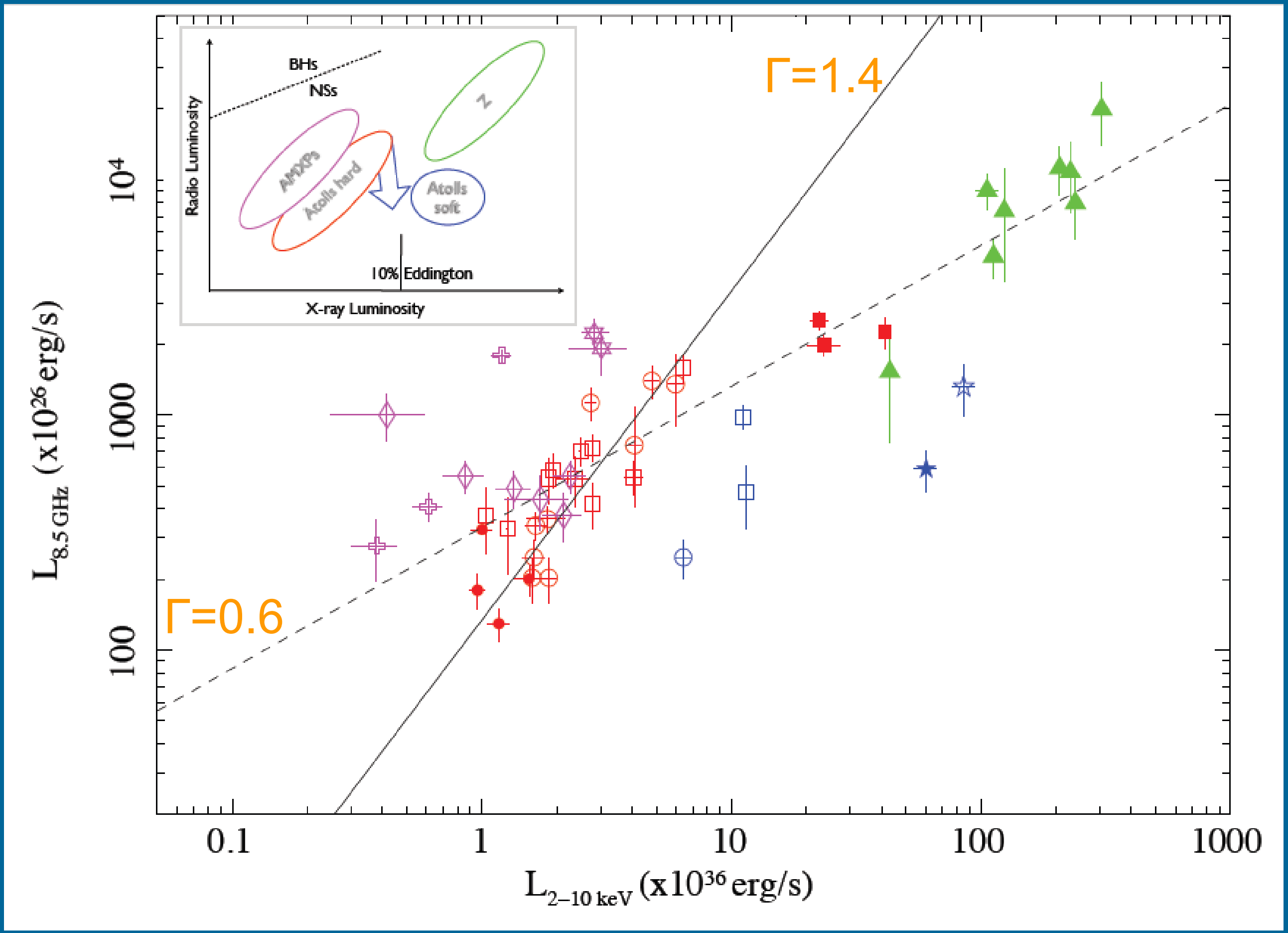

open circles, 4U 1728-34;
filled squares, MXB 1730-335;
open squares, Aql X-1;
filled circles, 4U 0614+091;
Open star, Ser X-1;
filled star, 4U 1820-30;
filled triangles are Z sources;
open diamonds, SAX J1808.4-3658;
open crosses are IGR J00291+5934;
stars of David, XTE J0929-314.
Colors:
red, atolls in hard state or
in outburst, up to the peak;
blue, atolls in steady soft state;
green, Zsources; magenta, AMXPs.

1104.1115

A jet from normally magnetized NS

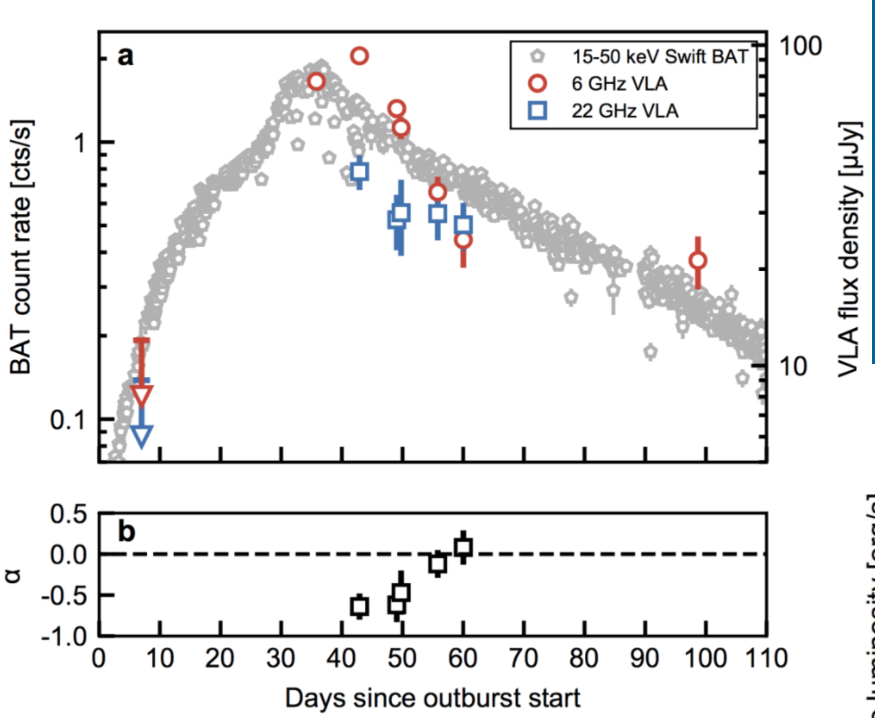

VLA detection of emission from Swift J0243.6+6124.
Spin period ~10 sec.
Before jets have been detected from rapidly spinning NSs.
Blandford-Znajek, not Blandford-Payne.

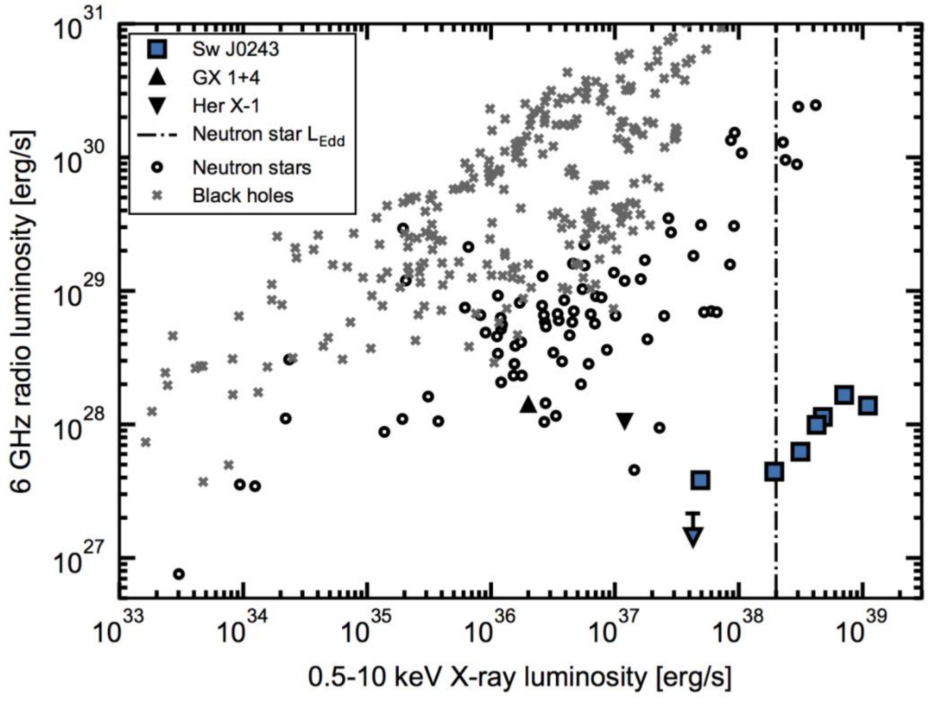

$$L_R \propto L_X^{0.54 \pm 0.16}$$

1809.10204

Radio census of accreting NSs

36 sources observed with VLA or ATCA.

13 sources detected.

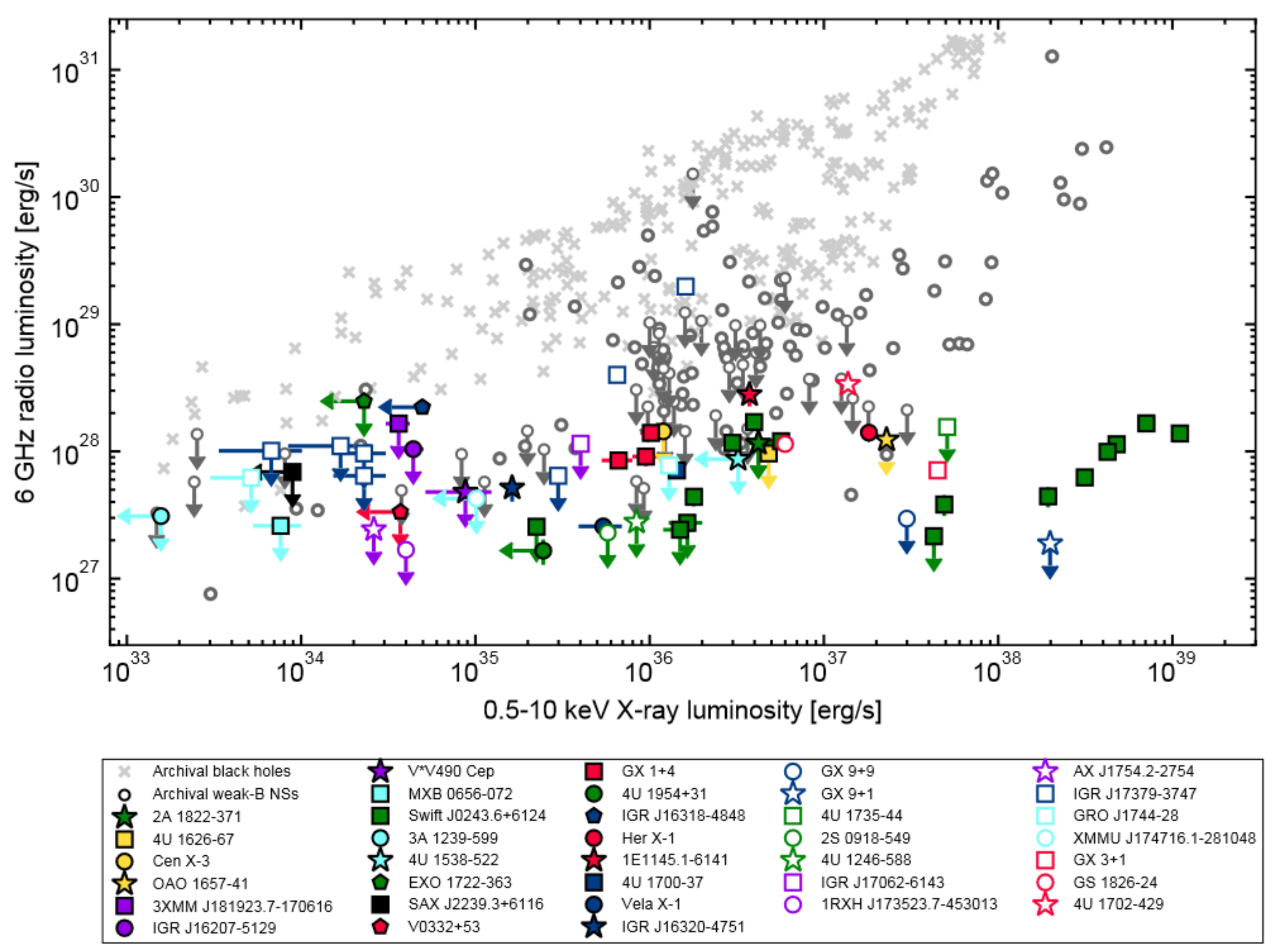

2107.05286

Spins: NSs vs. BHs

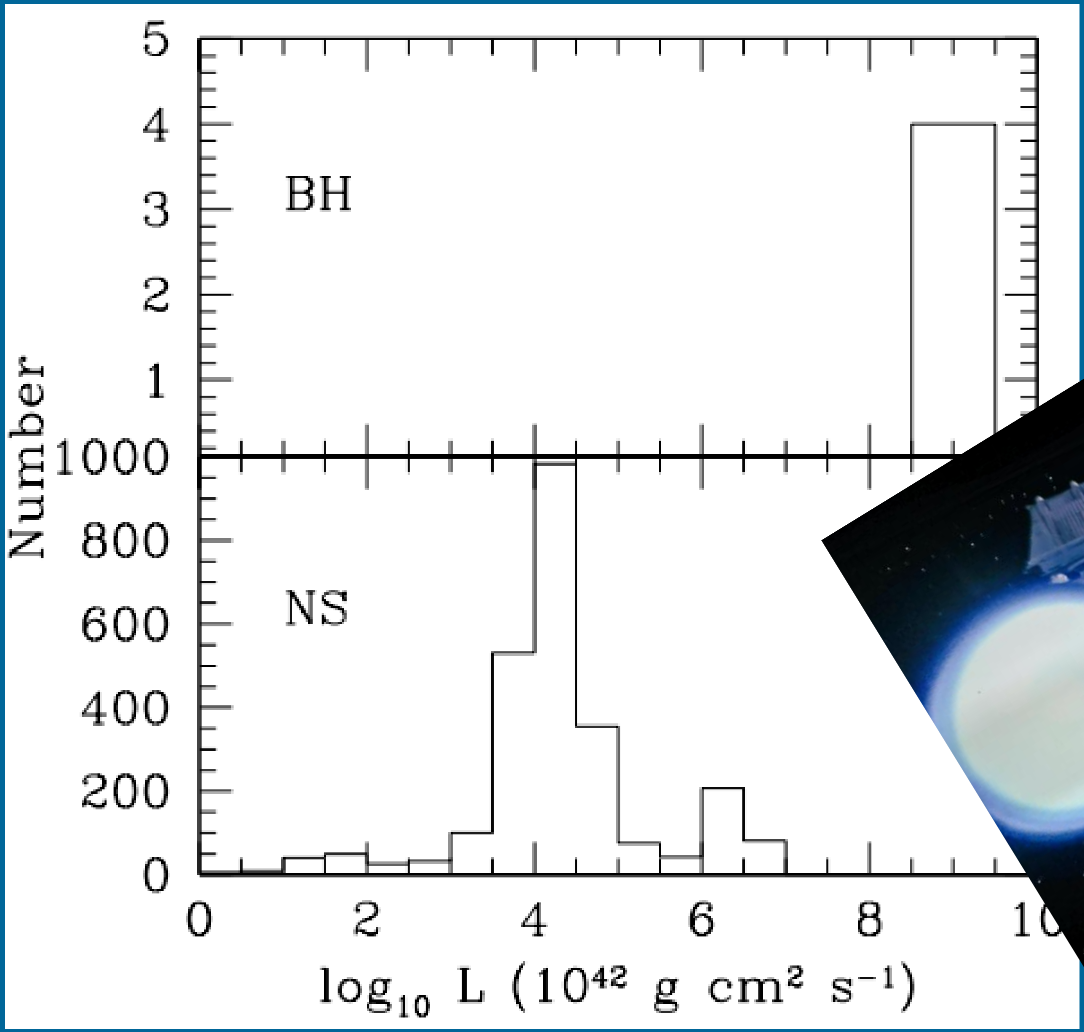

BHs win!!!!!
They nearly do not loose angular momentum.

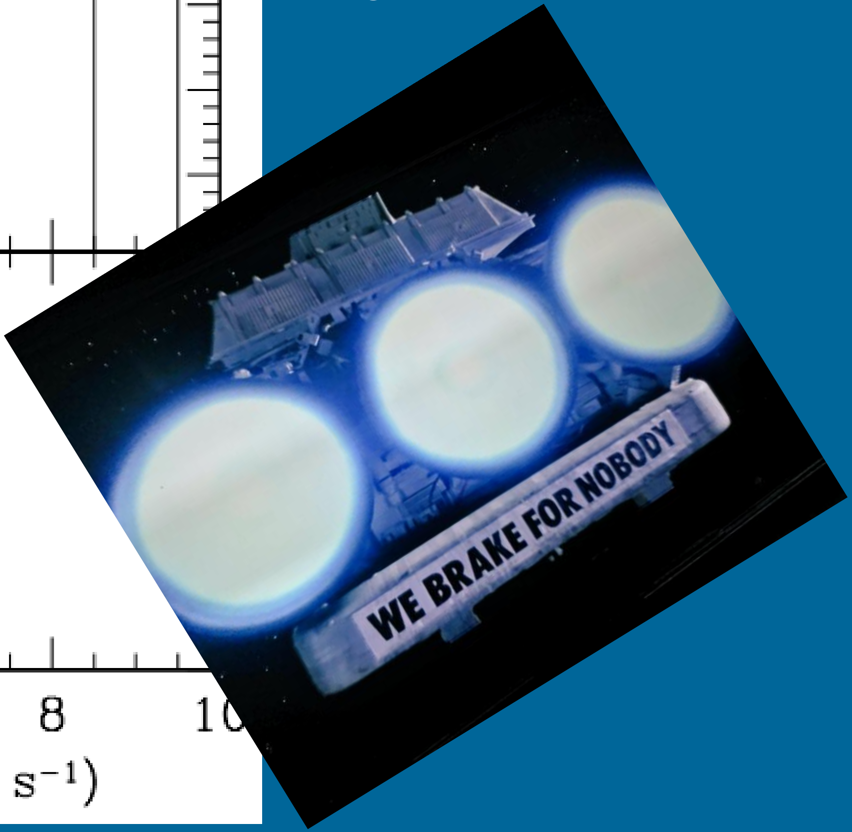

1408.4145

Mass and spin determinations are reviewed in 1408.4145 and spin in 1507.06153

Origin of BH spin

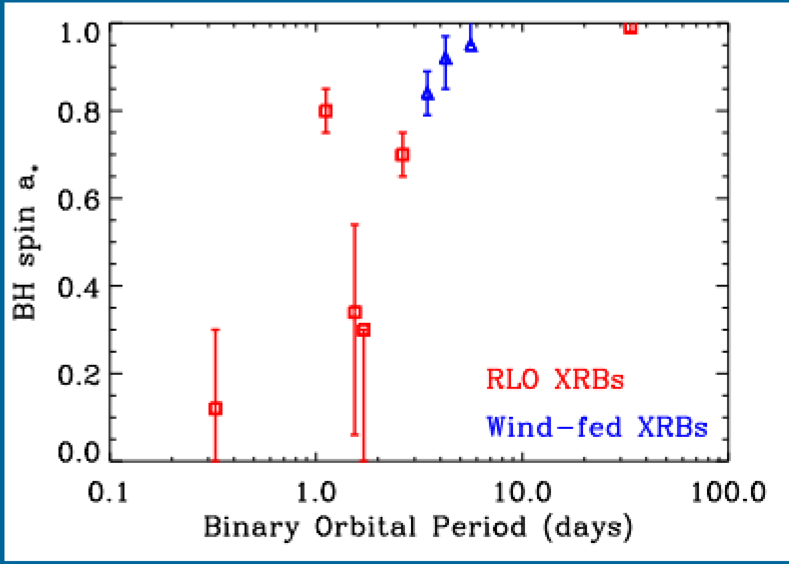

Spin is due to accretion.

BHs accrete (on average) ~1.5 solar mass

However, a BH in the system Swift J1728.9-3613 in a SNR has a=0.86, see 2303.04164

High spin estimate for EXO 1846–031 excludes a NS as an accretor. a=0.995-0.998 (2007.04324).

Source	MT Type[b]	P_{orb} (days)[b]	Spin a_*	Reference
GRS 1915+105	RLO	33.5	> 0.98	McClintock et al. (2006)
Cyg X-1	Wind	5.6	> 0.95	Gou et al. (2011)
LMC X–1	Wind	4.23	$0.92^{+0.05}_{-0.07}$	Gou et al. (2009)
M33 X–7	Wind	3.45	0.84 ± 0.05	Liu et al. (2008, 2010)
4U 1543–47	RLO	1.15	0.80 ± 0.05	Shafee et al. (2006)
GRO J1655–40	RLO	2.62	0.70 ± 0.05	Shafee et al. (2006)
XTE J1550–564	RLO	1.54	$0.34^{+0.20}_{-0.28}$	Steiner et al. (2011)
LMC X–3	RLO	1.7	< 0.3[c]	Davis et al. (2006)
A0620–00	RLO	0.33	0.12 ± 0.18	Gou et al. (2010)

1408.2661
New measurements for 4U1543 are consistent with the value above: 2002.11922

Spin (and mass) growth due to accretion

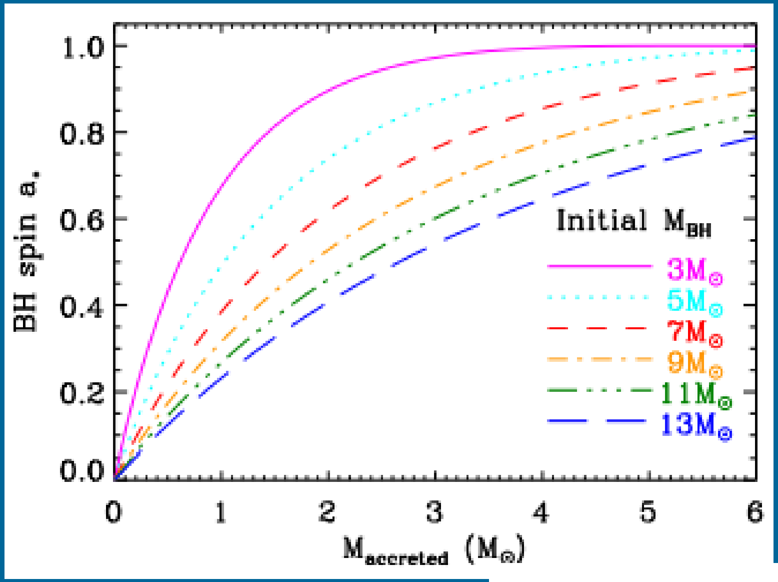

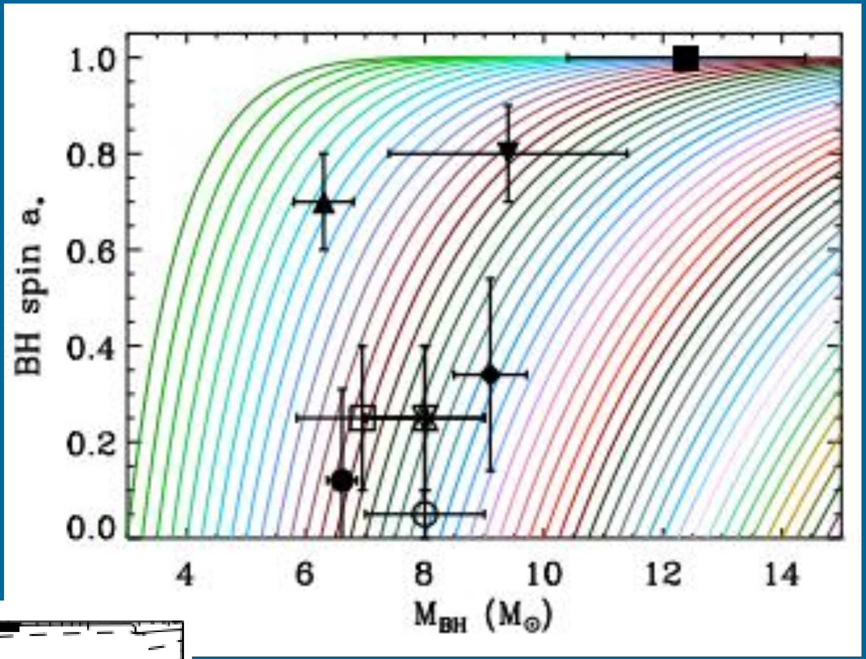

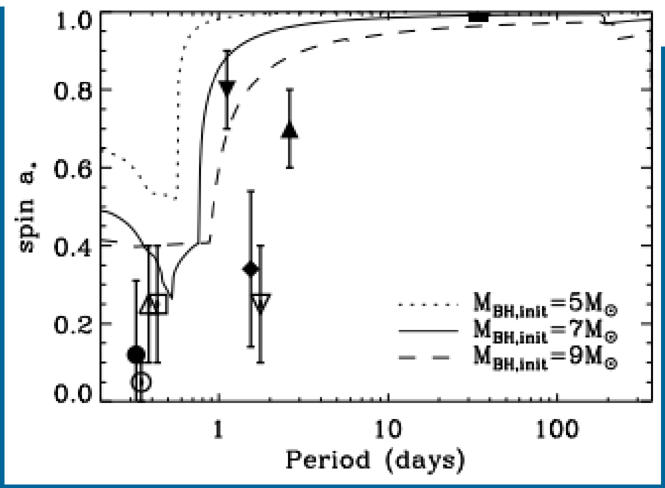

The hypothesis is that spin is gained due to accretion (at birth a=0).

1408.2661

Statistics

Various methods are used to determine the spin parameter of accreting BHs in binaries.

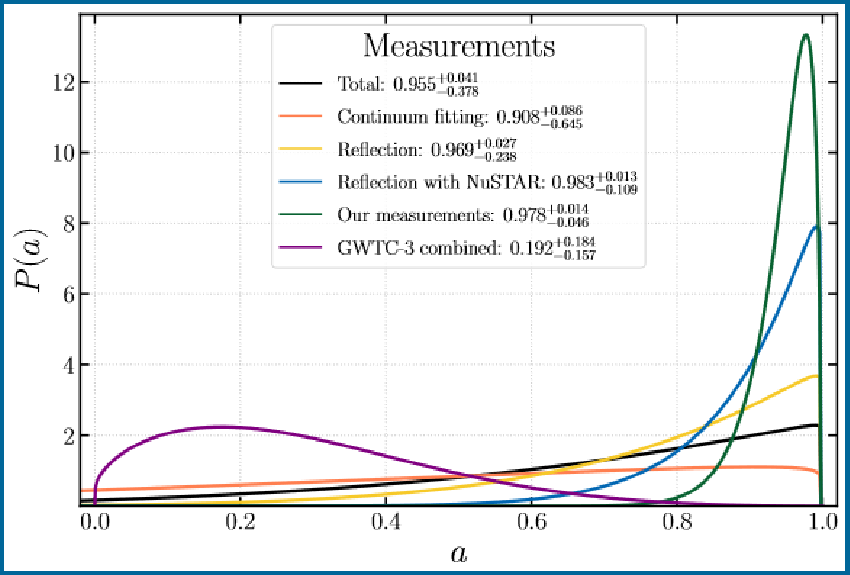

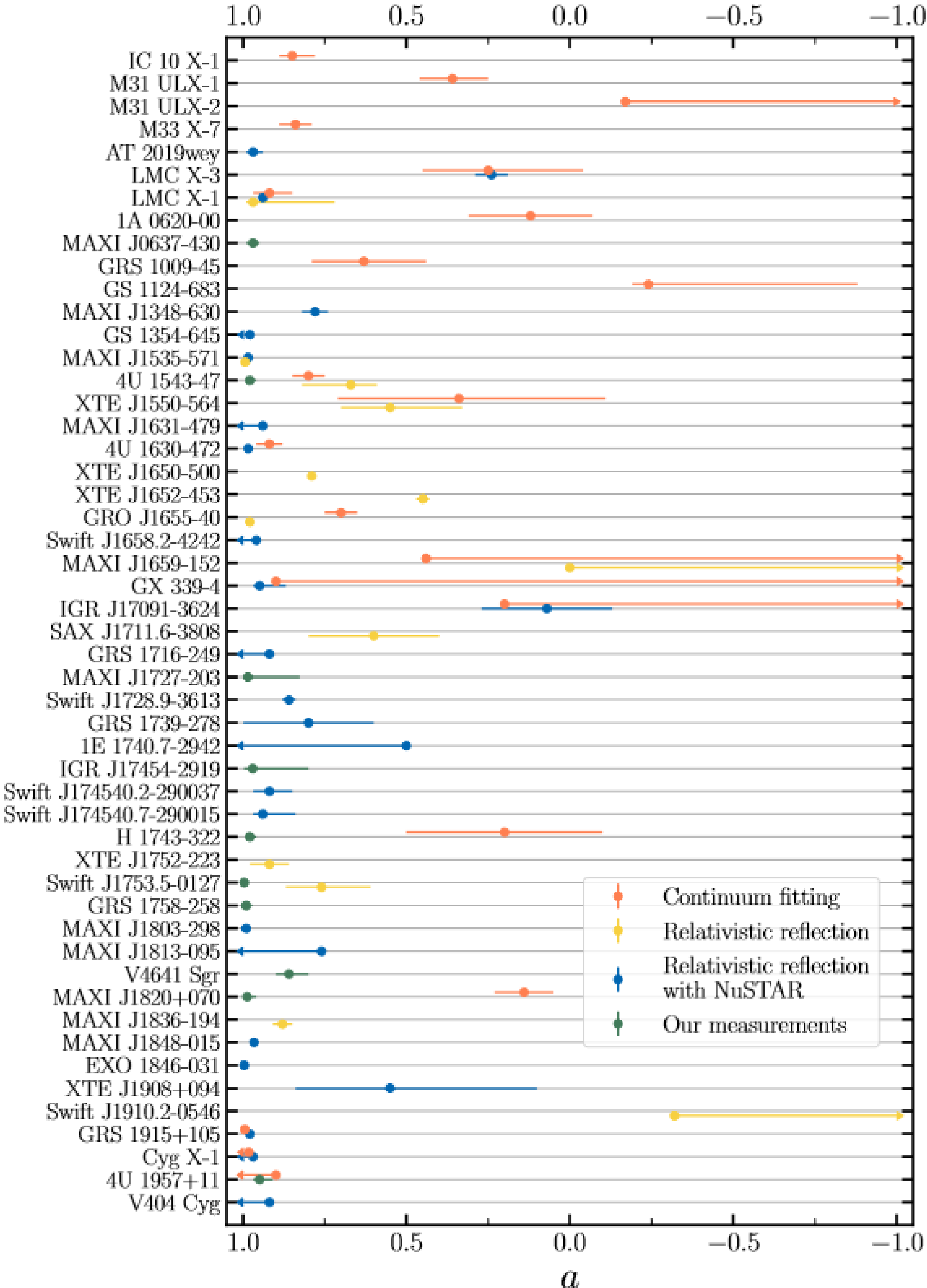

2210.02479, see also 2311.16225 about NuSTAR data on BH spins.

Misalignment

2109.07511

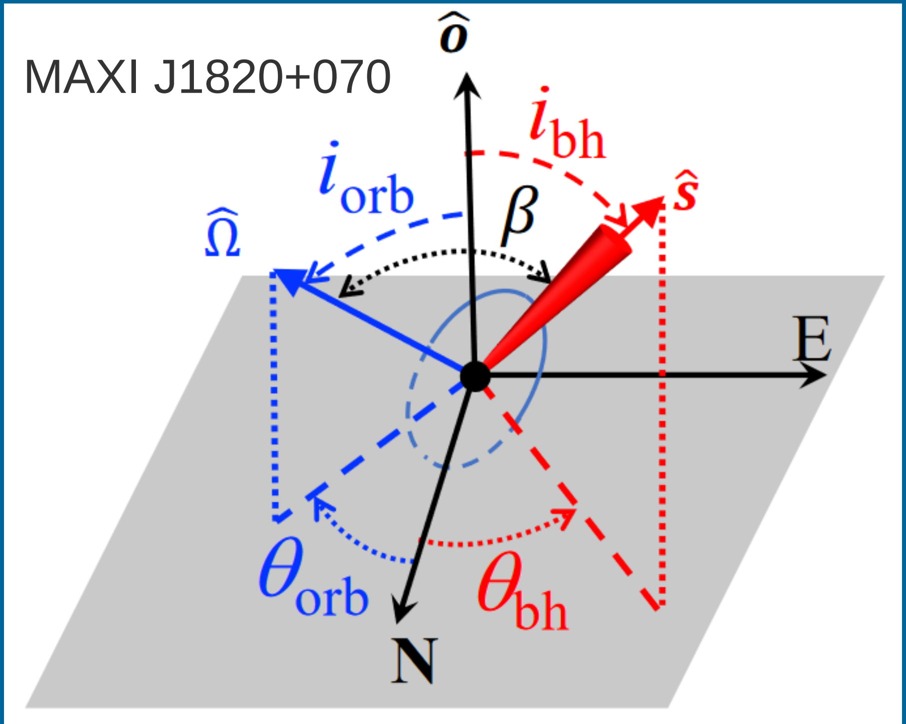

For MAXI J1820 the spin was estimated as a=0.8 (2109.14371)

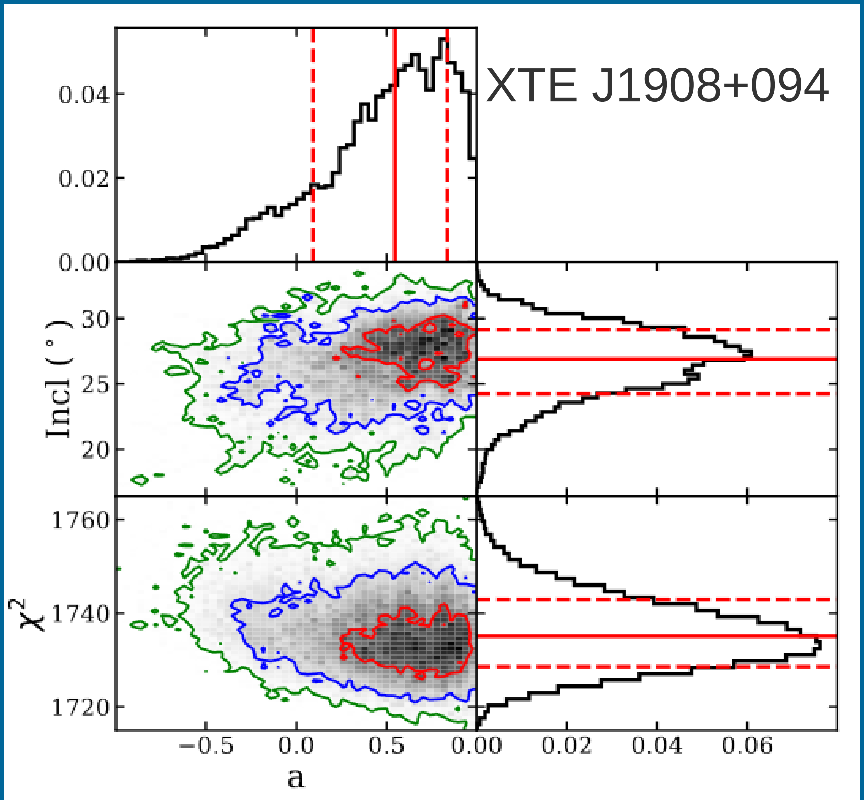

2107.02810

Orbital spin orientation is measured due to optical polarization observations. The BH spin – due to the jet observations.

Also huge data set on misalignment is available due to GW observations.

QPO

BH candidates demonstrate two main types of QPOs:
Low-frequency (0.1-30 Hz) and high-frequency (40-450 Hz).

Low-frequency QPOs are found in many well-studied objects.
They are observed during different states of sources.
Probably, in different states, different mechanisms of QPO are working.

High-frequency QPOs are known in a smaller number of sources.
It is supposed that the frequencies of these QPOs correspond to the ISCO.

Recent reviews: Ingram, Motta 2001.08758

Different types of variability in BH sources are also discussed in
1407.7373 and 1603.07872.

About NS QPOs see a review in 2010.08291

BH low-frequency QPOs in various states

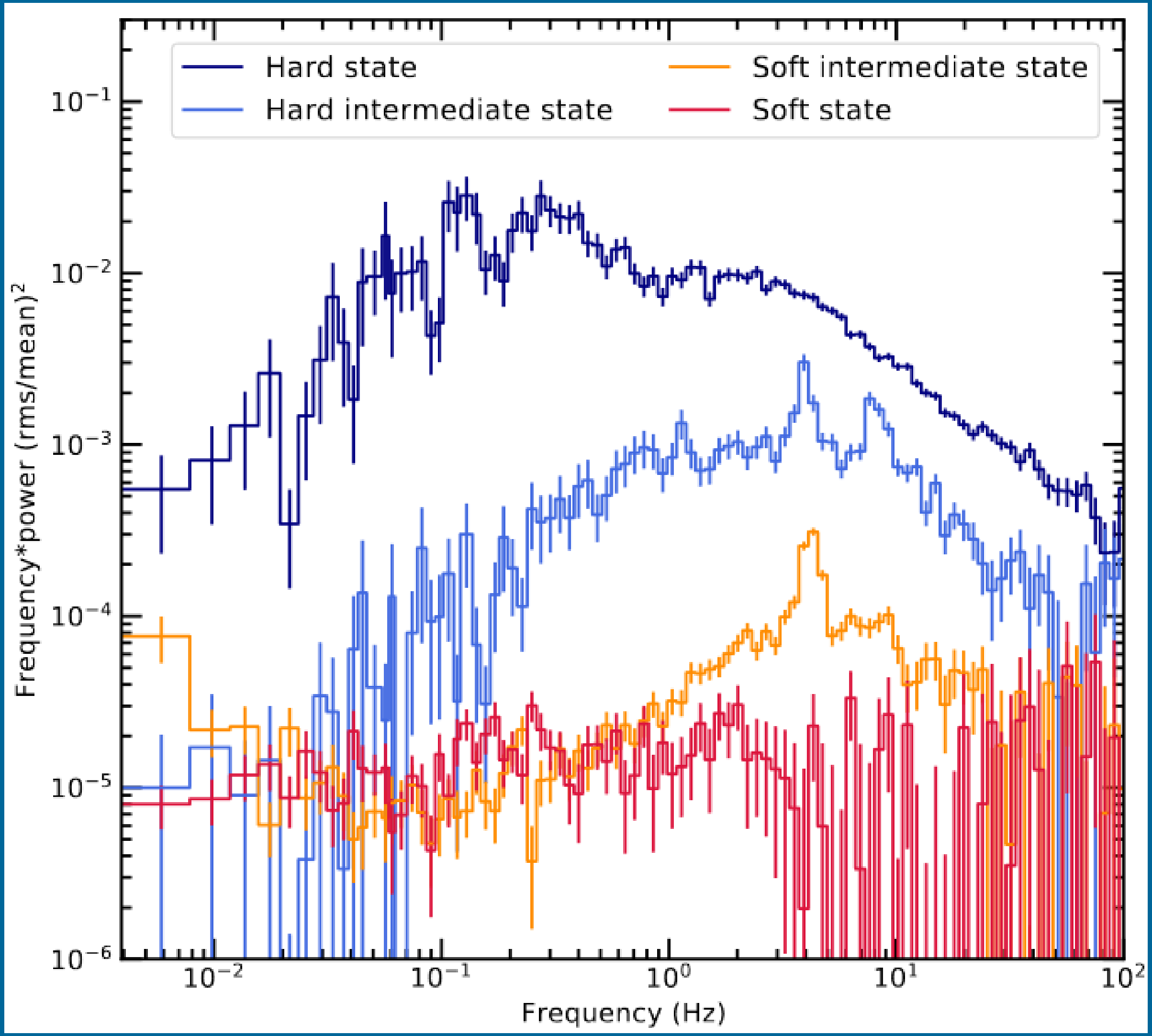

The power spectral density of MAXI J1820+070 in four spectral states.

2206.14410

Low-frequency QPO

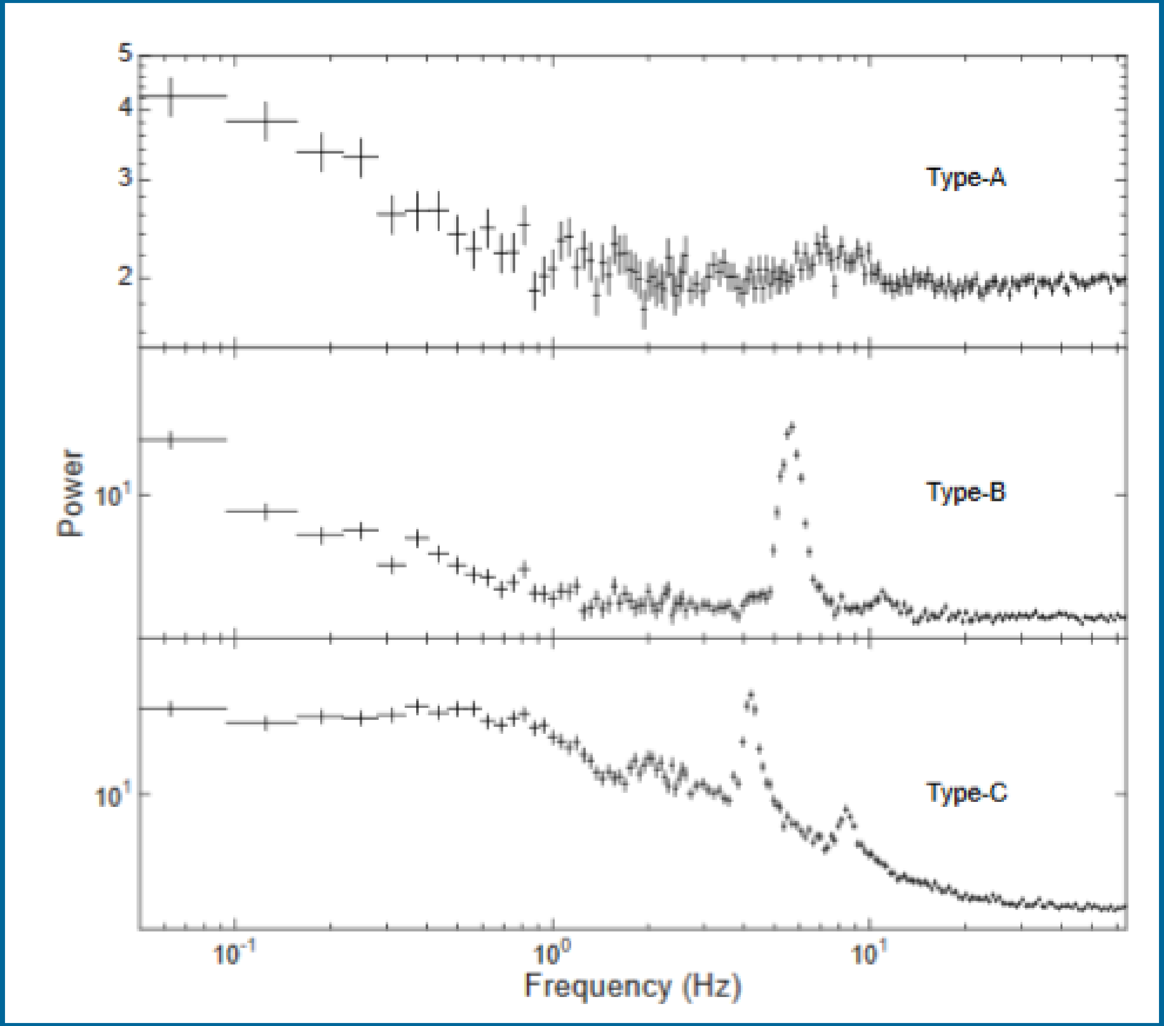

Disc instabilities ?

Jets?

Lense-Thirring precession?
(see e.g., 2206.14410)

1603.07885

Low-frequency QPO due to a jet?

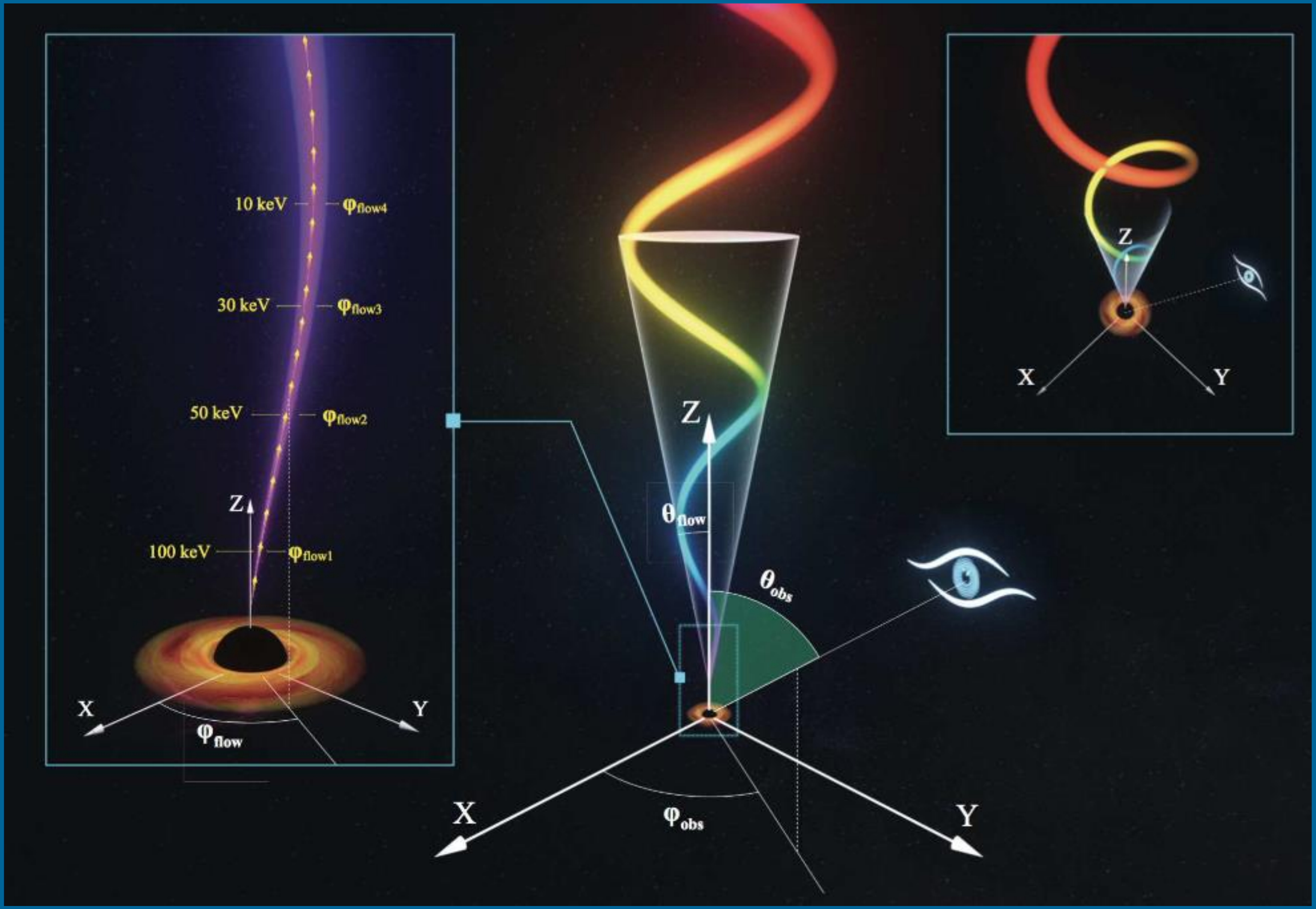

MAXI J1820+070

Observations with Insight-HXMT up to 200 keV.

2009.10607

GRS 1915+105

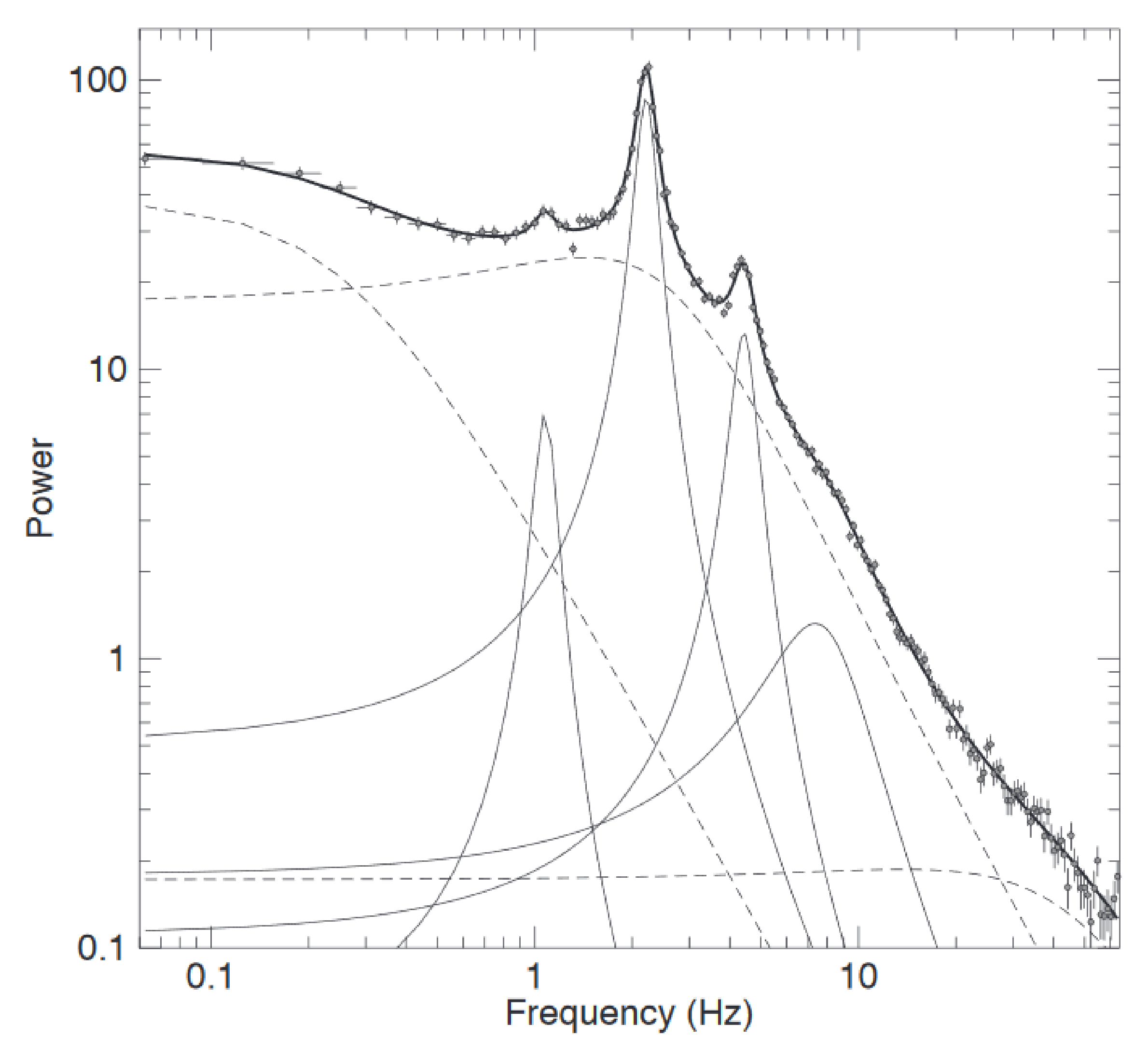

Low-frequency QPO.

Peaks are harmonically related. The main is the highest peak.

1902.06586

GRS 1915+105

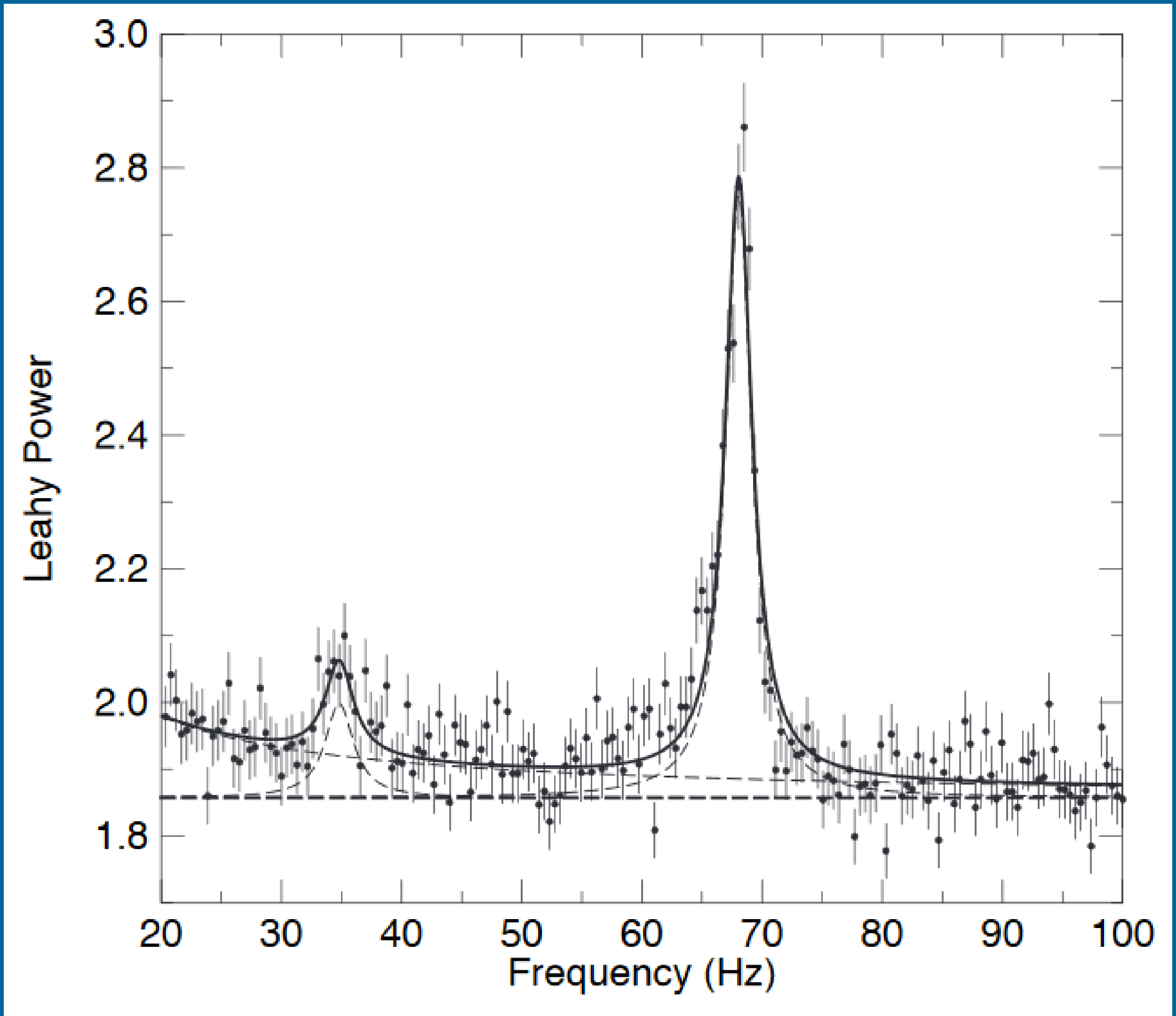

High-frequency QPO

1902.06586

QPO and flux from a disc

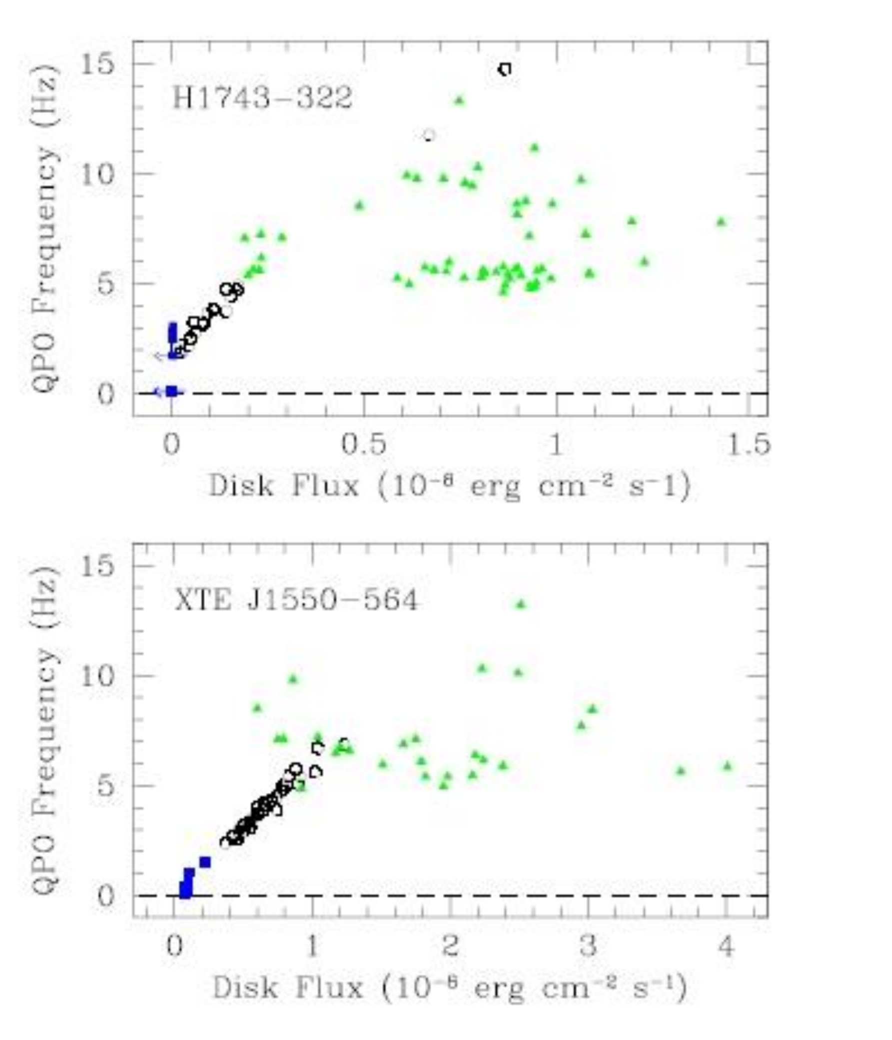

SPL – green triangles
Hard – blue squares
Intermediate states – black circles

Low-frequency QPOs
(their frequency and amplitude)
correlate with spectral parameters.

Probably, QPO mechanisms
in the hard state
and in the SPL state are different.

(Remillard, McClintock astro-ph/0606352)

QPO at high (for BHs) frequency

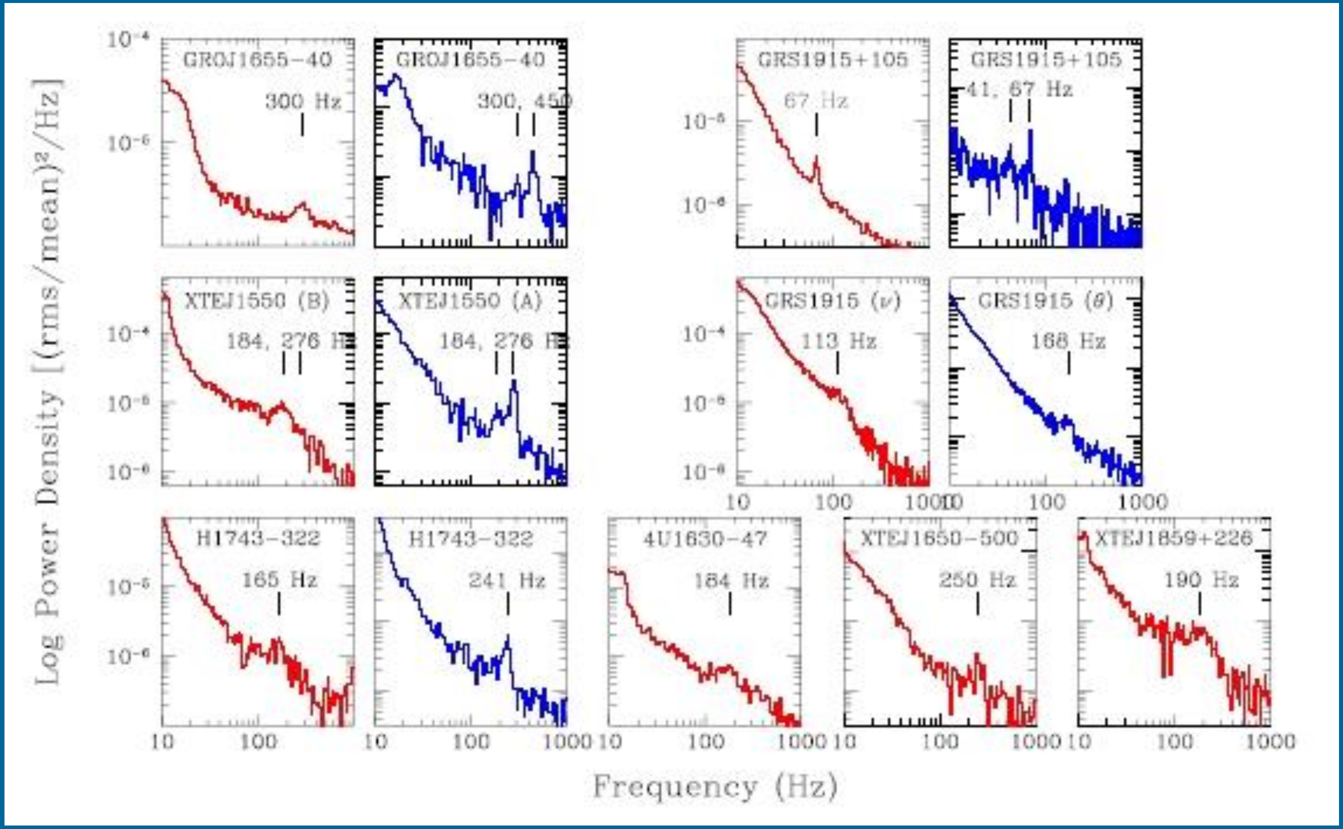

All QPO at >100 Hz are observed only in the SPL state.

Blue curves: for the range 13-30 keV.
Red curves: for a wider range (towards lower energies).

(Remillard, McClintock astro-ph/0606352)

Possible interpretations

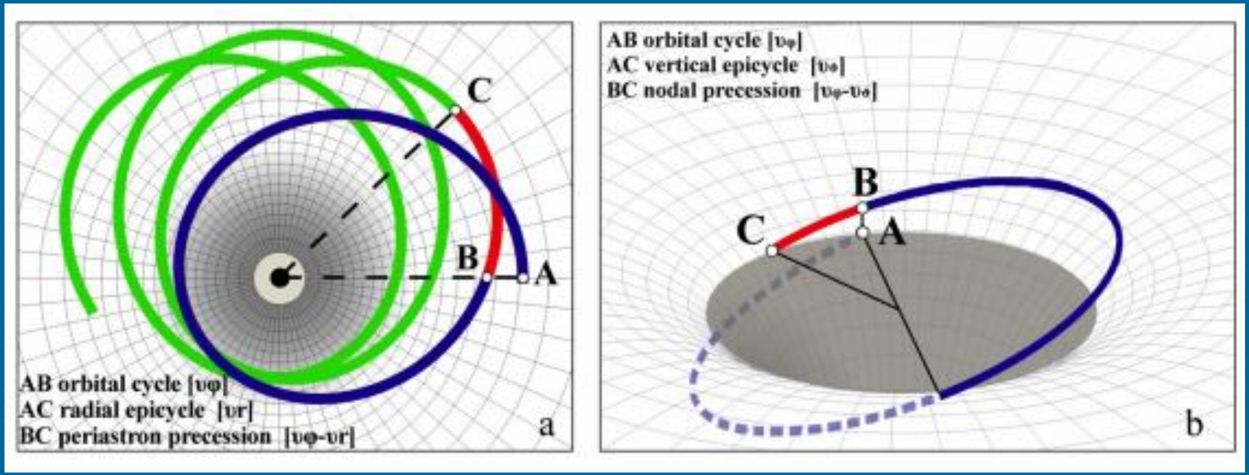

ν_φ – *Keplerian frequency*
ν_r – *radial epicyclic*
ν_θ – *vertical epicyclic*

periastron precession frequency $\nu_\varphi - \nu_r$
nodal precession frequency $\nu_\varphi - \nu_\theta$

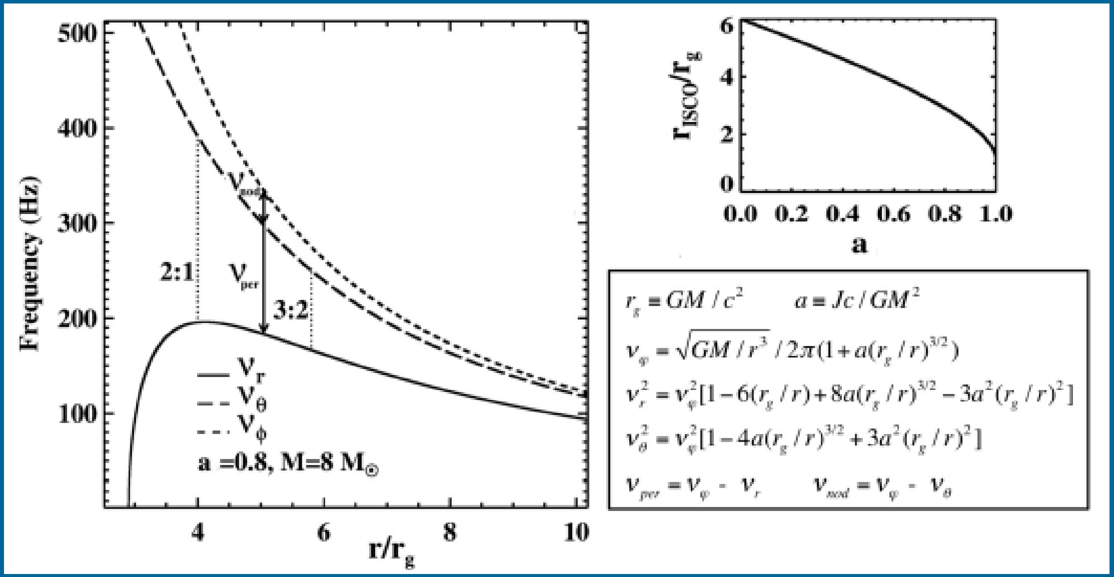

1407.7373

Correlations

Such measurement allow to derive a model dependent estimate of the mass and the spin in the framework of the relativistic precession.

GRO J1655-40

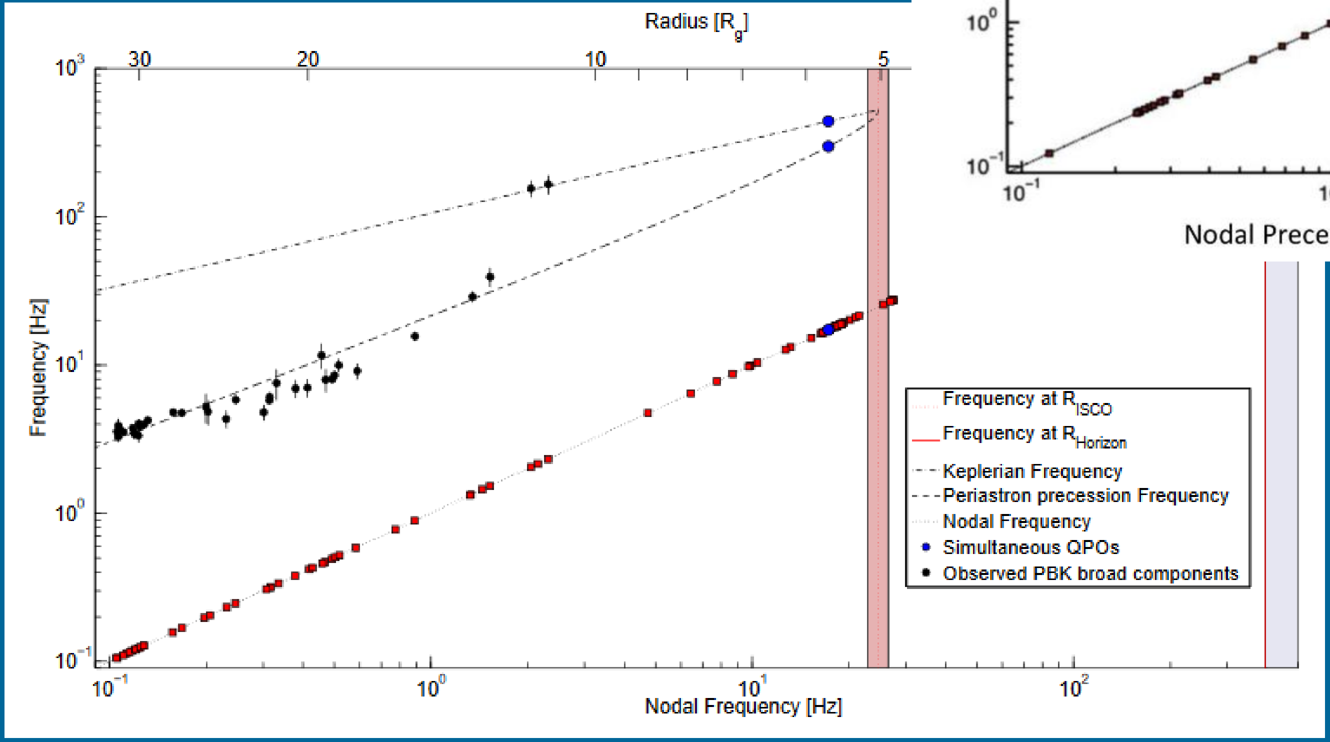

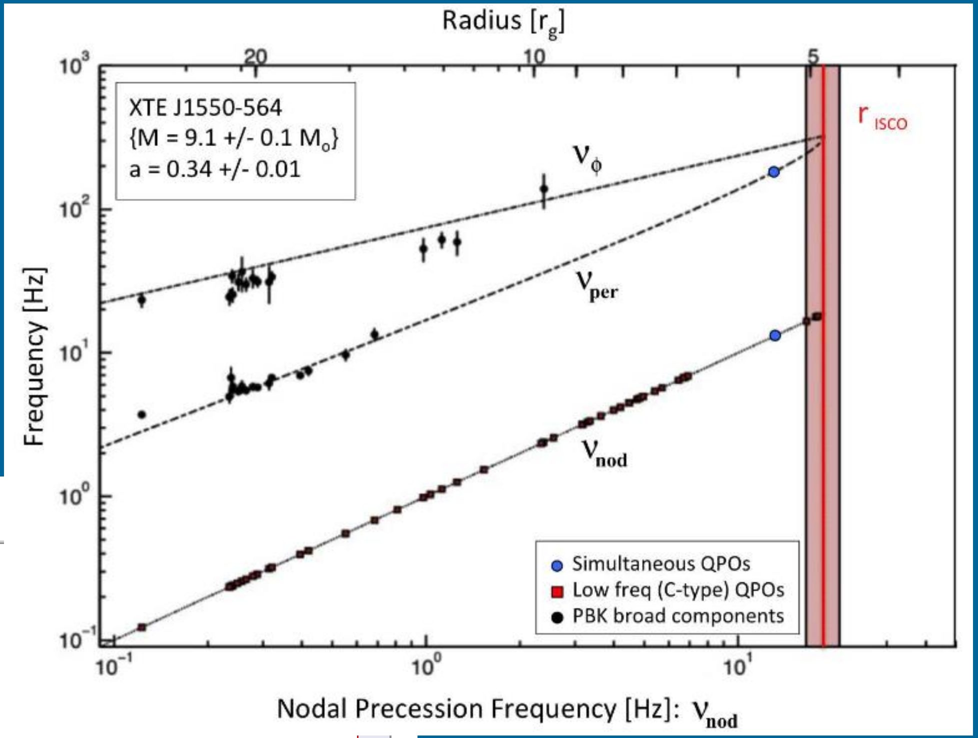

XTE J1550-564

Recently, similar data were also obtained for XTE J1859+226, see 2209.10376

1902.06586

Rotation and ISCO

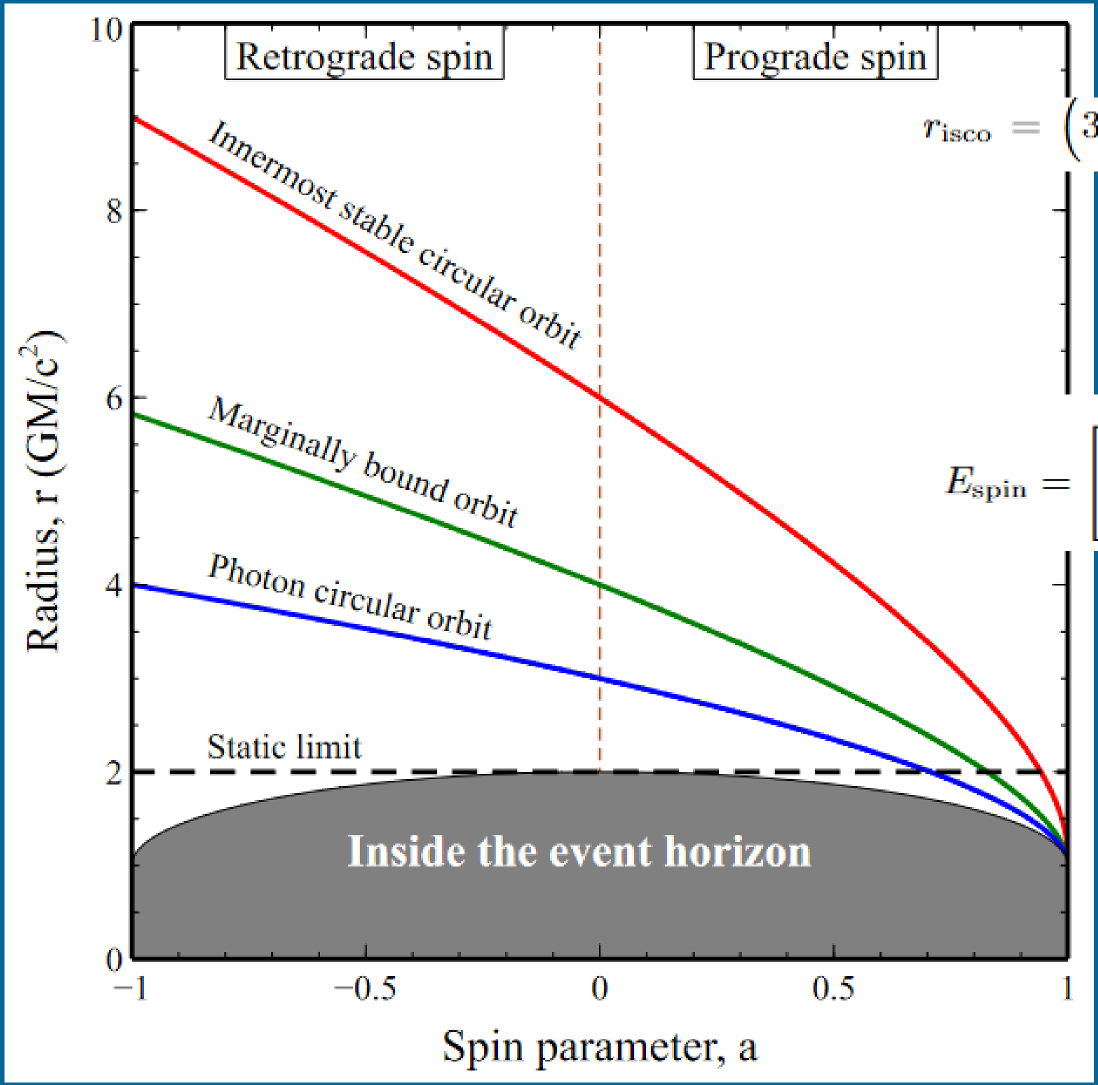

$$r_{\rm isco} = \left(3 + Z_2 \mp [(3 - Z_1)(3 + Z_1 + 2Z_2)]^{1/2}\right) r_g,$$

$$r_{\rm mb} = \left(2 \mp a + 2\sqrt{1 \mp a}\right) r_g,$$

$$r_{\rm ph} = 2\left(1 + \cos\left[\frac{2}{3}\cos^{-1}(\mp a)\right]\right) r_g,$$

$$E_{\rm spin} = \left[1 - \frac{1}{2}\left(\left[1 + \sqrt{1 - a^2}\right]^2 + a^2\right)^{1/2}\right] Mc^2,$$

2011.08948

QPOs and BH masses

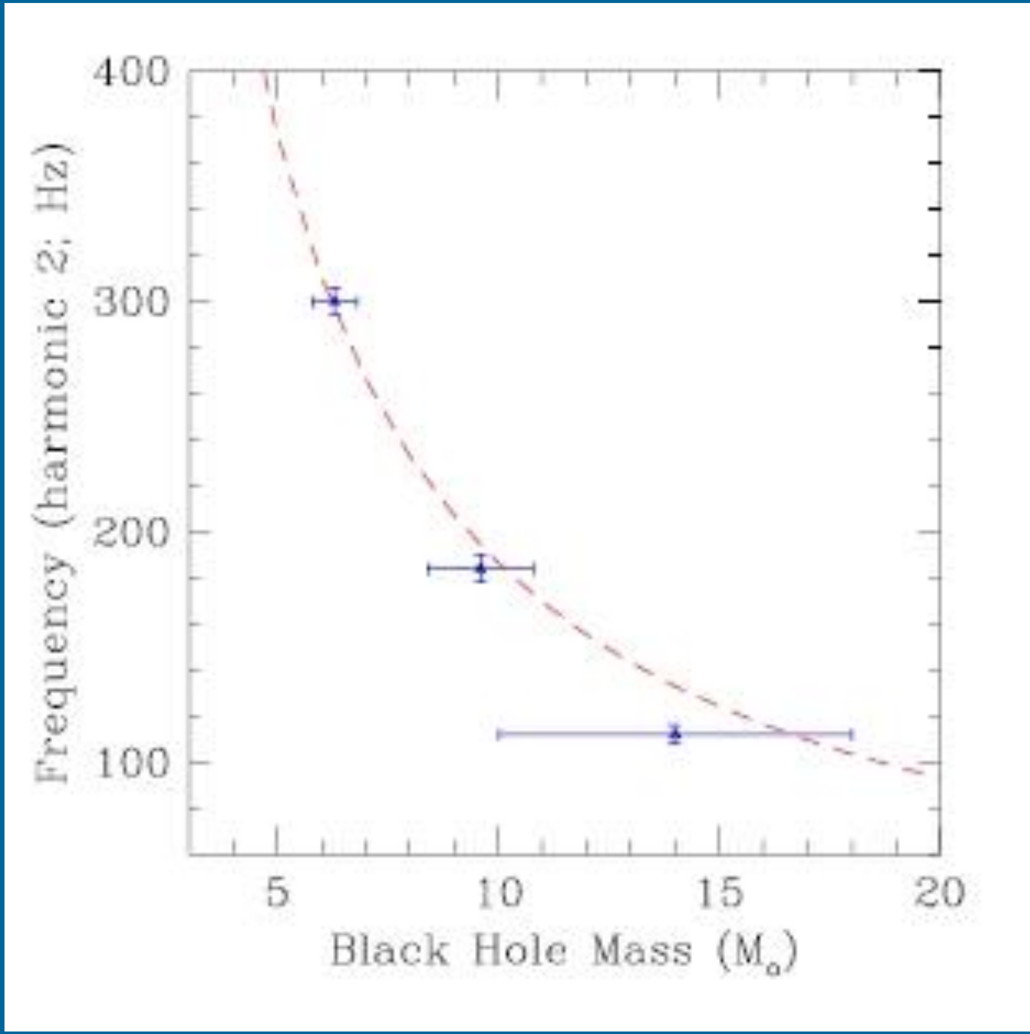

XTE J1550-564,
GRO J1655-40,
GRS 1915+105

Dashed line is plotted for the relation
v_0 = 931 Hz $(M/M_O)^{-1}$
The ordinate shows $2v_0$

(Remillard, McClintock astro-ph/0606352)

Extragalactic BHs: the case of M31

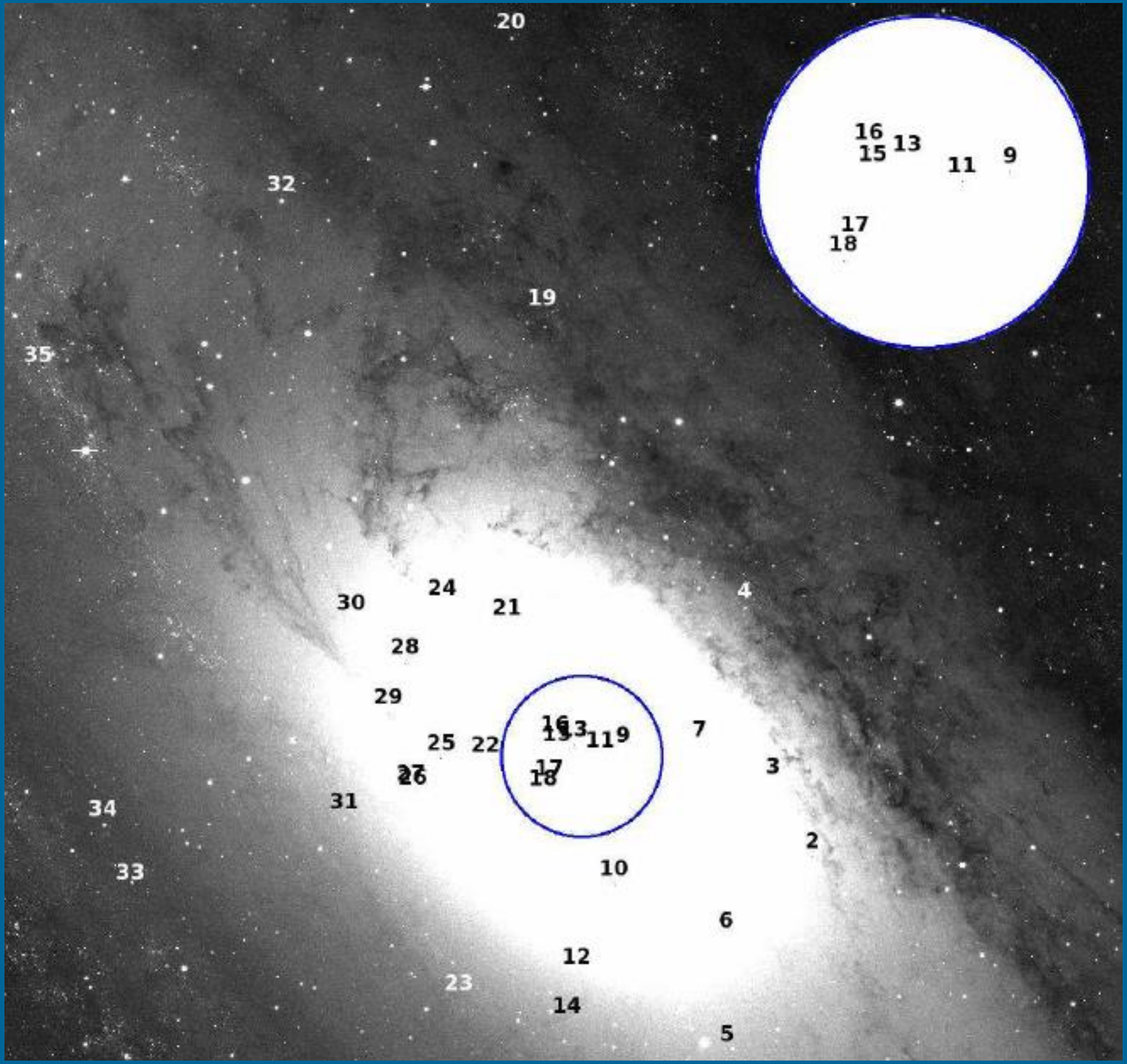

Chandra identification of 26 new black hole candidates in the central region of M31

arXiv:1304.7780

50 BHCs in M31

Src	ID	$D_{M31*}/'$	L^{x}_{Max}	Γ_{Max}	L^{x}_{Min}	Γ_{Min}	N_O	DC 1	DC 2	χ^2_{con}/dof
S109	BH1	15.85	37 (5)	1.5 (3)	14.1 (17)	1.4 (3)[a]	P			230/76
S111	T1	6.24	18.3 (17)	2.0 (4)	<0.06	1.9 (5)[a]	2	0.04	0.06	234/79
S117	T2	5.11	53 (3)	4.9 (6)	<0.04	1.7	1	0.05	0.05	3957/99
S122	BH2	5.28	15 (2)	1.47 (7)[a]	1.73 (15)	1.47 (7)[a]	P			1527/164
S151	BH3	4.06	31 (2)	2.5 (5)	4.31 (17)	1.552 (15)[a]	P			28720/166
S159	BH4	4.63	5.5 (5)	1.89 (7)[a]	0.39 (0.10)	1.89 (7)[a]	P			3999/167
S167	BH5	6.85	7.9 (1.6)	1.5 (1)[a]	1.7 (2)	1.5 (1)[a]	P			568/157
S168	BH6	4.83	19.0 (18)	1.58 (3)[a]	0.6(2)	1.58 (3)[a]	P			5639/162
S179	BH7	2.49	21 (2)	2.7 (5)	4.9(13)	1.69 (3)[a]	P			669/168
S199	BH8	19	19 (3)	1.8 (4)	<0.4	1.37 (15)[a]	Many	0.33	0.33	664/26
S214	BH9	0.9	8.5 (4)	2.36 (16)[a]	0.05	2.36 (16)[a]	3	0.08	0.09	3482/94
S223	BH10	2.78	4.5(4)	1.64 (5)[a]	0.55(7)	1.64 (5)[a]	P			4983/167
S233	T5	0.66	9.8(13)	2.0 (5)	<0.04	1.7	2	0.02	0.06	317/100
S236	BH11	0.41	23(2)	1.41 (7)[a]	<0.05	1.41 (7)[a]	1 (turn off)	0.16	0.12	2319/95
S251	U2	9.2	320 (8)	3.9 (5)	<0.4	1.7	1	0.11	0.08	61651/69
S265	BH12	4.52	9.0(18)	2.5 (9)	1.5(2)	2.08 (4)	P			3701/167
S269	BH13	0.26	4.9(3)	1.78 (5)[a]	0.76(8)	1.78 (5)[a]	P			3625/170
S276	BH14	5.55	14 (2)	2.9 (7)	<0.05	2.6 (3)[a]	1	0.30	0.17	8381/98
S286	BH15	0.5	7.9 (9)	1.61 (4)[a]	1.2 (2)	1.61 (4)[a]	P			3472/170
S287		2.1	20.5 (5)	3.67 (13)	0.07(2)	1.7	1	0.05	0.03	82/92
S289	BH16	0.62	26.3 (6)	1.58 (3)[a]	0.6 (2)	1.58 (3)[a]	P			16817/164
S293	B128	4.96	5.9 (5)	1.64 (10)[a]	<0.03	1.64 (10)[a]	2	0.14	0.13	2348/87
S297	BH17	0.89	8.0 (3)	1.91 (4)[a]	0.73 (14)	1.91 (4)[a]	P			4602/170
S299	BH18	1.12	20 (2)	1.50 (2)[2]	6.8 (8)	1.8 (3)	P			842/170
S300	BH19	9.26	21 (3)	1.9 (6)	0.75(18)	1.84 (5)[a]	P			9096/127
S322		1.62	13 (2)	2.5 (6)	<0.04	1.7	1	0.02	0.04	227/72
S327	BH20	15.1	62 (3)	1.14 (14)	30 (2)	1.89 (2)[a]	P			587/73
S330	T8	8.4	2.7 (4)	2.10 (17)[a]	<0.06	2.10 (17)[a]	1 (turn on)	0.73	0.79	2941/158
S331	T13	1.6	6.1 (6)	4.02 (17)	<0.0016	1.7	1	0.018	0.05	171/45
S335	BH21	3.2	20.6(17)	1.9 (4)	5.6 (4)	1.7	P			441/108
S339	T9 / U1	2.4	394 (2)	?	<0.025	1.74 (2)[a]	1	0.06	0.04	37255/89
S345	BH22	2	23 (2)	1.70 (5)[a]	0.82 (18)	1.7	P			5782/108
S353		3.5	5.8 (15)	1.6 (3)[a]	<0.05	1.70 (5)[a]	5	0.20	0.21	1984/112
S358	BH23	5.7	8.9(13)	2.5 (6)	<0.18	1.6 (3)[a]	P			651/167
S365		2.8	14(2)	2.9 (9)	<0.009	1.78 (4)	1	0.06	0.04	503/60
S372	BH24	4.3	7.2(13)	1.8 (4)	2.8(3)	2.37 (19)[a]	P			801/168
S373	BH25	2.9	7.2 (11)	1.9 (6)	3.1(9)	1.78 (8)	P			406/107
S386	BH26	3.6	8.2 (13)	1.84 (5)[a]	1.3 (2)	1.4 (3)	P			5245/170
S389	BH27	3.6	13.0 (18)	2.01 (5)[a]	0.37 (9)	1.84 (5)[a]	P			14549/170
S391	BH28	4.2	7.7 (3)	1.69 (4)[a]	1.8 (2)	2.1 (5)	P			2885/169
S396	BH29	4.1	46.8 (5)	1.46 (8)[a]	<0.07	1.69 (4)[a]	1	0.05	0.05	20445/99
S411	BH30	5.6	12 (2)	1.9 (6)	<0.16	1.46 (8)[a]	Many	0.26	0.42	2667/145
S415	BH31	5.1	20 (3)	1.6 (3)	7.5 (14)	1.9 (2)[a]	P			511/102
S438	BH32	13.2	14.2 (12)	1.6 (2)	<0.007	1.47 (2)[a]	3	0.70	0.13	3195/76
S448		6.9	97 (6)	3.8 (4)	<0.04	1.58 (2)[a]	2	0.06	0.10	3198/89
S484	BH33	9.8	10 (3)	1.94 (6)[a]	1.4 (2)	1.7	P			1450/111
S487	BH34	10.1	10.2 (13)	1.9 (5)	3.3 (11)	1.94 (6)[a]	P			100/39
S497	BH35	13.9	12.8 (15)	1.7 (4)	1.07 (16)	1.49 (5)[a]	P			2578/78

Classification is mainly based on spectral properties.

1406.6091

Ultraluminous X-ray sources

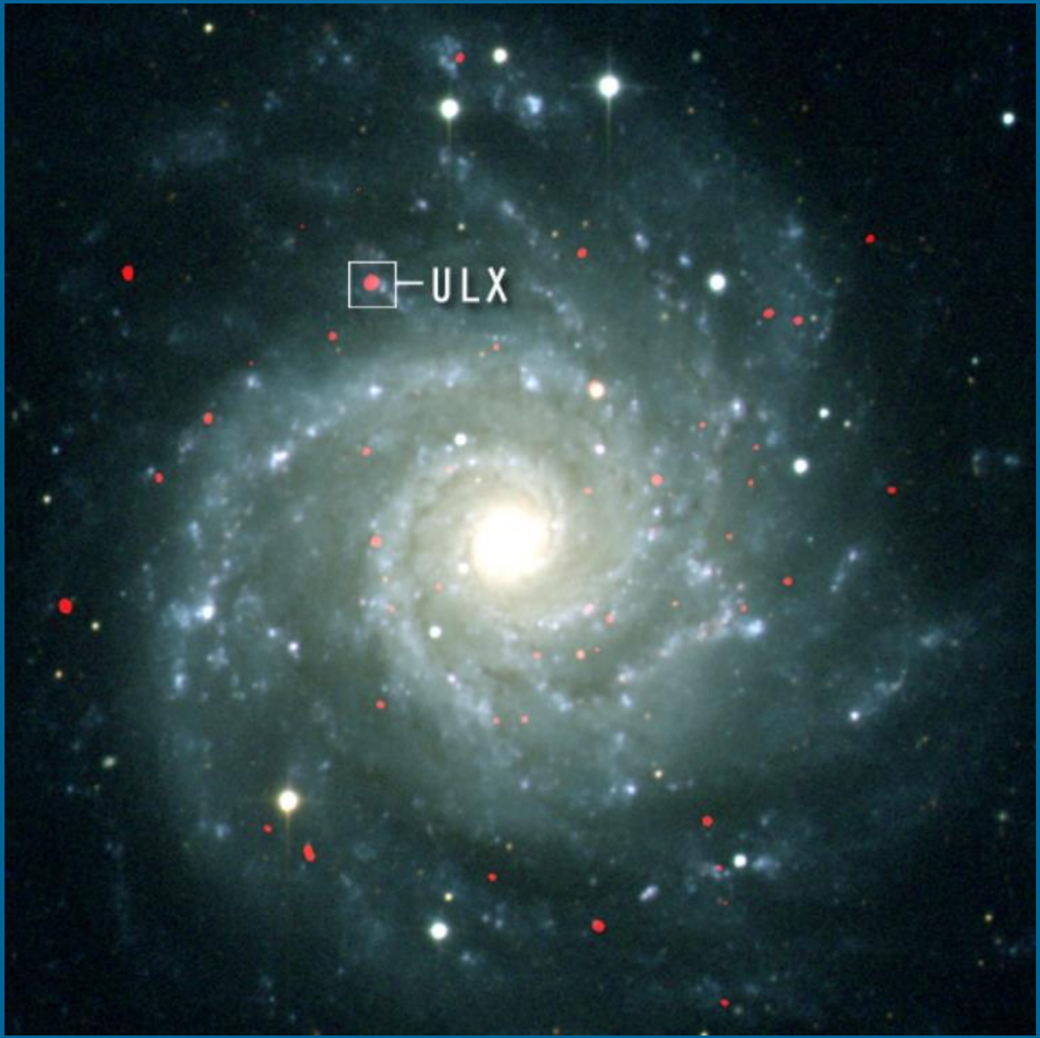

ULXs are sources with fluxes which correspond to an isotropic luminosity larger than the Eddington limit for a 10 solar mass object.

ULXs in NGC 4490 and 4485

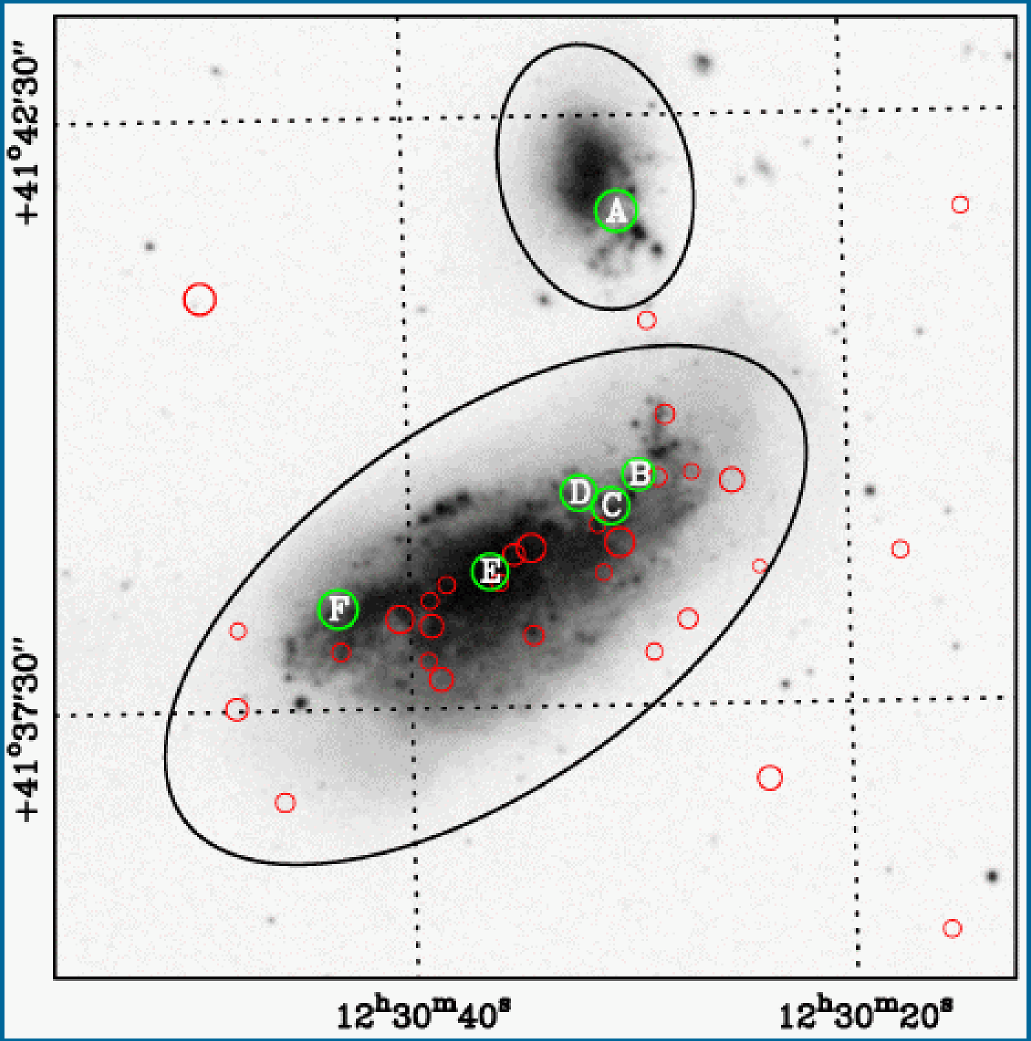

Six marked sources are ULXs

Spectrum of the ULX in NGC 1313

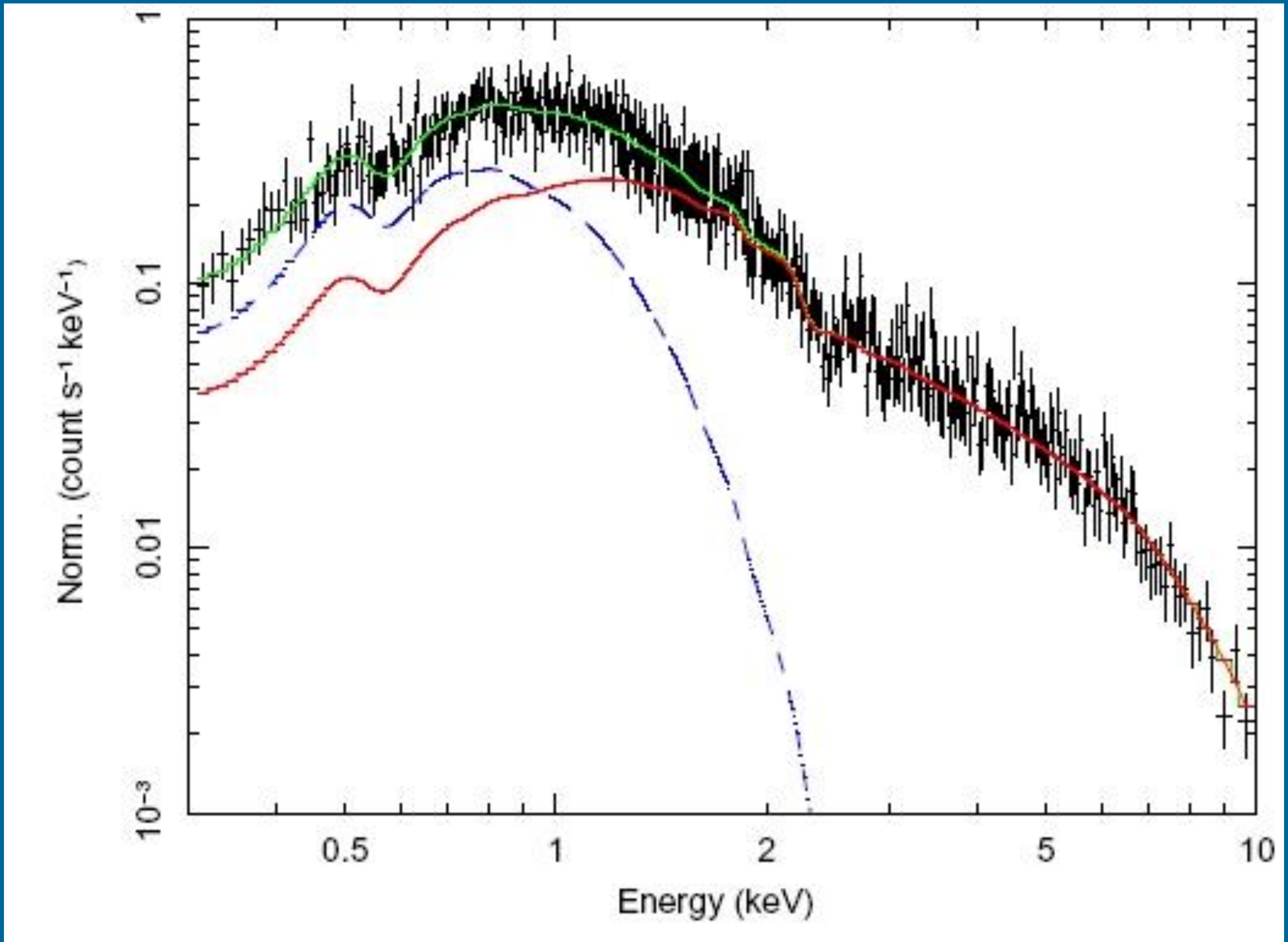

NGC 1313 X-1

Green line –
the IMBH model.

Red – power-law.

Blue – multi-color disc.

arXiv 0706.2562

ULX in galaxies of different types

In the following two slides there are images of
several galaxies from the SDSS in which positions of ULXs are marked.

Crosses (x) mark sources with luminosities $>10^{39}$ erg/s.
Pluses (+) mark sources with luminosities $>5\ 10^{38}$ erg/s.

The size of one square element of the grid is 1.2 arcminute
(except IZW 18, in which case the size is 0.24 arcminute in right ascension and 0.18 in declination).

Galaxies NGC 4636, NGC 1132, NGC 4697, NGC 1399 are ellipticals,
IZW 18 – irregular, the rest are spiral galaxies.
Ellipses mark the 25-th magnitude isophotes
(this a typical way to mark the size of a galaxy).

ULX in galaxies of different types

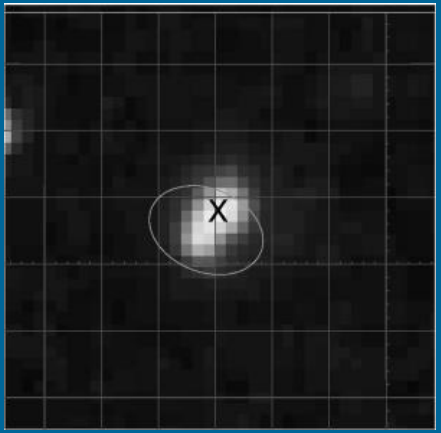

IZW 18

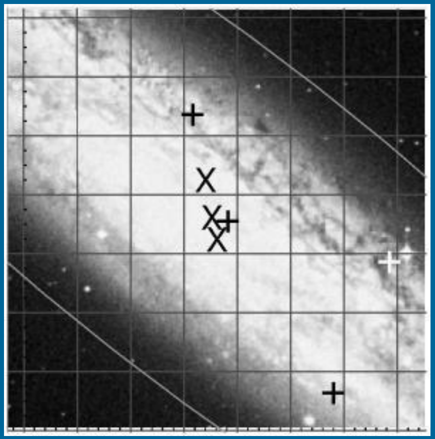

NGC 253

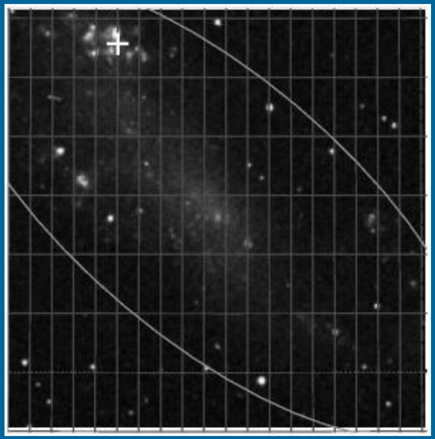

IC 2574

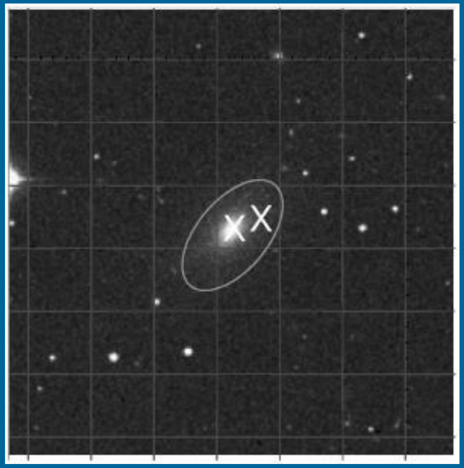

NGC 1132

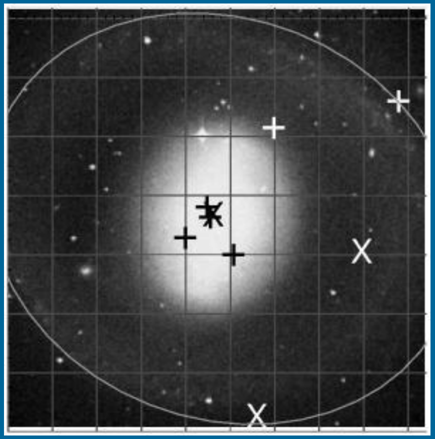

NGC 1291

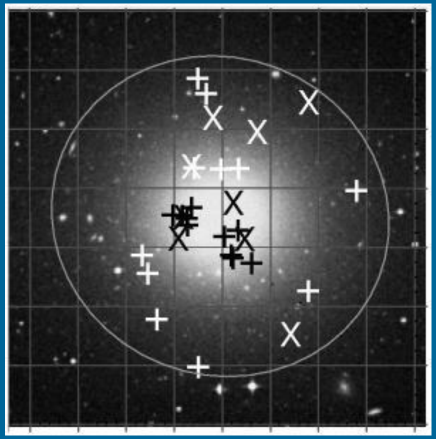

NGC 1399

ULX in galaxies of different types

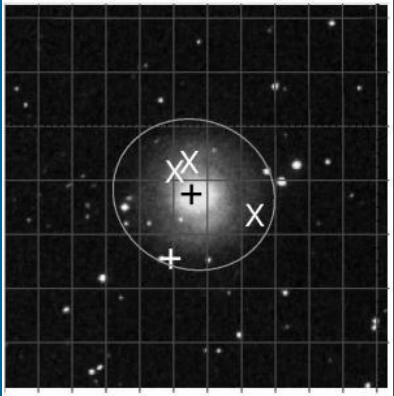

NGC 2681

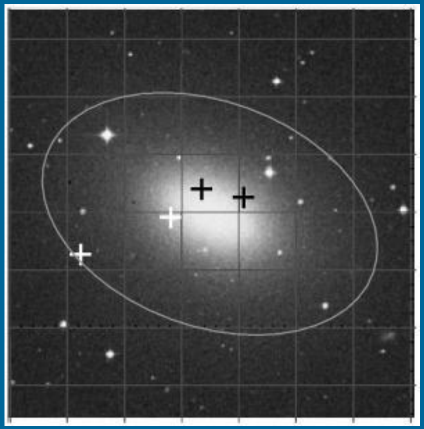

NGC 4697

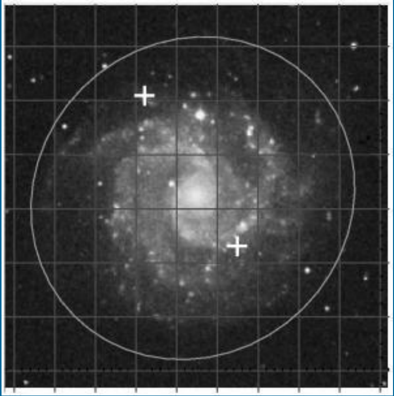

NGC 3184

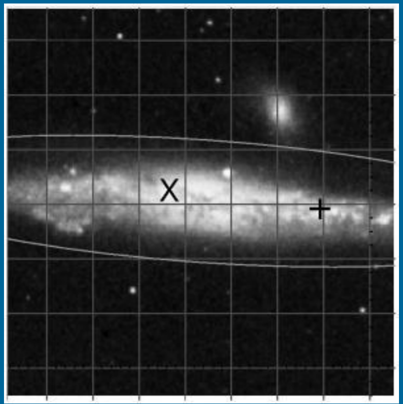

NGC 4631

Large sample of
host galaxies for ULX:
1108.1372

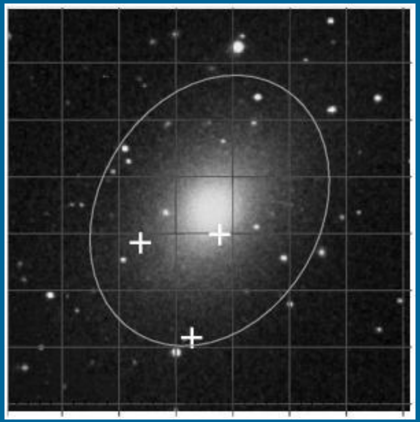

NGC 4636

Statistical studies of ULXs

A clean sample of 1342 ULXs and 191 HLXs.

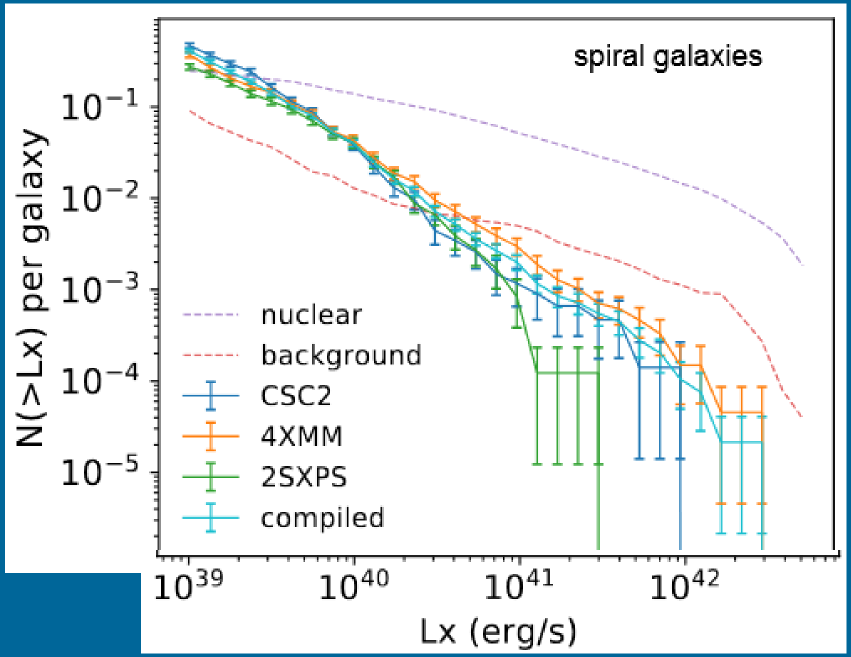

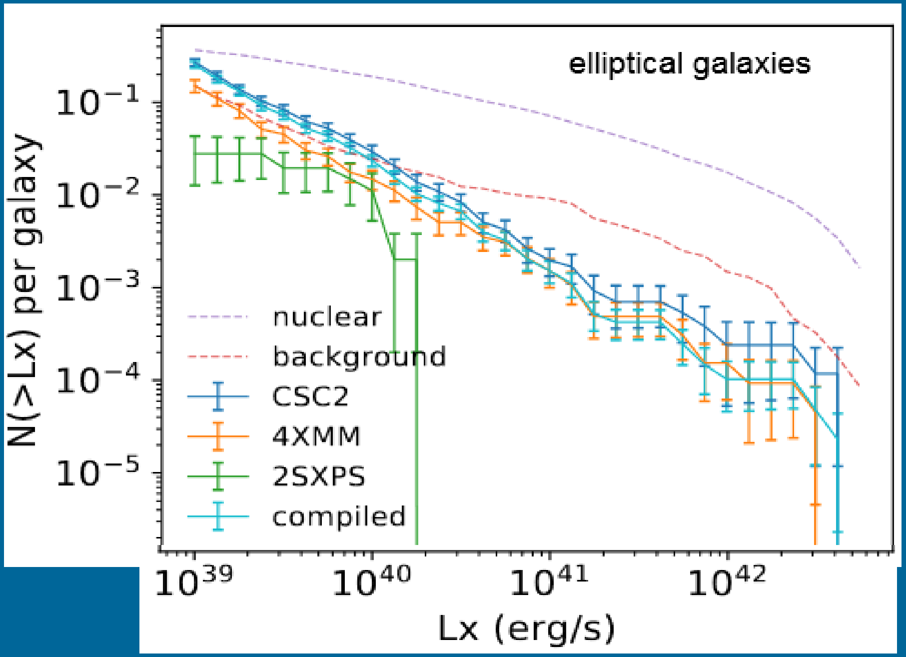

2304.11216

ULXs in globular clusters

Donors are low-mass stars.

GC in 21 early-type galaxies.
10 ULX candidates in GCs found.
24 our of GCs.

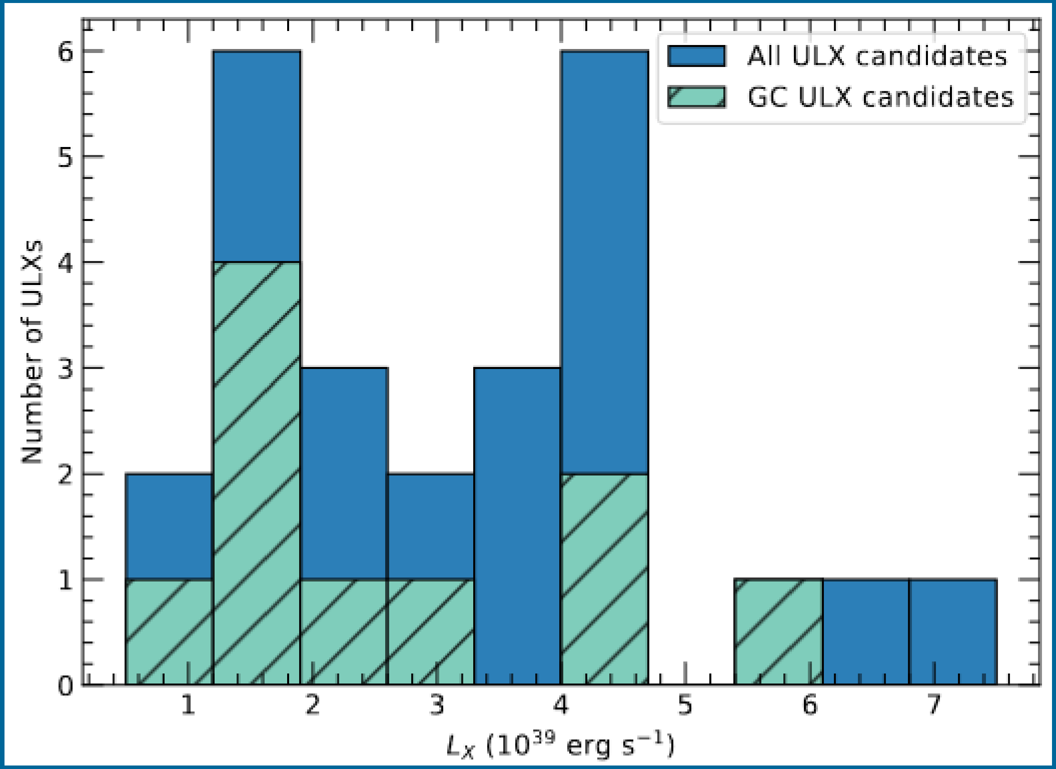

2211.07699

Properties of galaxies with ULXs

The authors used Chandra data to make a census of ULXs in galaxies at d<40 Mpc.
They present statistical properties of the galaxies with ULXs:
629 sources in 309 galaxies.

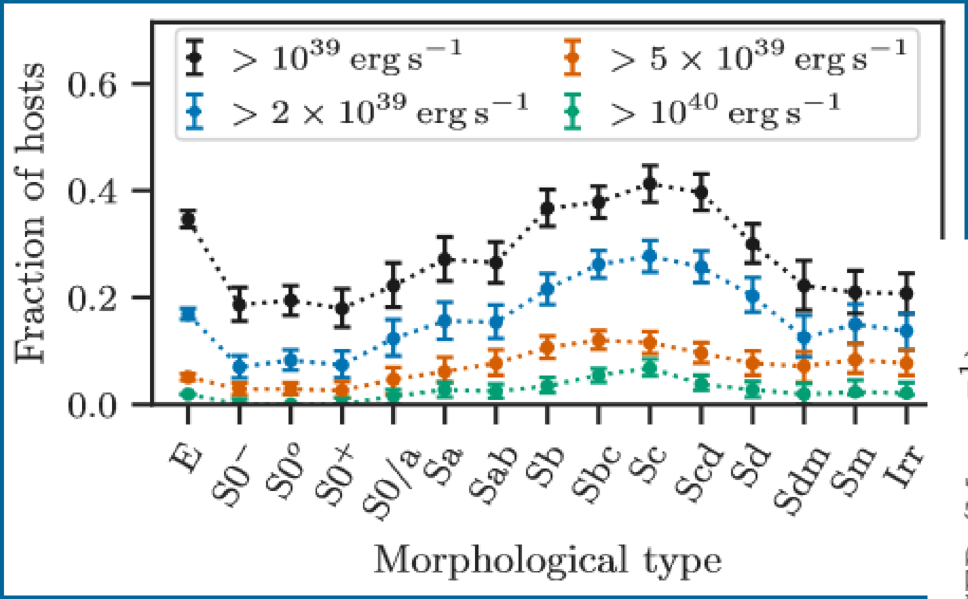

Numbers in boxes denote the number of galaxies in each bin.

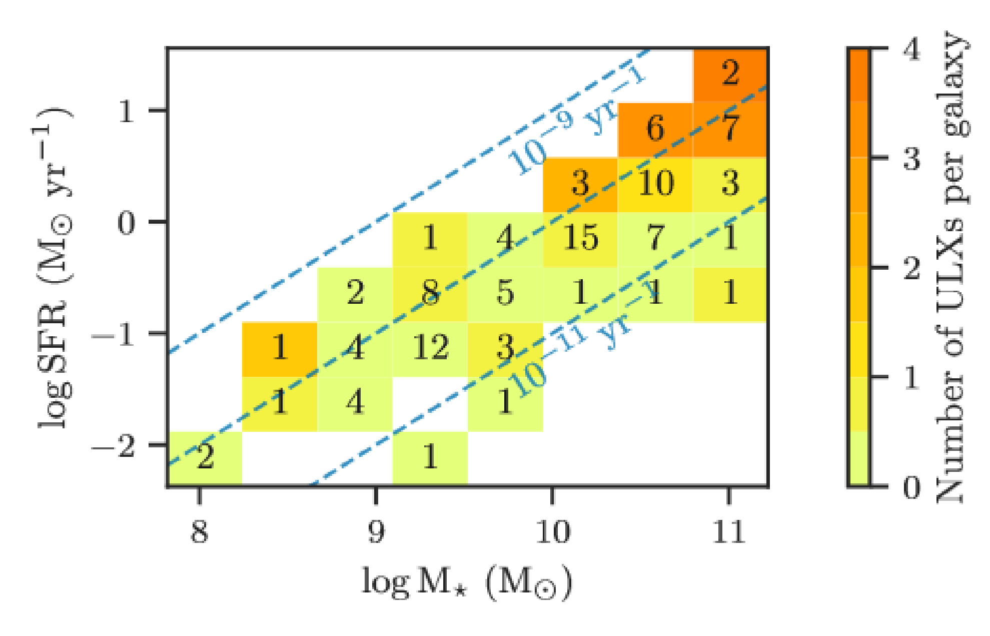

The source X-1 in M82

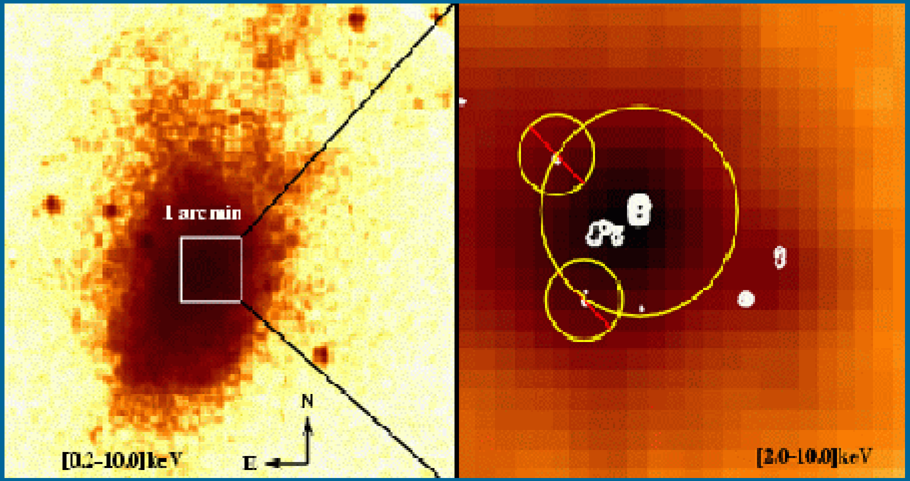

The source M82 X-1 is one of the most luminous, and so it is the best candidate to be an intermediate mass BH.

QPOs are observed in this source. Their properties support the hypothesis of an intermediate mass BH.

QPO was recently detected (1309.6101).
Scaling points to masses 10^4-10^5 solar masses.

Pasham et al. (2014) estimated the mass to be 400 Msolar
Nature **513**, 74–76 (04 September 2014)

M82, stellar clusters and ULXs

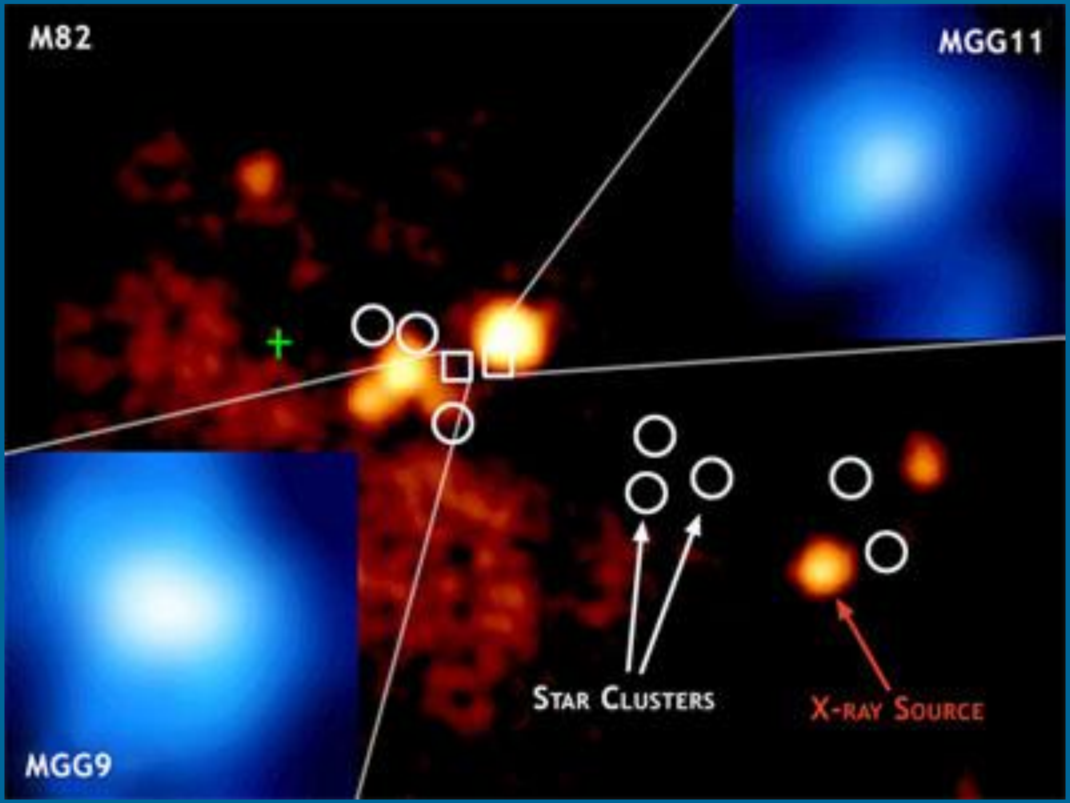

Intermediate mass BHs can be formed in dense stellar clusters.

See, however, 0710.1181 where the authors show that for solar metallicity even very massive stars most probably cannot produce BHs massive enough.

McCrady et al (2003)

http://www.nature.com/nature/journal/v428/n6984/full/nature02448.html

X41.4+60 in M82

79-day burst. Isotropic luminosity ~5 10^{40} erg/s
Hard state. Usually L~0.3 L_{edd}, here there are indications (photon index Γ= 1.6) that it is even ~0.1 L_{edd}.

QPOs.

Altogether: mass ~ few 1000 Solar.

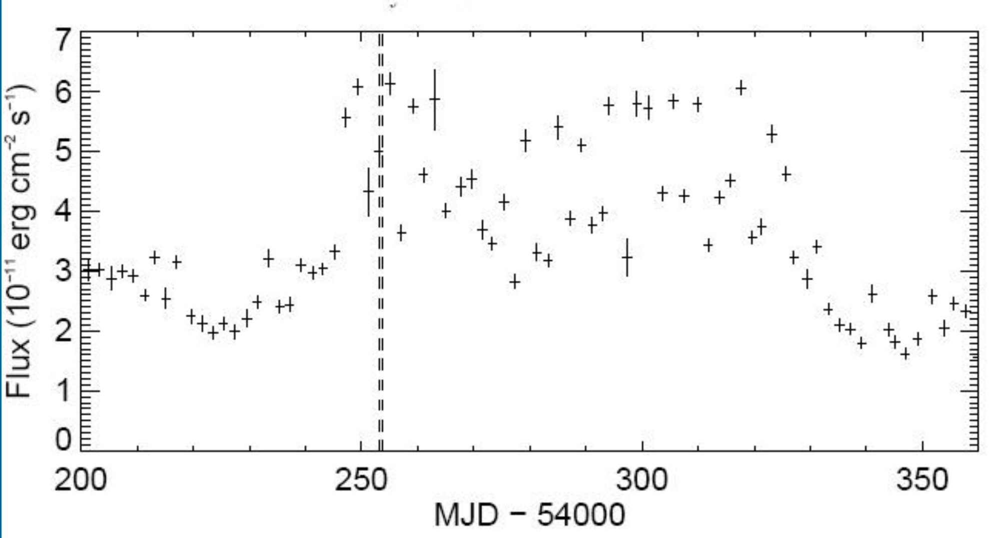

RXTE + Chandra observations

(Kaaret et al. 0810.5134)

The most luminous ULX:
HLX-1 in the galaxy ESO 243-49,

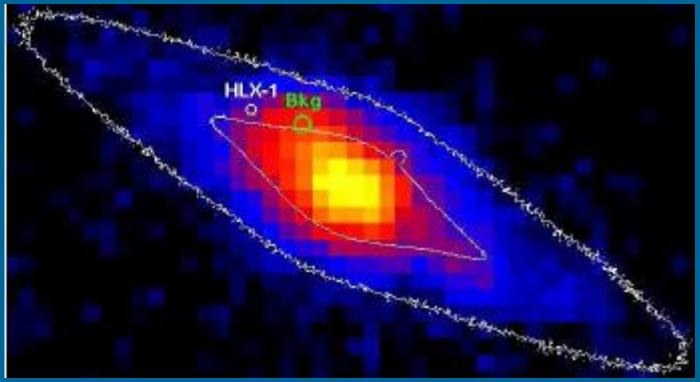

$L>10^{42}$ erg/s
$M \sim 500 M_{\odot}$

1011.1254, 1104.2614

New data about this source: 1108.4405; 1203.4237; 1210.4169; 1210.4924

Origin of IMBHs

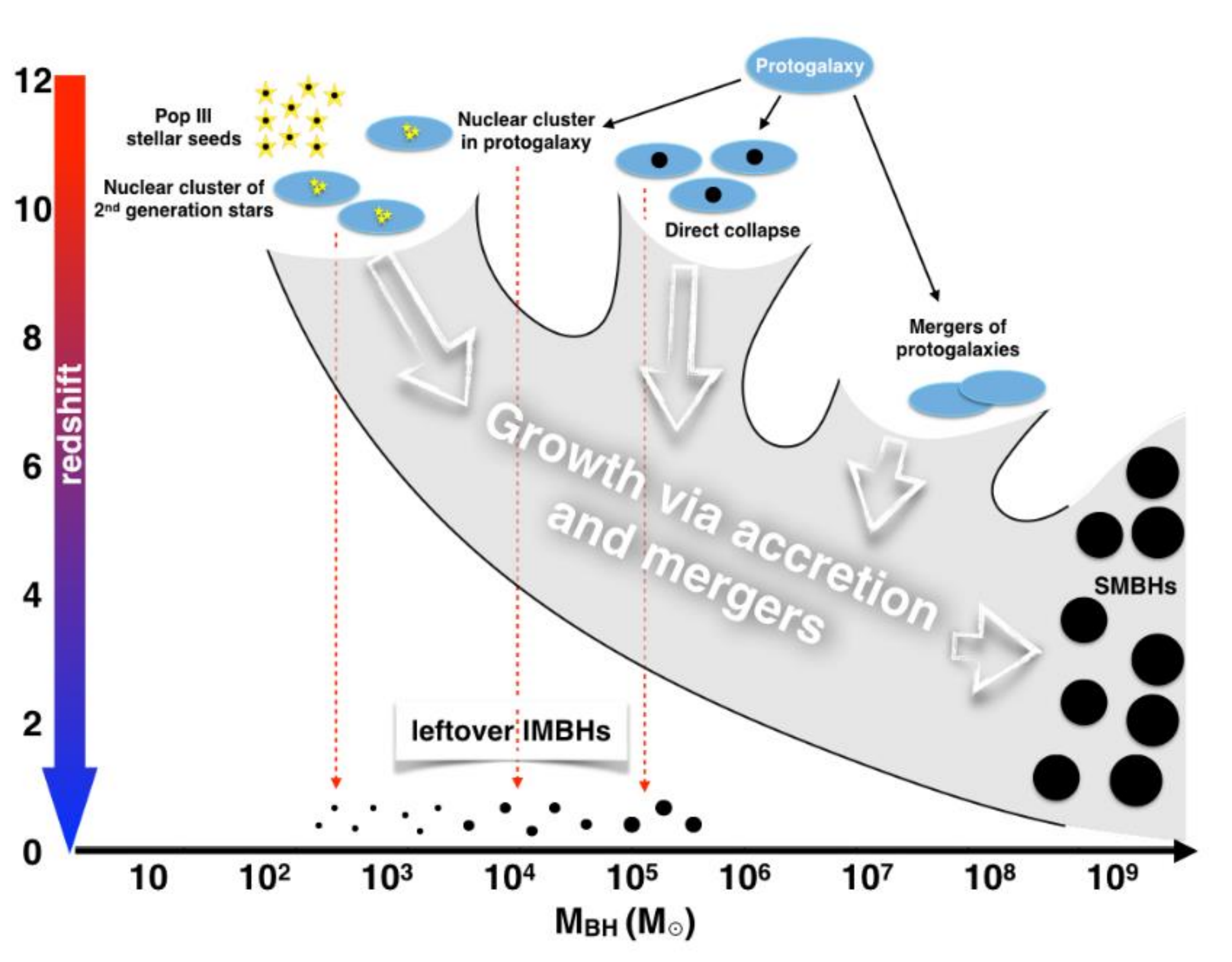

1705.09667 See also a review in 1801.01095

State transitions in ESO 243-49 HLX-1

Mass is estimated to be 10^4-10^5 Msolar

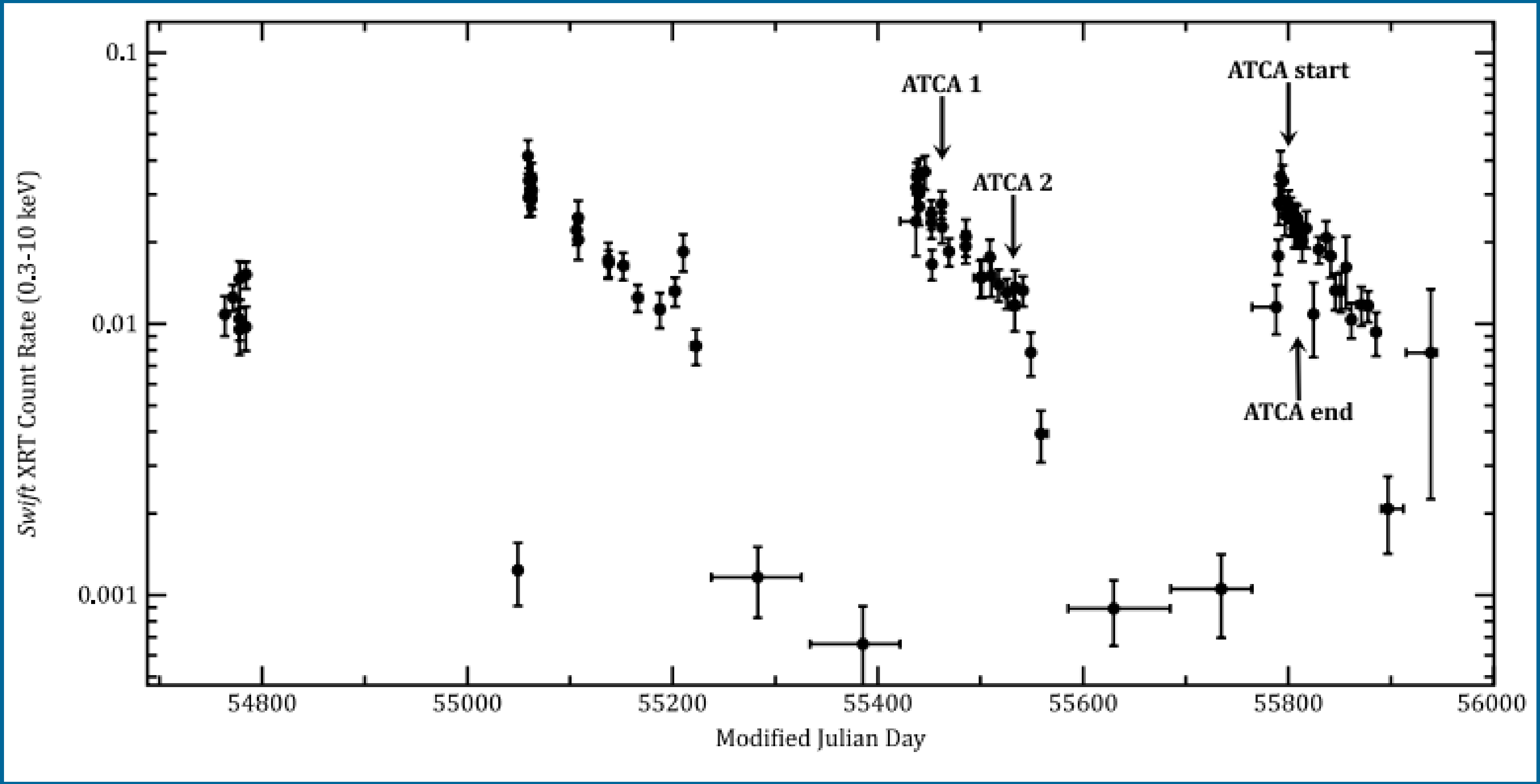

1311.6918

More mass estimates for HLX-1

Taking into account all uncertainties the mass is still large

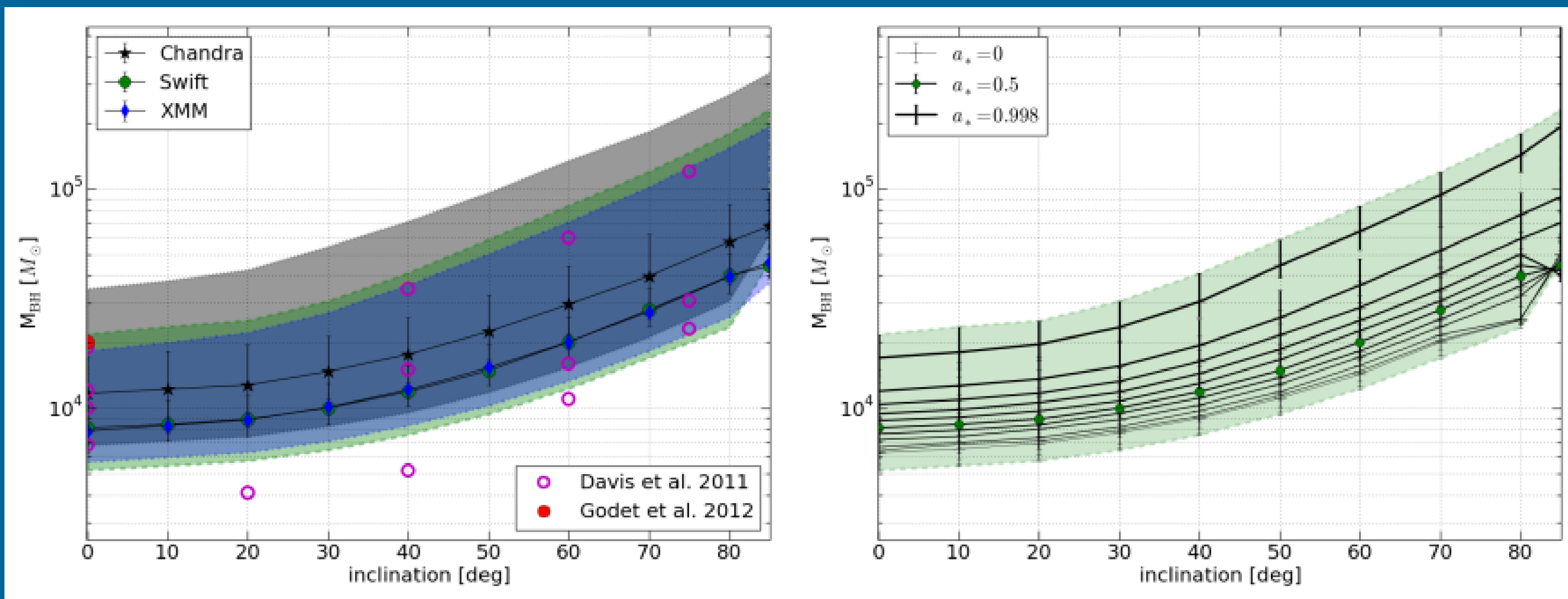

Accretion model for this source was presented in 1402.4863

1403.6407

Heavy BH in M82

Pasham et al. (Nature 2014) дают оценку массы для X-1 около 400 масс Солнца.

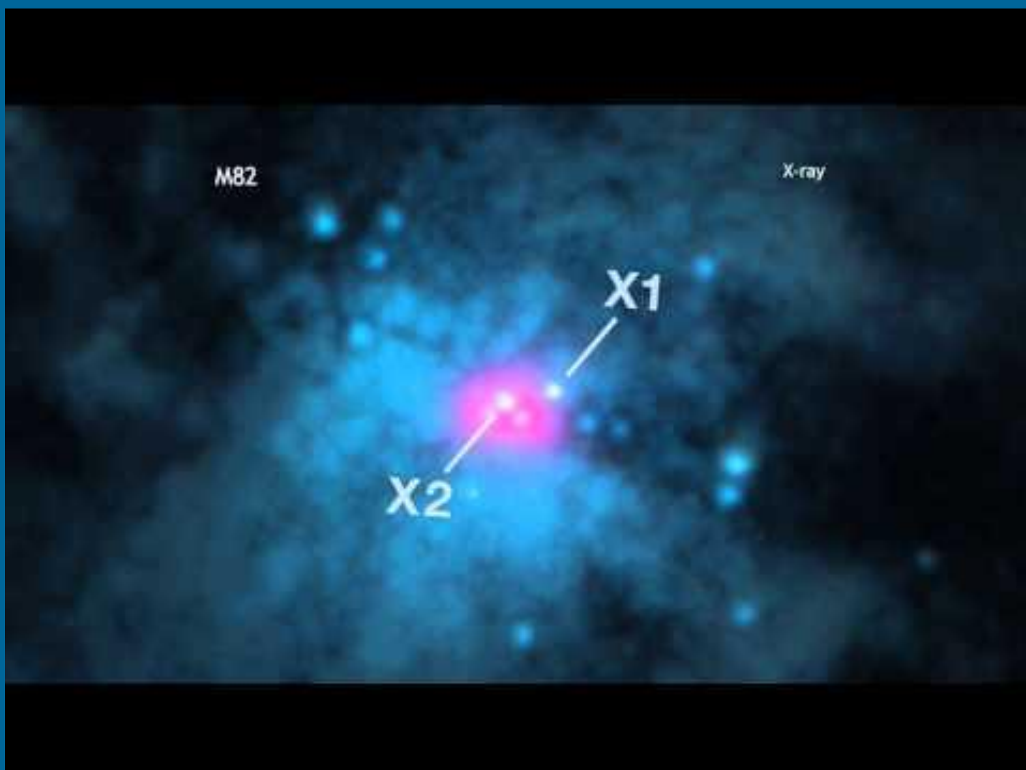

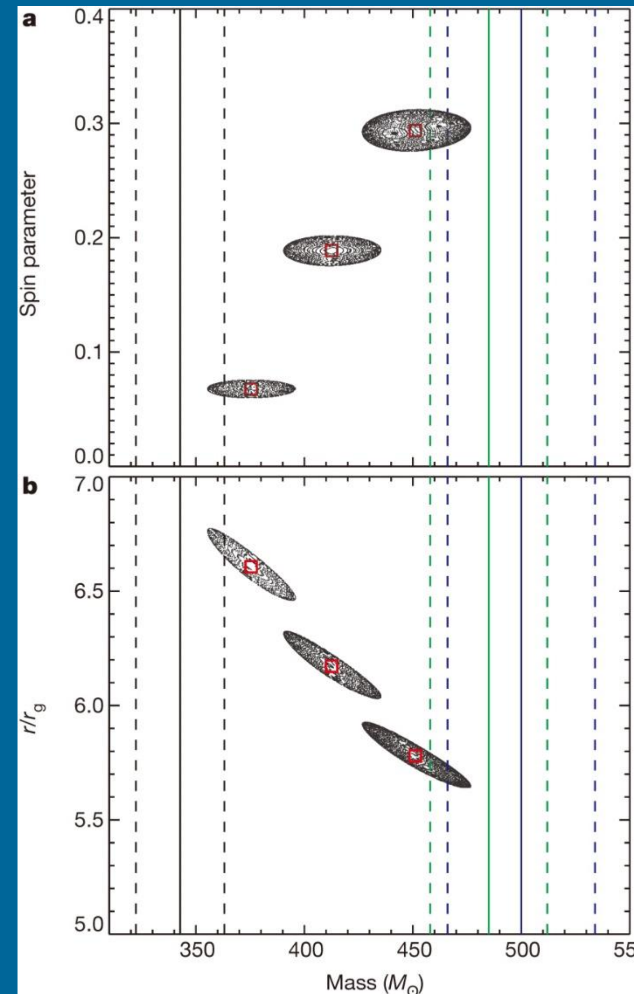

1501.03180

IMBH in an ULXs

For the first time for one source there are both – spectral and timing – data showing evidence in favor of an IMBH.

$M_{BH} \sim 10^3 - 10^4 M_{solar}$

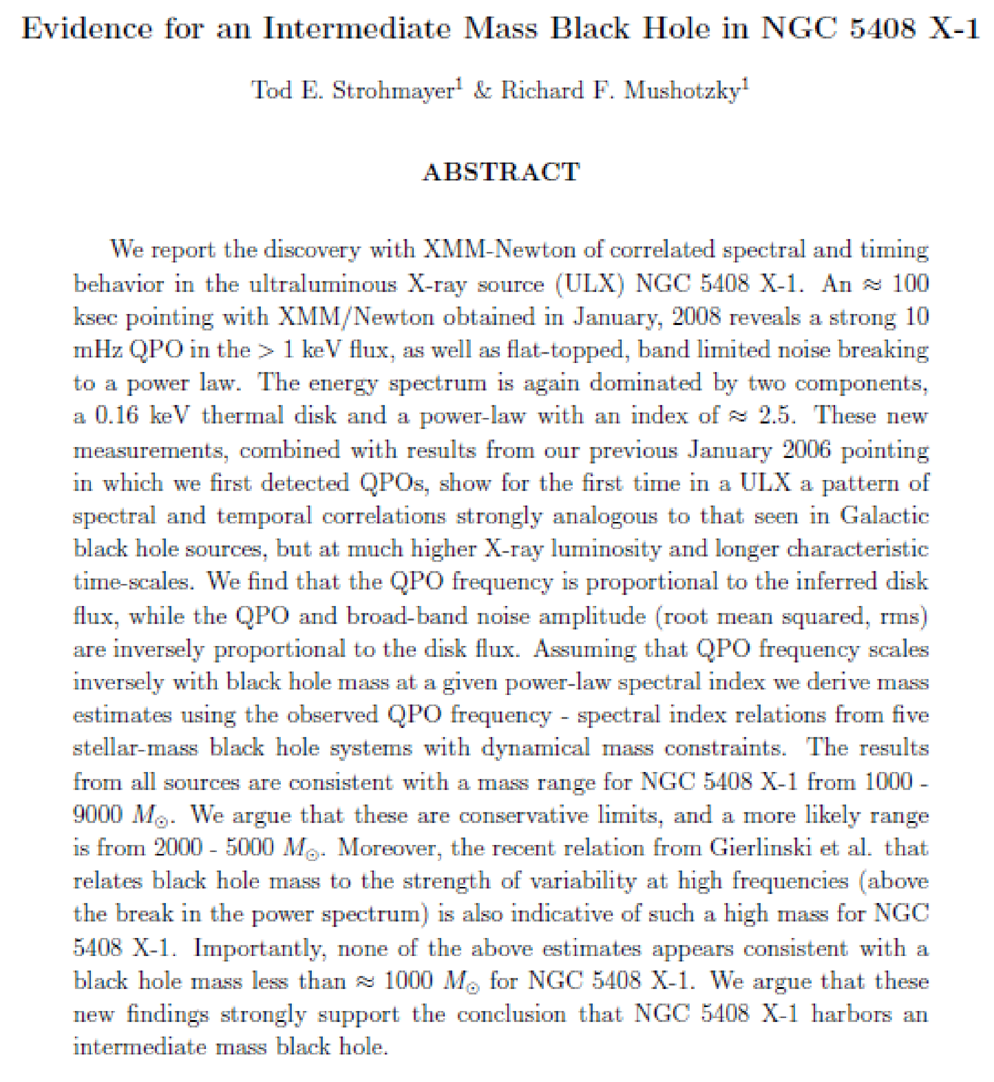
Evidence for an Intermediate Mass Black Hole in NGC 5408 X-1

Tod E. Strohmayer[1] & Richard F. Mushotzky[1]

ABSTRACT

We report the discovery with XMM-Newton of correlated spectral and timing behavior in the ultraluminous X-ray source (ULX) NGC 5408 X-1. An ≈ 100 ksec pointing with XMM/Newton obtained in January, 2008 reveals a strong 10 mHz QPO in the > 1 keV flux, as well as flat-topped, band limited noise breaking to a power law. The energy spectrum is again dominated by two components, a 0.16 keV thermal disk and a power-law with an index of ≈ 2.5. These new measurements, combined with results from our previous January 2006 pointing in which we first detected QPOs, show for the first time in a ULX a pattern of spectral and temporal correlations strongly analogous to that seen in Galactic black hole sources, but at much higher X-ray luminosity and longer characteristic time-scales. We find that the QPO frequency is proportional to the inferred disk flux, while the QPO and broad-band noise amplitude (root mean squared, rms) are inversely proportional to the disk flux. Assuming that QPO frequency scales inversely with black hole mass at a given power-law spectral index we derive mass estimates using the observed QPO frequency - spectral index relations from five stellar-mass black hole systems with dynamical mass constraints. The results from all sources are consistent with a mass range for NGC 5408 X-1 from 1000 - 9000 $M_\odot$. We argue that these are conservative limits, and a more likely range is from 2000 - 5000 $M_\odot$. Moreover, the recent relation from Gierlinski et al. that relates black hole mass to the strength of variability at high frequencies (above the break in the power spectrum) is also indicative of such a high mass for NGC 5408 X-1. Importantly, none of the above estimates appears consistent with a black hole mass less than ≈ 1000 $M_\odot$ for NGC 5408 X-1. We argue that these new findings strongly support the conclusion that NGC 5408 X-1 harbors an intermediate mass black hole.

0911.1076

Low-frequency QPO (2008 data)

NGC 5408 X-1 behaves very much like a Galactic stellar-mass BH system with the exception that its characteristic X-ray time-scales are 100 times longer, and its luminosity is greater by a roughly similar factor.

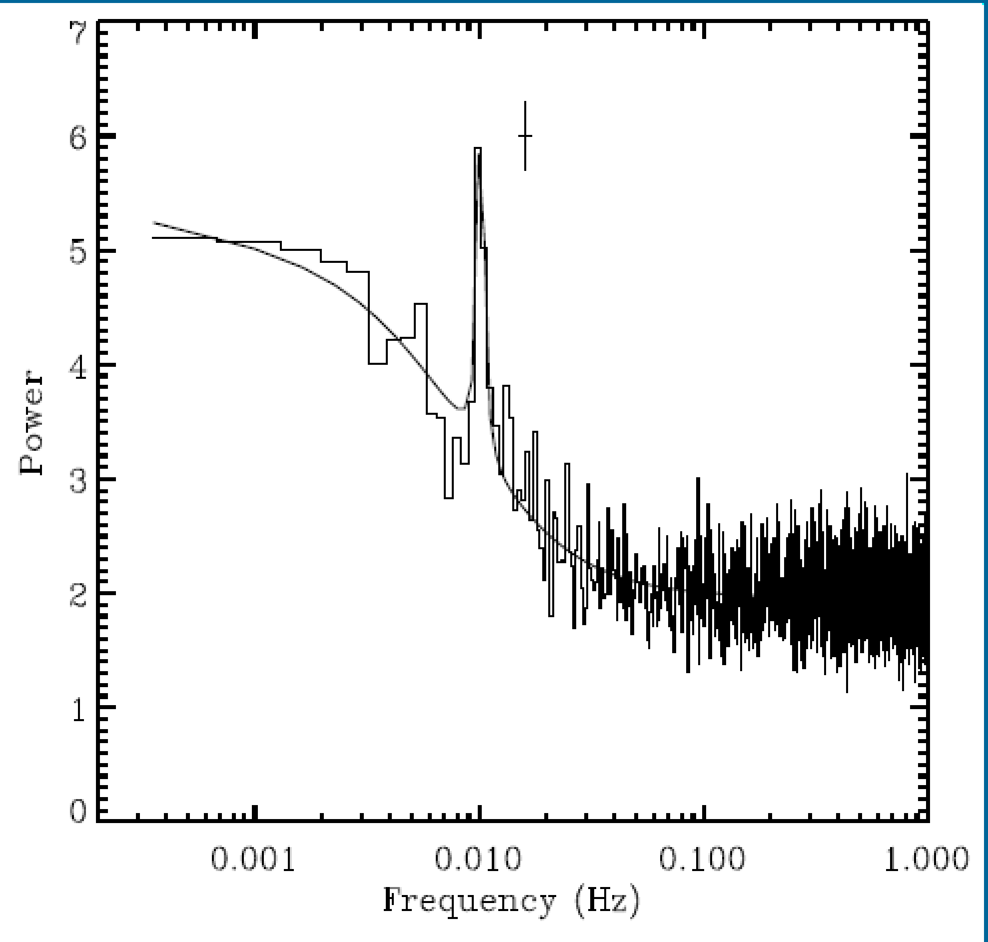

E>1 keV

0911.1076

Comparison of two observations

Obs1 – 2006
Obs2 – 2008

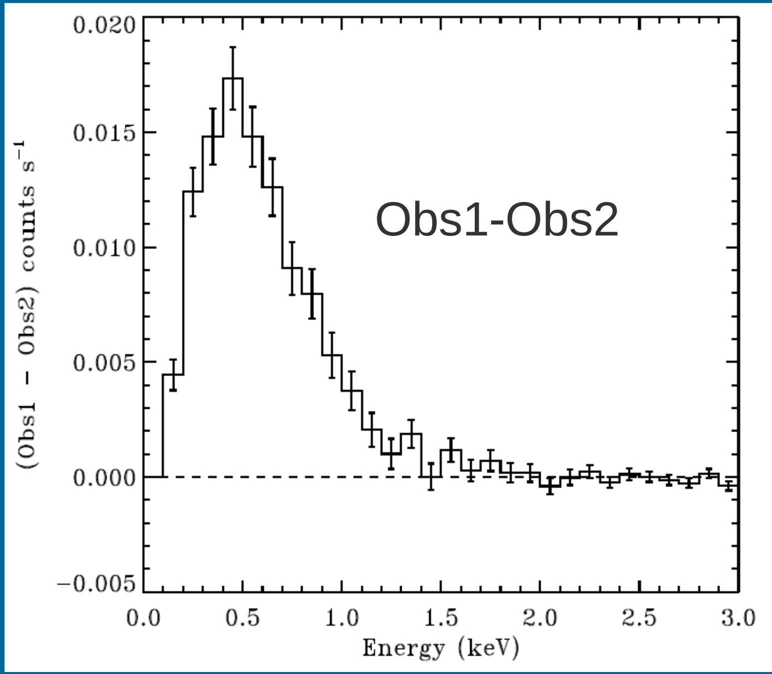

Obs1 was brighter, but all difference is due to soft (disc) component.

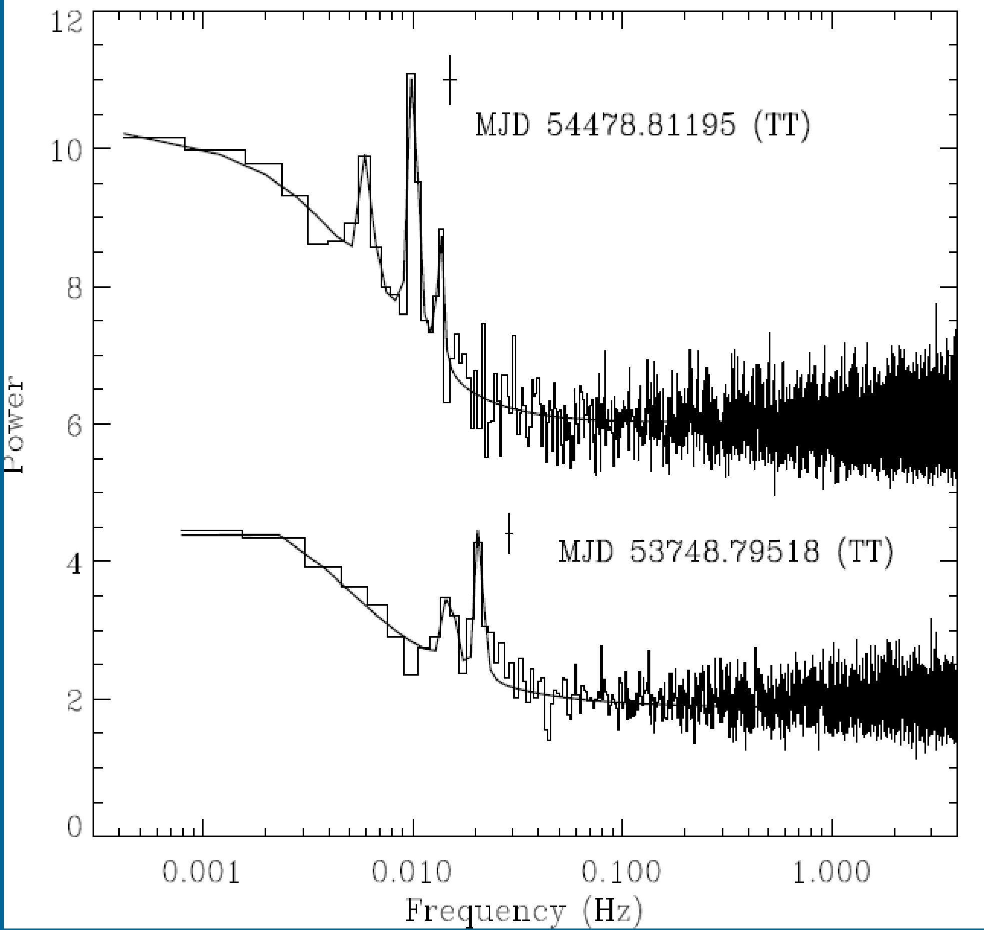

0911.1076

Jet from an ULX in NGC 2276

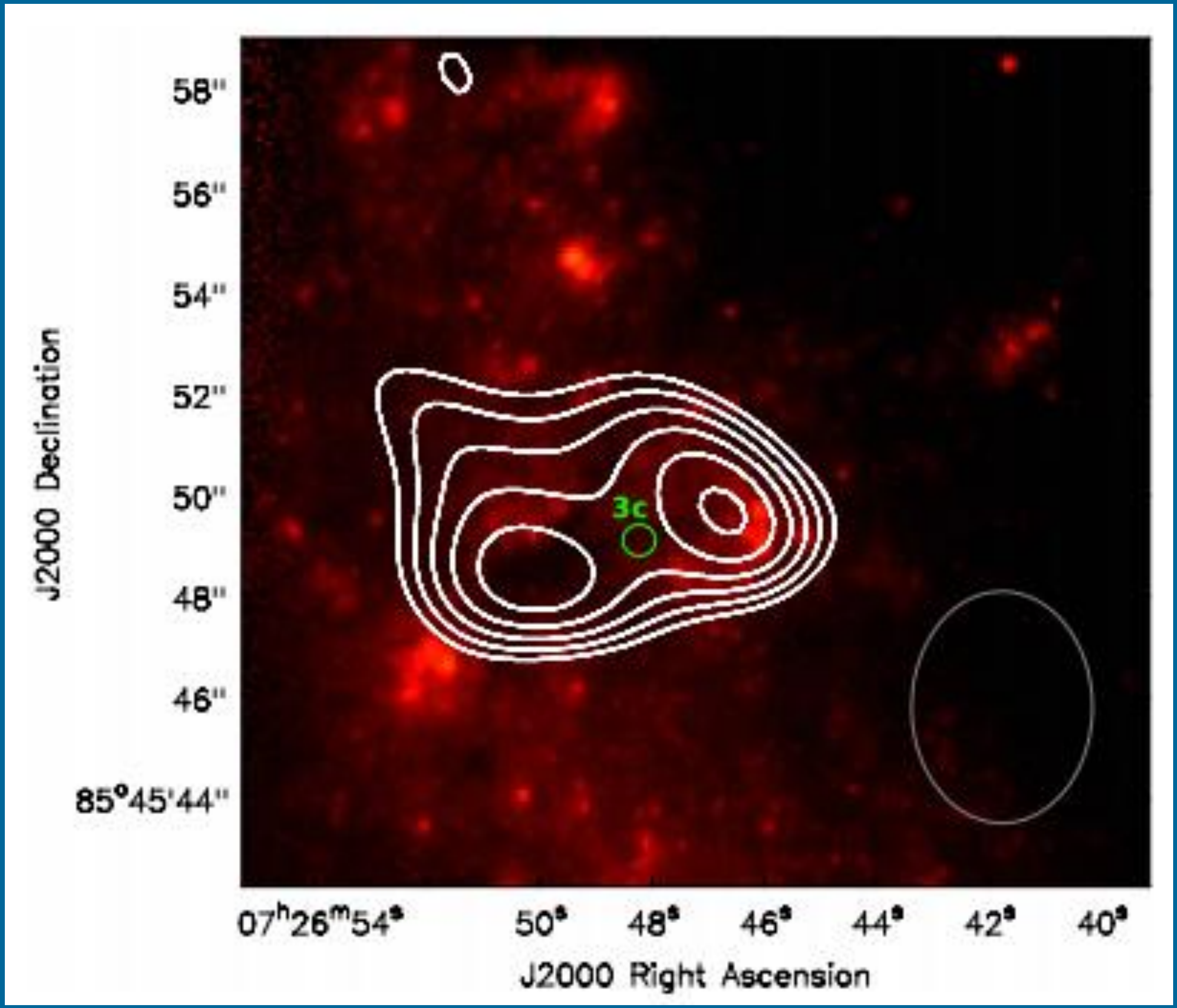

650 pc radio lobes
Scaling from usual BHs gives the mass estimate $4.7\ 10^3 < M < 8.5\ 10^5$

1309.5721

Jet from ULX Holmberg II X-1

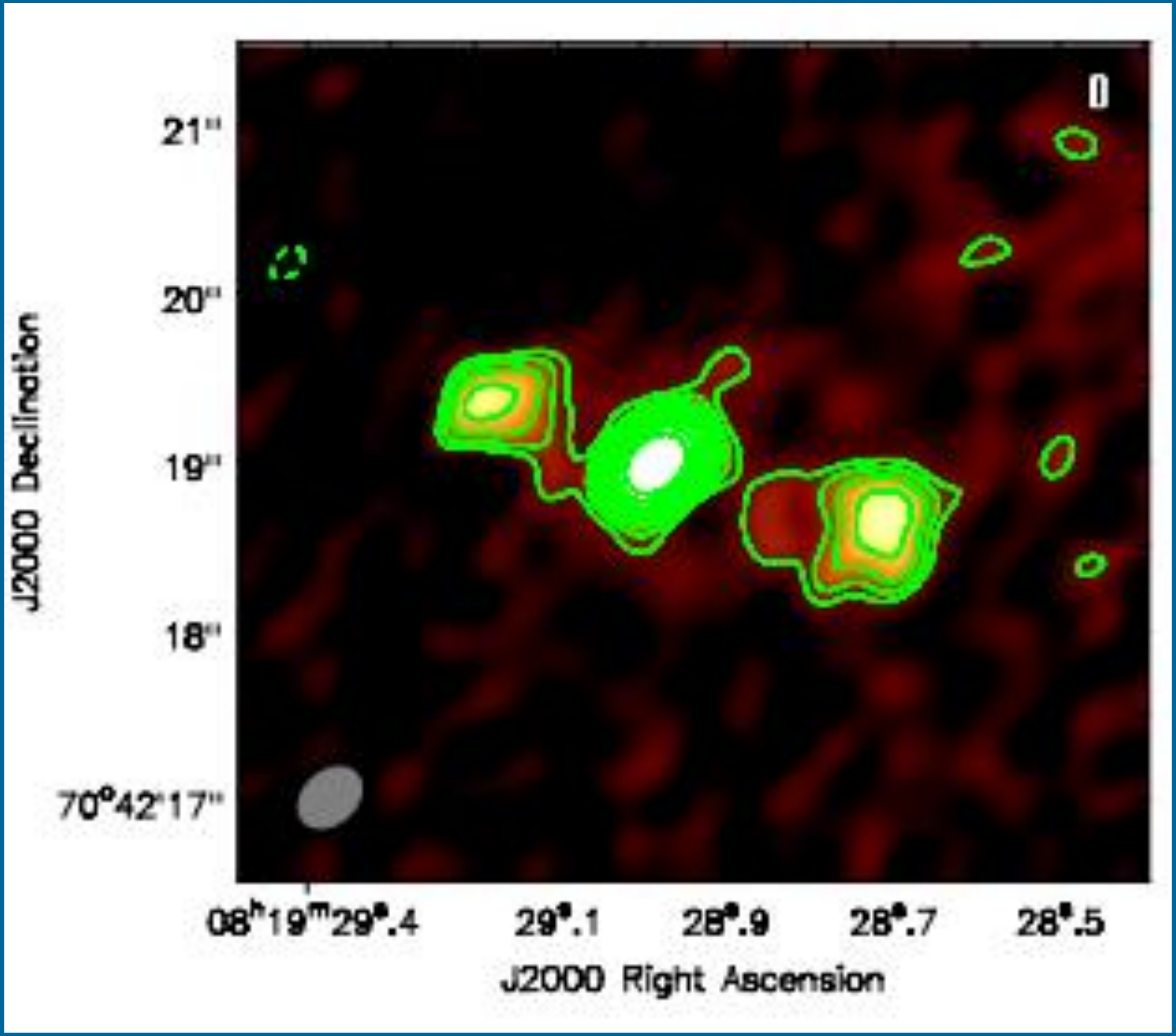

Mass limits are poor:
M> 25 Msolar

1311.4867

Strange accretion in the ULX in M101

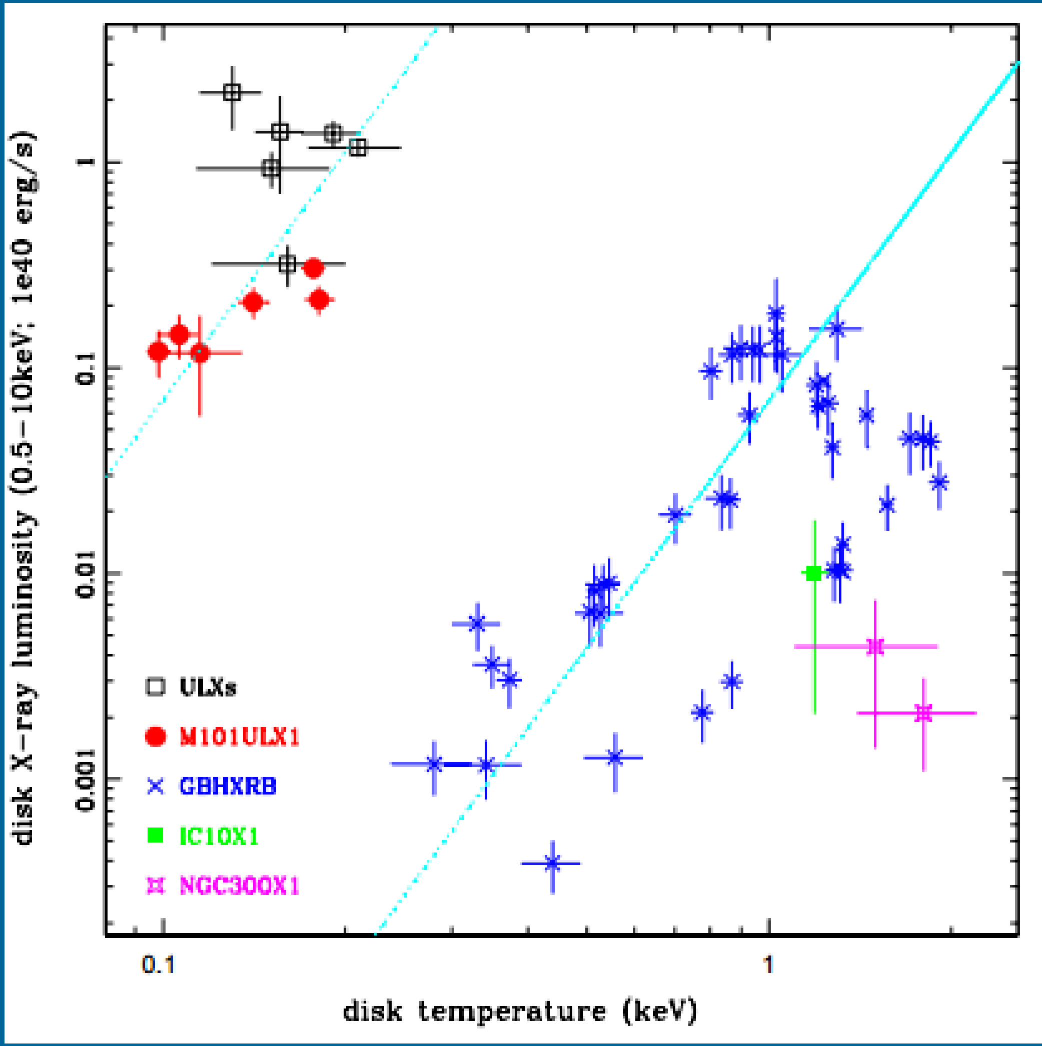

The authors determined the orbital period and determined properties of the companion.

The BH mass is estimated to be ~20-30 Msolar.

However, soft X-ray spectra is unexpected for such low mass.

1312.0337

Normal BH in an ULX

P13 in the galaxy NGC 7793
BH mass 7-15 Msolar
(depending on rotation)

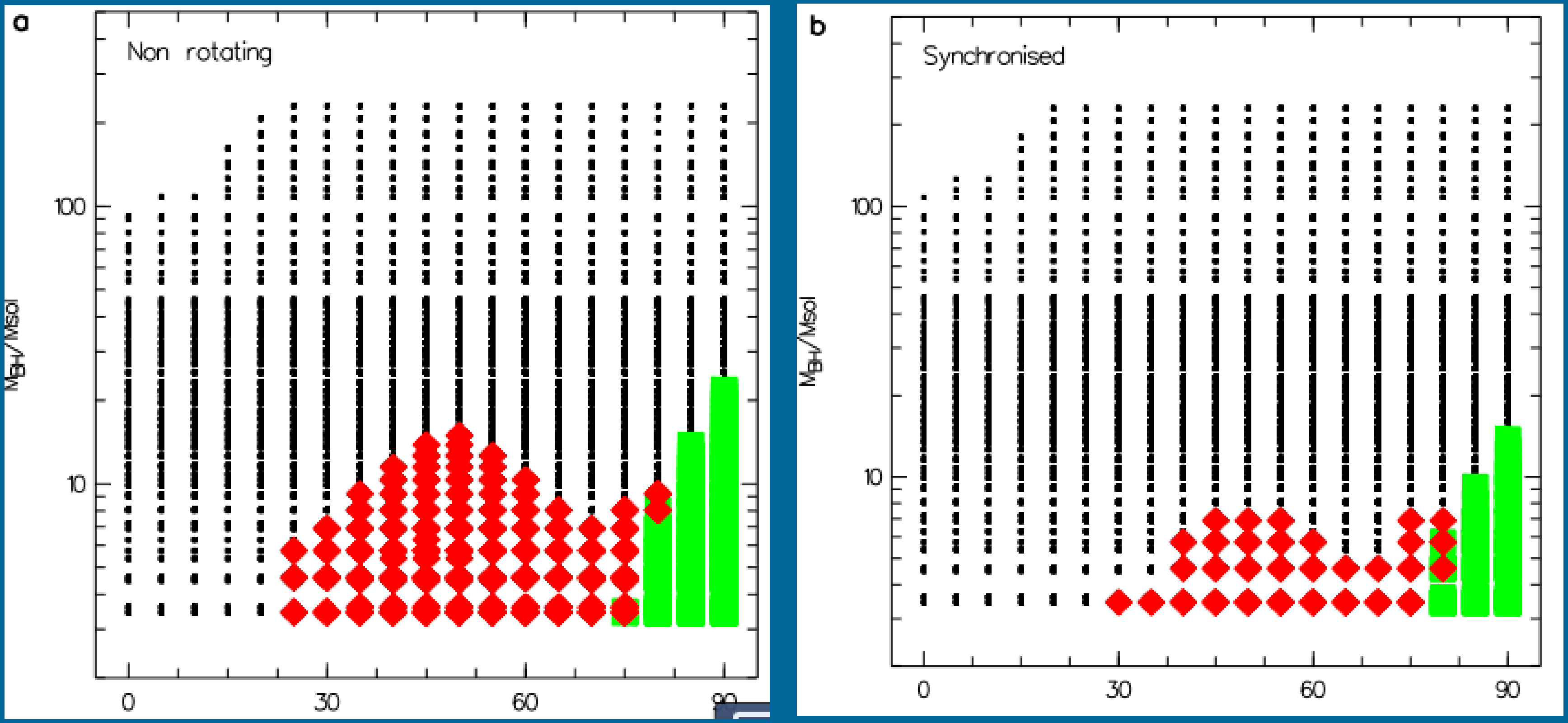

1410.4250

Funneling in the Galactic source Cyg X-3

Polarization measurements. IXPE.

The intrinsic luminosity exceeds the Eddington limit
for a neutron star accretor at opening angles α~8,
while for α~16 this limit is exceeded even for a black hole of 20 solar masses.

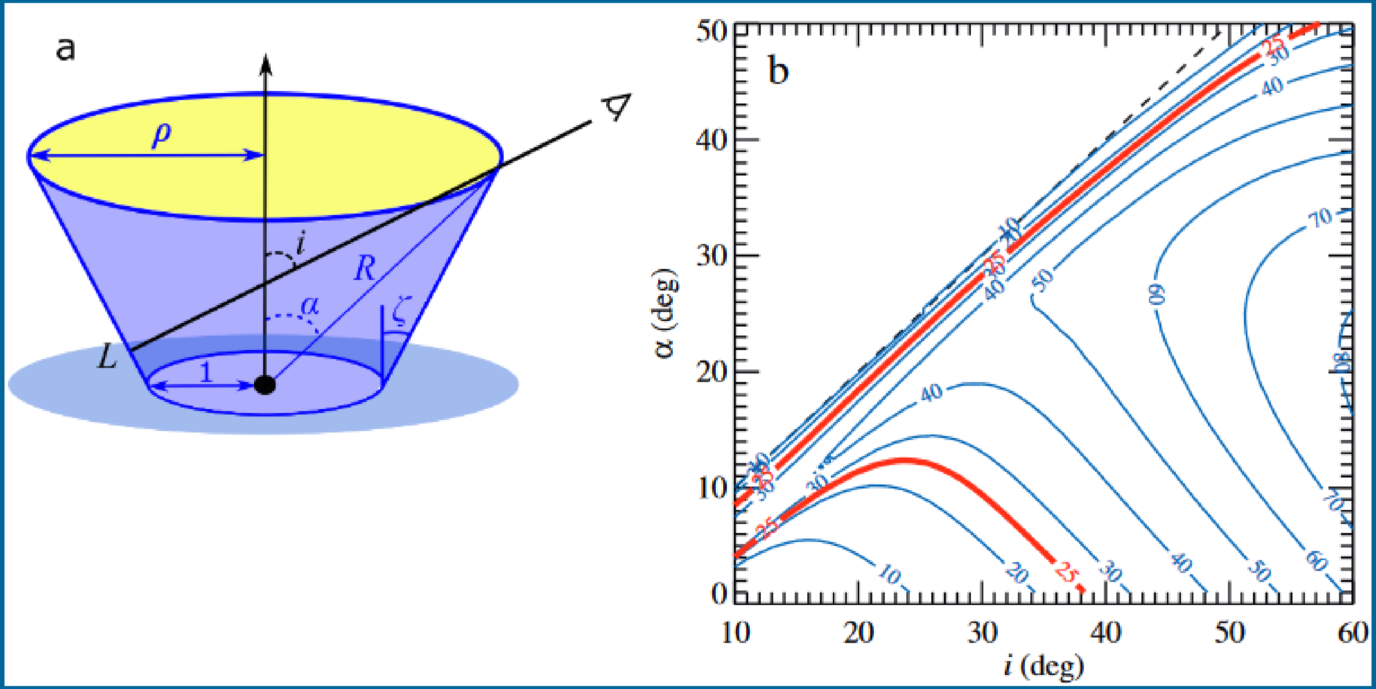

Cyg X-3 is viewed as a ULX to an extragalactic observer located along the axis of the funnel.

2303.01174

A NS in an ULX!!!!

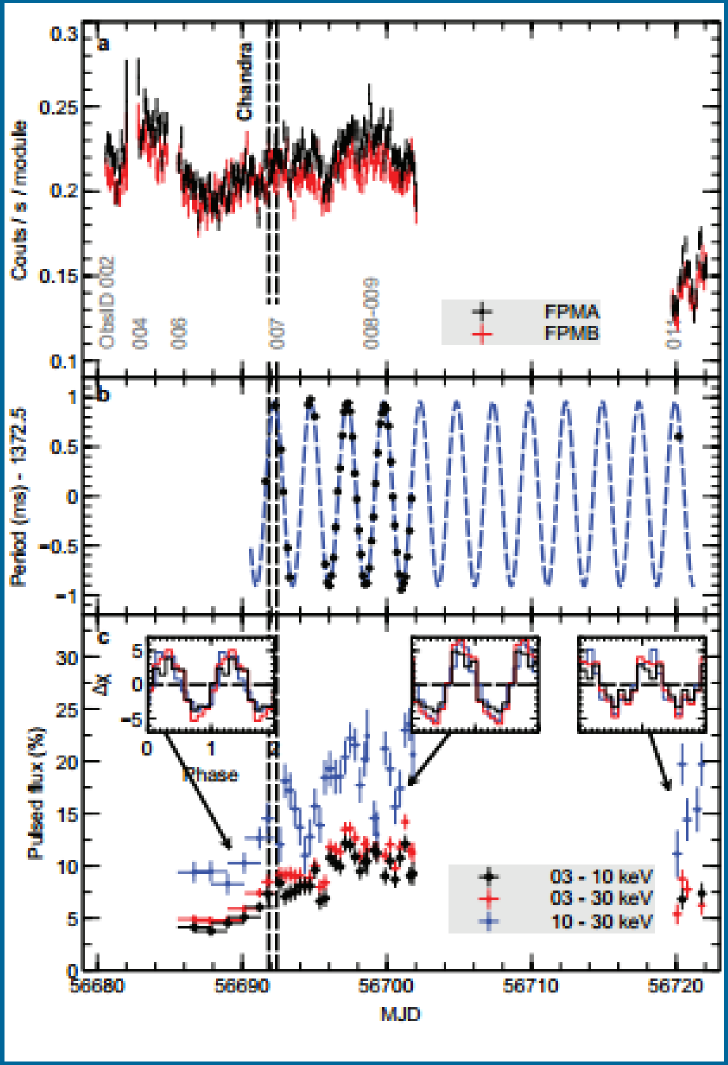

Pulsations with 1.37 s period found!

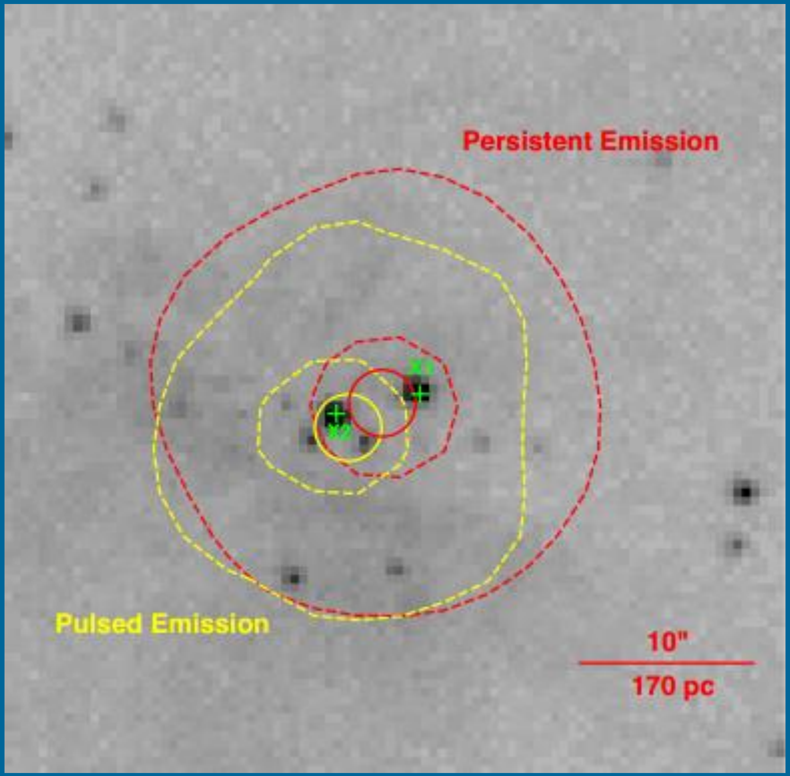

New search through archive data for other examples of pulsars in ULX failed to find any (1410.7264)

1410.3590

Cyclotron line in ULX M51

~10^{12} G dipolar field.
Strong dipole field is excluded,
but strong multipoles are still possible.

<u>A big question: are there magnetars in ULX?</u>

Some studies suggest that – no
(see 1903.03624 and 2309.00034).

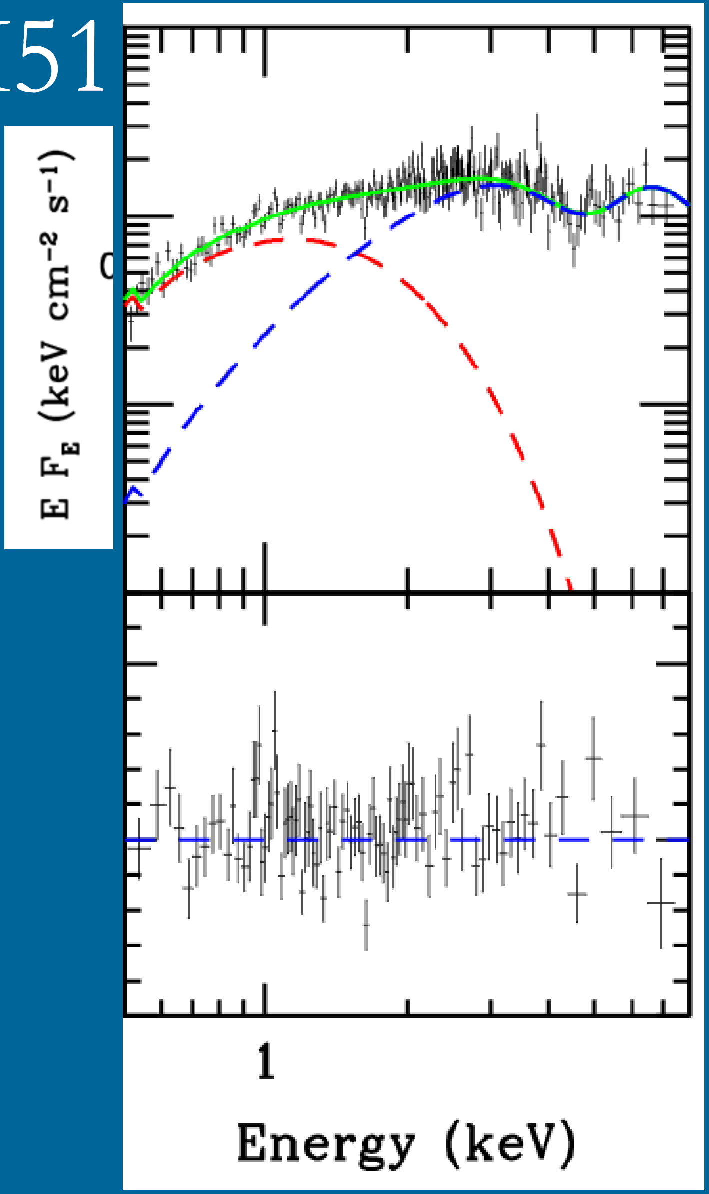

1902.04058

Fantastic spin evolution of the ULX in NGC 300

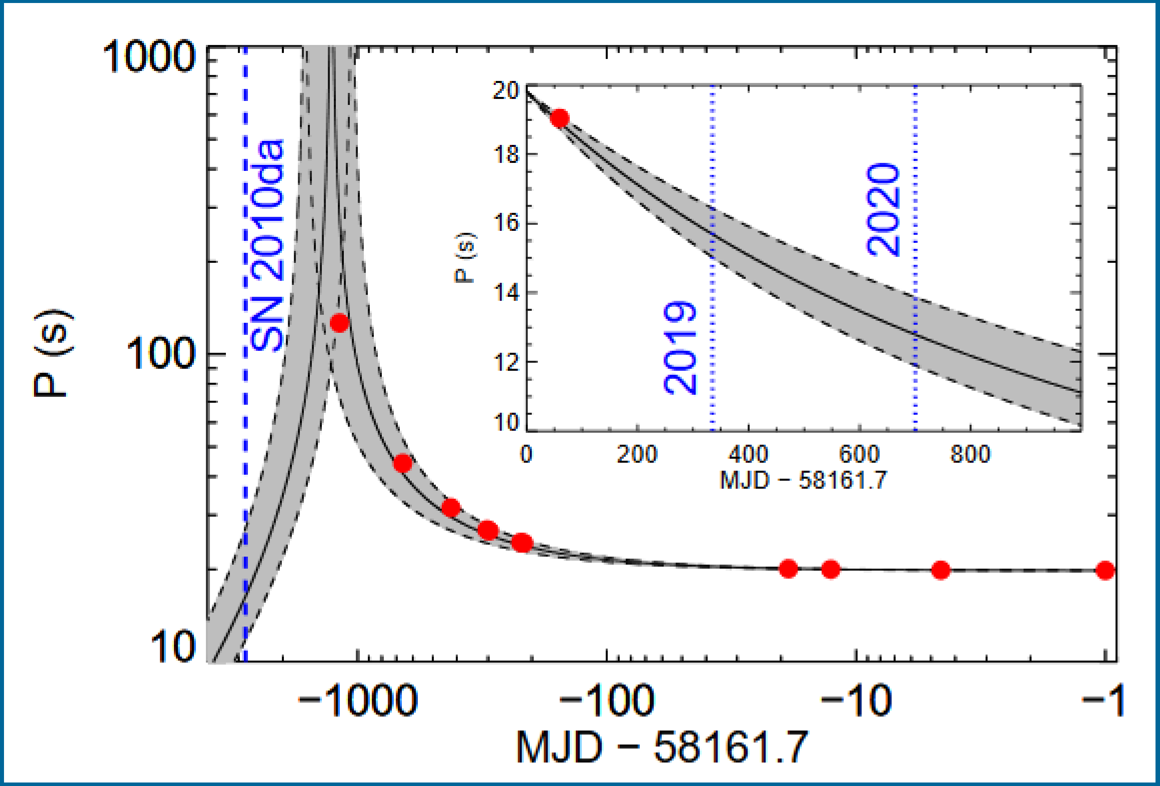

Torque reversal in 2014?

About SN2010da see 1605.07245.
This might be not a core collapse, but an eruption on a massive evolved star.

Donor star discovered (1909.02171)!
It is a red supergiant.

1811.11907

Propeller states in ULXs

Source	State	N_H $\times 10^{20}$ cm^{-2}	kT_{soft} keV	$L_{disc,\,o}$ $\times 10^{39}$ erg/s	$L_{NS,\,o}$ $\times 10^{39}$ erg/s	$\Delta L / L_{disc,\,o}$	χ^2/dof
IC 342 X-1	High Propeller	0.80±0.02	0.87±0.02	$5.9^{+0.2}_{-0.1}$	5.1±0.2 -	0.86±0.04	476/417
NGC 1313 X-1	High Propeller	0.15±0.01	0.57±0.01	$4.7^{+0.09}_{-0.07}$	4.2±0.2 -	$0.90^{+0.05}_{-0.04}$	717/390
Circinus ULX5	High Propeller	0.63±0.01	$1.13^{+0.01}_{-0.02}$	5.15±0.05	8^{+8}_{-3} -	$1.5^{+1.6}_{-0.6}$	518/374

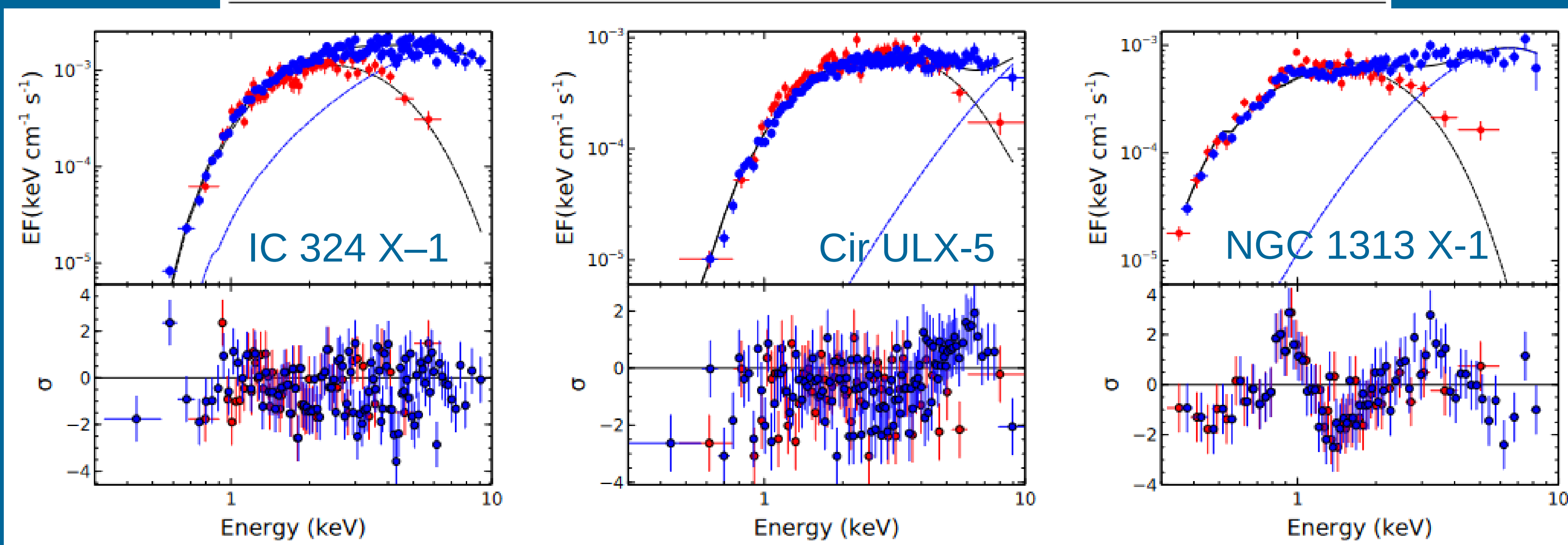

2211.13758

The population of ULXs

Most probably, the population of ULXs in not uniform.

1. Intermediate mass BHs
2. Collimated emission from normal stellar mass BHs
3. Accreting neutron stars
4. Different types of sources (pulsars, SNR, contamination)
5. Background sources.

Background sources

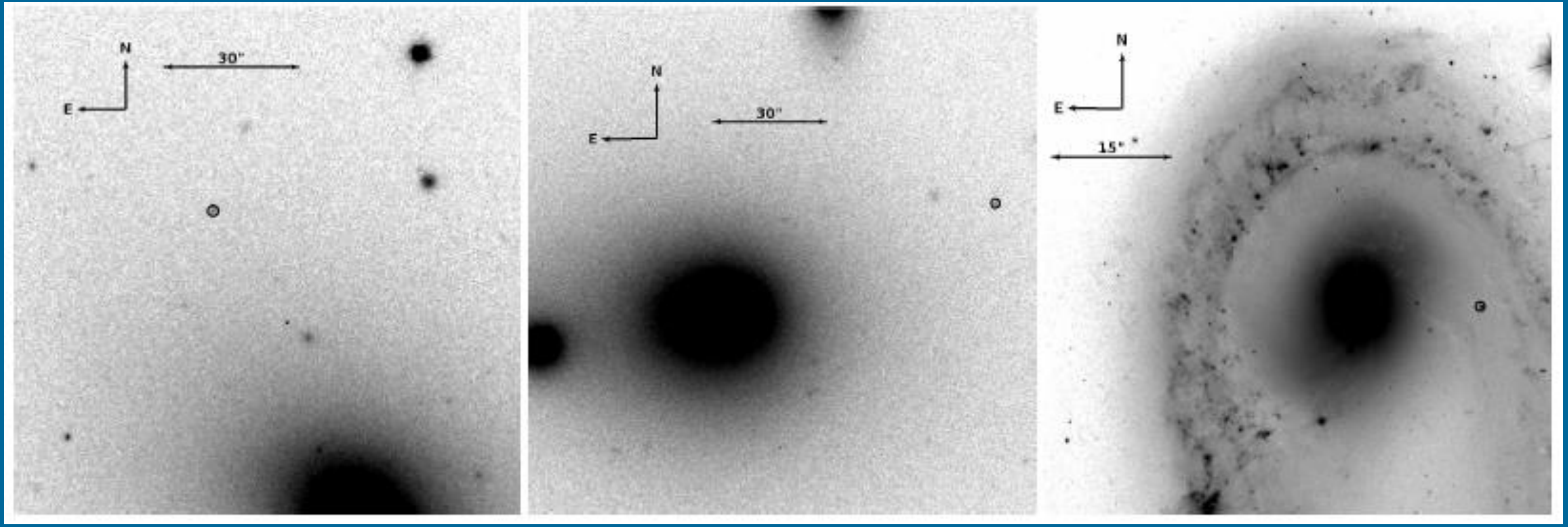

Three out of four studied objects appeared to be background AGNs.
The only true ULX is in a spiral galaxy. Two out of false – in ellipticals.

1305.0821

List of reviews

- Modeling accretion: Done et al. arXiv:0708.0148
- Accretion discs: Lasota 1505.02172
- Accretion onto BHs: Bu, Zhang 2310.20637
- BH binaries: Kalemci et al. 2206.14410 ←
- BH states: Belloni arXiv: 0909.2474; Dunn et al. arXiv: 0912.0142
- X-ray observations of ULXs: Roberts. arXiv:0706.2562
- BH binaries and microquasars: Zhang. arXiv: 1302.5485
- BH transients: Belloni. arXiv:1109.3388, 1603.07872
- ULXs: Fabrika 2105.10537, King et al. 2302.10605
- QPO: Ingram, Motta 2001.08758
- BH spin: Middleton 1507.06153, Reynolds 2011.08948
- IMBHs: Koliapanos 1801.01095, Mezcua 1705.09667
- BH coalescence: Schutz 1804.06308
- BH-BH binaries (stellar and supermassive): Celoria et al. 1807.11489
- General review on accreting NSs and BHs. Psaltis. astro-ph/0410536

IMBH in 47 Tuc?

Cluster dynamics was probed with radio pulsars.

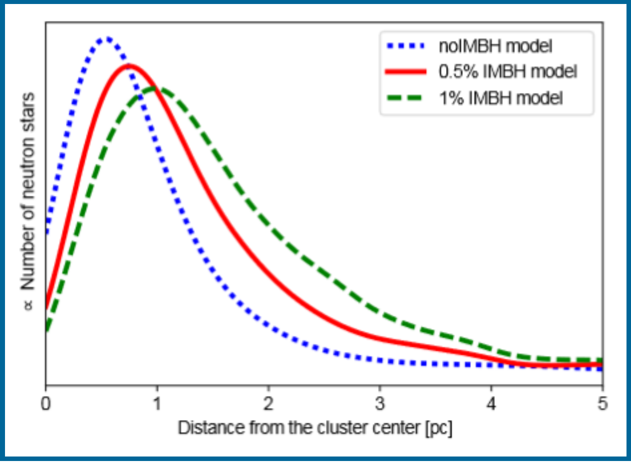

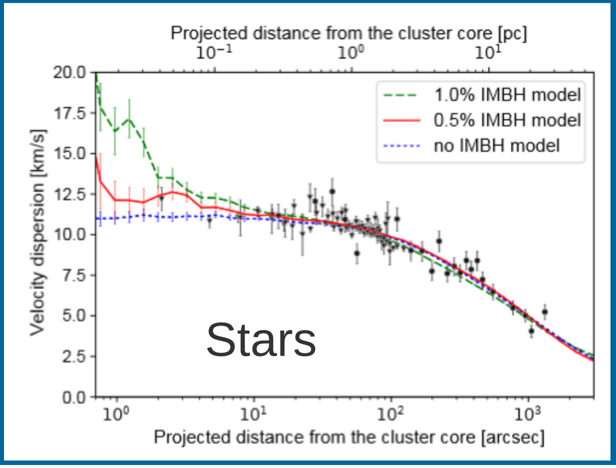

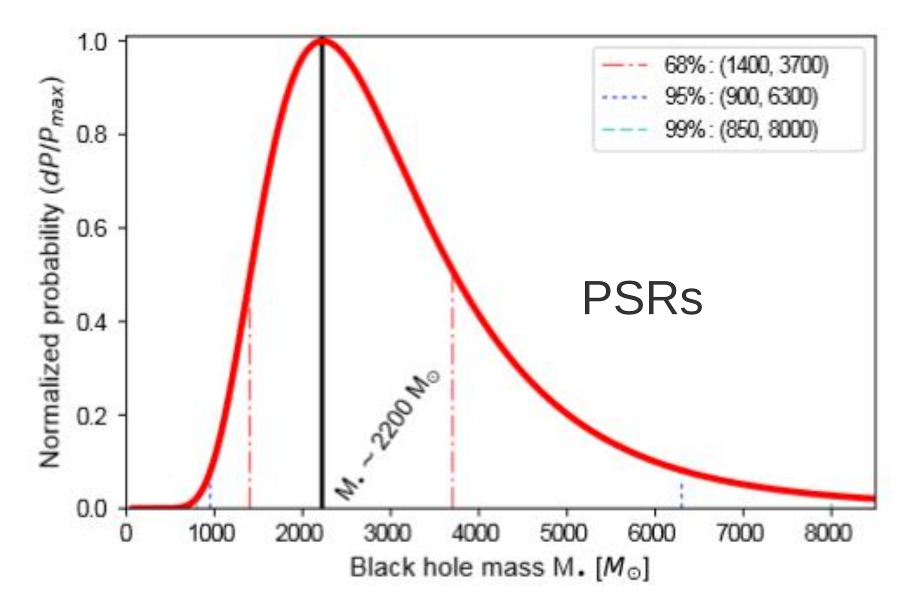

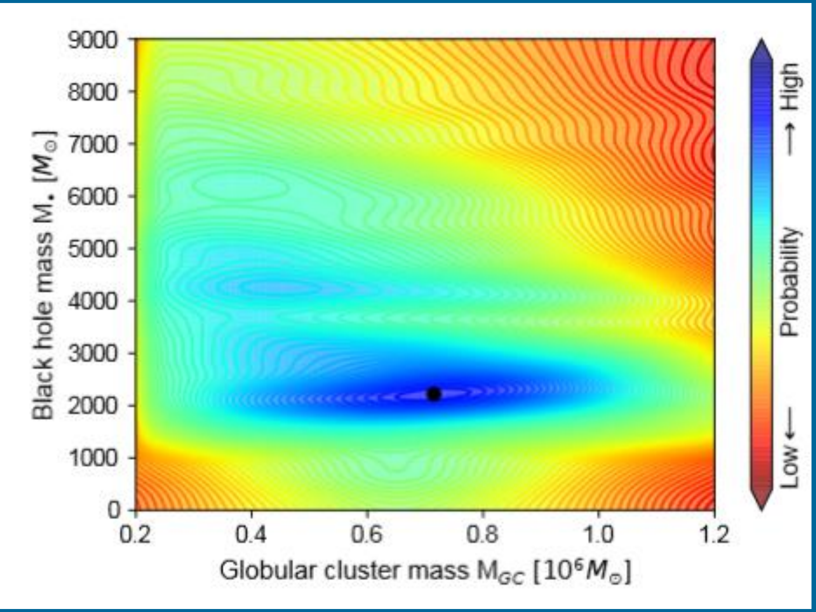

1702.02149

Summary of states with jets in BH binaries

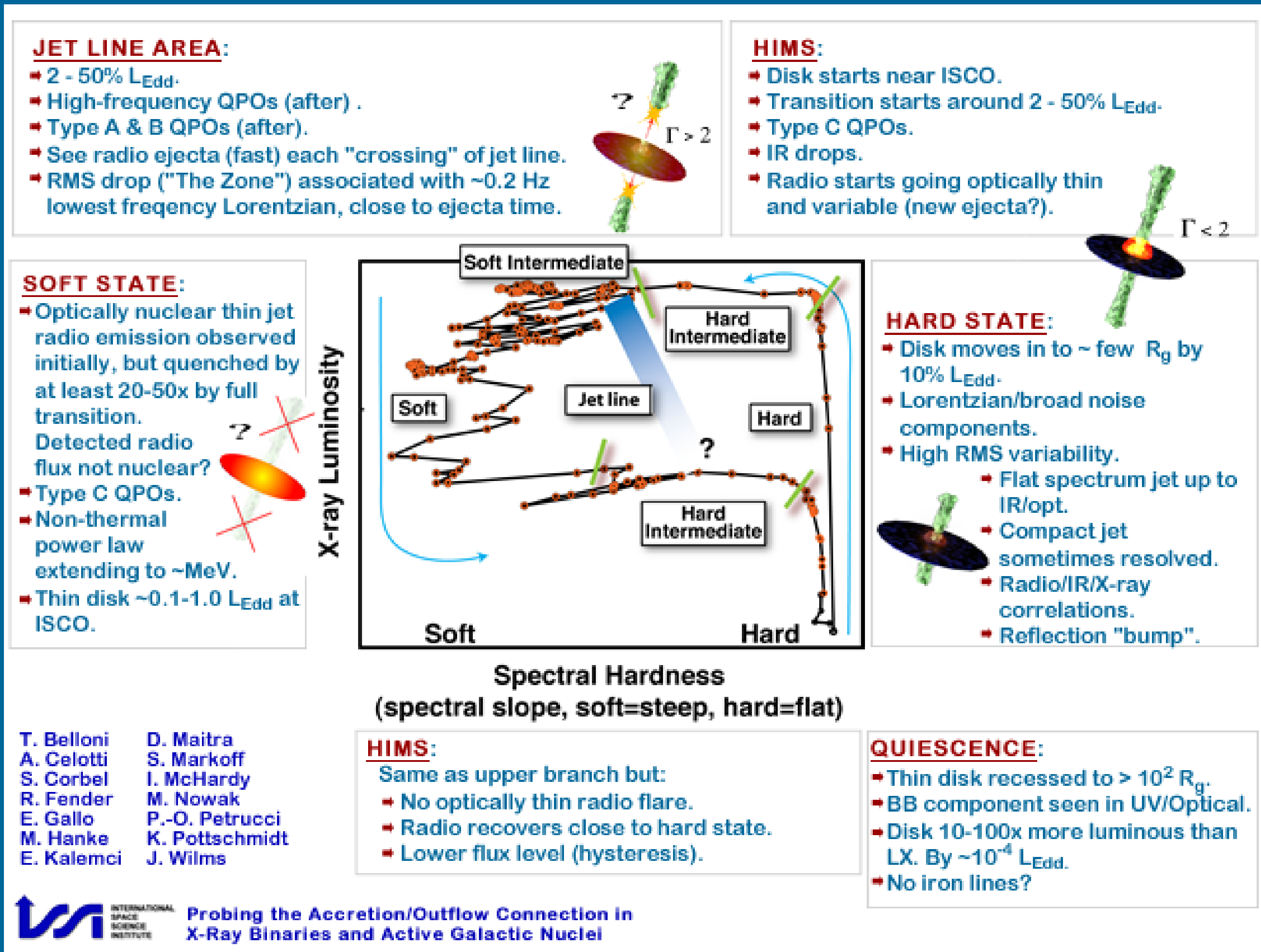

http://www.issibern.ch/teams/proaccretion/Images/newcomplete_72dpi.png